การออปติไมซ์ของการเผาไหม้เชื้อเพลิงผสมในเครื่องเผาไหม้ฟลูอิไดซ์เบดแบบหมุนเวียน

นางสาวชุติมา มณฑาทิพย์

วิทยานิพนธ์นี้เป็นส่วนหนึ่งของการศึกษาตามหลักสูตรปริญญาวิศวกรรมศาสตรมหาบัณฑิต
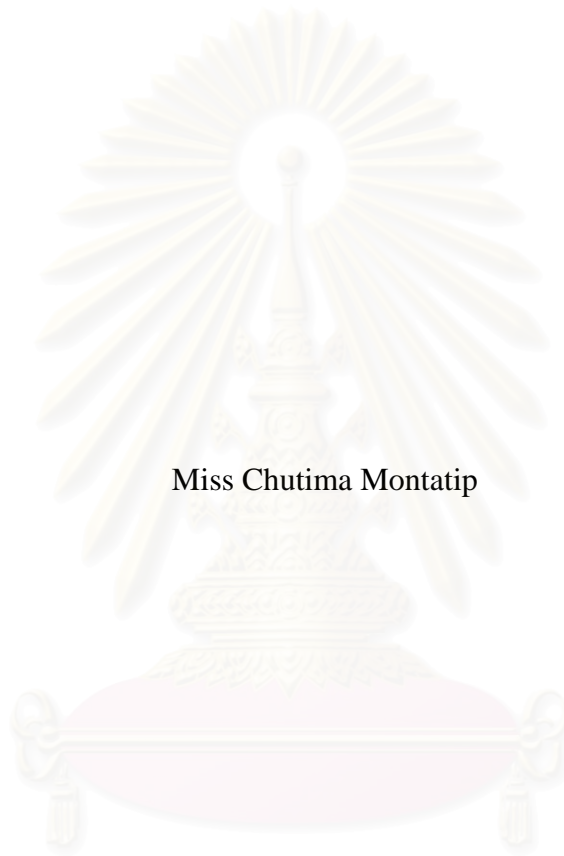สาขาวิชาวิศวกรรมเคมี   ภาควิชาวิศวกรรมเคมี
คณะวิศวกรรมศาสตร์ จุฬาลงกรณ์มหาวิทยาลัย
ปีการศึกษา 2550
ลิขสิทธิ์ของจุฬาลงกรณ์มหาวิทยาลัย

OPTIMIZATION OF CO-COMBUSTION IN CIRCULATING FLUIDIZED BED
COMBUSTOR

Miss Chutima Montatip

A Thesis Submitted in Partial Fulfillment of the Requirements
for the Degree of Master of Engineering Program in Chemical Engineering
Department of Chemical Engineering
Faculty of Engineering
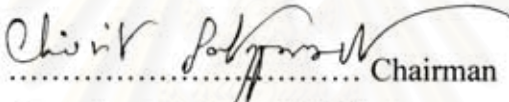Chulalongkorn University
Academic year 2007
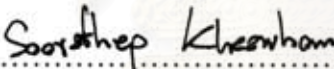
Thesis Title   OPTIMIZATION OF CO-COMBUSTION IN CIRCULATING
                    FLUIDIZED BED COMBUSTOR
By   Miss Chutima Montatip
Field of Study   Chemical Engineering
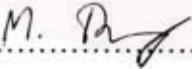Thesis Advisor   Soorathep Khaewhom, Ph.D.

Accepted by the Faculty of Engineering, Chulalongkorn University in Partial Fulfillment of the Requirements for the Master's Degree

.... Dean of the Faculty of Engineering
(Associate Professor Boonsom Lerdhirunwong, Dr.Ing.)
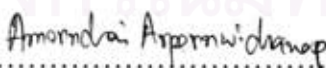
THESIS COMMITTEE

.... Chairman
(Associate Professor Chairit Satayaprasert, Dr.Ing.)

.... Thesis Advisor
(Soorathep Kheawhom, Ph.D.)

.... Member
(Associate Professor Muenduen Phisalaphong, Ph.D.)

.... Member
(Assistant Professor Okorn Mekasuwandumrong, D.Eng.)

.... Member
(Assistant Professor Amornchai Arpornwichanop, D.Eng.)

ชุดิมา มณฑาทิพย์ : การออปติไมซ์ของการเผาไหม้เชื้อเพลิงผสมในเครื่องเผาไหม้ฟลูอิไดซ์เบดแบบ
หมุนเวียน (OPTIMIZATION OF CO-COMBUSTION IN CIRCULATING FLUIDIZED BED
COMBUSTOR) อ. ที่ปรึกษา: คร. สุรเทพ เขียวหอม,113 หน้า.

การเผาไหม้ด้วยฟลูอิไดซ์เบดแบบหมุนเวียนได้รับความสนใจในการวิจัยค้นคว้าอย่าง
กว้างขวาง เนื่องจากเป็นระบบที่มีสมรรถนะทางด้านประสิทธิภาพการเผาไหม้ เศรษฐศาสตร์ และ
สิ่งแวดล้อมสูง เทคโนโลยีการเผาไหม้ฟลูอิไดซ์เบดแบบหมุนเวียนสามารถเผาไหม้ได้กับเชื้อเพลิงที่มี
คุณภาพต่ำเช่น ถ่านหิน, ชีวมวล และขยะอินทรีย์ เตาเผาฟลูอิไดซ์เบดแบบหมุนเวียนสามารถเผาไหม้
เชื้อเพลิงพร้อมกับหินปูนเพื่อดักจับซัลเฟอร์ไดออกไซด์ขณะทำการเผาไหม้พร้อมๆกันได้ และอุณหภูมิ
ที่ใช้ในการเผาไหม้ไม่สูงมาก จึงทำให้ผลิตสารประกอบไนโตรเจนออกไซด์ออกมาน้อย ในงานวิจัยนี้
ศึกษาการเผาไหม้ของเชื้อเพลิงชีวมวลที่ได้มาจากวัสดุเหลือทิ้งทางการเกษตร เช่นชานอ้อย, เปลือกไม้
และแกลบร่วมกับถ่านหินลิกไนต์ในเตาเผาฟลูอิไดซ์เบดแบบหมุนเวียน โดยใช้โปรแกรมสำเร็จรูปและ
แบบจำลองการเกิดปฏิกิริยาที่ปรับปรุงขึ้น พร้อมกับแบบจำลองทางจลนศาสตร์ที่ใช้ในการสร้าง
แบบจำลองระบบการเผาไหม้ในเตาเผาไหม้ฟลูอิไดซ์เบดแบบหมุนเวียน ในการทดลองนี้ศึกษาผลของ
สภาวะในการดำเนินการต่างๆ เช่น อุณหภูมิการเผาไหม้, ปริมาณของอากาศ, อัตราส่วนของชีวมวลใน
เชื้อเพลิงผสม และชนิดของเชื้อเพลิงชีวมวล ที่มีต่อสมรรถนะทางด้านสิ่งแวดล้อม และประสิทธิภาพใน
การเผาไหม้ของคาร์บอน รวมถึงศึกษาผลของอัตราส่วนโดยโมลระหว่างปริมาณของแคลเซียมต่อ
ซัลเฟอร์ที่มีต่อประสิทธิภาพการดักจับซัลเฟอร์ไดออกไซด์ การผสมเชื้อเพลิงชีวมวลเข้ากับลิกไนต์ใน
สายป้อนจะมีผลให้ประสิทธิภาพในการเผาไหม้ของคาร์บอนสูงขึ้น และในขณะเดียวกันยังลดปริมาณ
ของคาร์บอนไดออกไซด์ คาร์บอนมอนออกไซด์ และซัลเฟอร์ไดออกไซด์ที่ปล่อยออกจากกระบวนการ
ด้วย

ภาควิชา	วิศวกรรมเคมี	ลายมือชื่อนิสิต...
สาขาวิชา	วิศวกรรมเคมี	ลายมือชื่ออาจารย์ที่ปรึกษา.........................
ปีการศึกษา	2547	

4770627821: MAJOR CHEMICAL ENGINEERING
KEY WORD: CIRCULATING FLUIDIZED BED COMBUSTOR/CO-COMBUSTION/
BIOMASS/ENVIRONMENTAL IMPACTS/CARBON EFFICIENCY/OPTIMIZATION

CHUTIMA MONTATIP: OPTIMIZATION OF CO-COMBUSTION IN CIRCULATING FLUIDIZED BED COMBUSTOR. THESIS ADVISOR: SOORATHEP KHEAWHOM, Ph.D.113 pp.

Circulating fluidized bed combustion has been received wide research attention due to its high combustion efficiency, high economic and environmental performances for burning low-grade coals, biomass and organic wastes. A Circulating fluidized bed combustor can burn coal and limestone that capture sulfur dioxide in the combustion. The combustion takes place at moderate temperature resulting in reduction of NOx generated. In this paper, biomass from agricultural wastes including bagasse, bark and rice husk co-fired with lignite coal in circulating fluidized bed combustor is investigated. Commercial software with customized reaction model and kinetic subroutines is used to perform a simulation. We analyze the effects of various different operating parameters including combustion temperature, air flow rate, ratio of biomass in mixed fuel and type of biomass on the environmental performances and carbon combustion efficiency. Moreover, the effect of Ca/S molar ratio on sulfur retention is also studied. The presence of biomass in the feed significantly improves carbon combustion efficiency, and at the same time reduces amount of carbon dioxide, carbon monoxide and sulfur dioxide released.

สถาบันวิทยบริการ
จุฬาลงกรณ์มหาวิทยาลัย

Department Chemical Engineering   Student's signature... C. Montt ...

Field of study   Chemical Engineering   Advisor's signature.... Soorathep Kheawhom

Academic year 2007

ACKNOWLEDGEMENTS

CONTENTS

LIST OF TABLE

TABLE   PAGE

LIST OF FIGURE

FIGURE   PAGE

FIGURE

NOMENCLATURES

a	:	Decay constant
b	:	Stoichiometric coefficient of gas in the combustion reaction
BFB	:	Bubbling Fluidized Bed
CFB	:	Circulating Fluidized Bed
CFBC	:	Circulating Fluidized Bed Combustor
C_{Ag}	:	Concentration of A (kmole/m^3)
C_{O2}	:	Oxygen concentration
D_A	:	Diffusivity coefficient of reactant A (m^2/s)
D_r	:	Diameter of riser (m)
d_p	:	Diameter of particle (m)
E_a	:	Activation energy (J/kmol)
Ec	:	Carbon combustion efficiency
f	:	Mole fraction of component
F	:	Volumetric flow rate of solid
F_A	:	Fuel flow rate in the feed (kg/s)
F_{fa}	:	Flow rate of fly ash (kg/s)
F_{bt}	:	Flow rate of bottom ash (kg/s)
F_{fg}	:	Flow rate of flue gas (kg/s)
F_r	:	Froude number
F_{rt}	:	Particle Froude number
FCC	:	Fluid Catalytic Cracking
g	:	Gravity force (m/s^2)
G_s	:	Solid circulation rate (kg/m^2 s)
k_1	:	First order reaction rate constant base on unit surface
k_c	:	Mass transfer coefficient
k_o	:	Frequency factor for lignite (m/K.s)
k_r	:	Kinetic rate constant
PCM	:	Progressive-Conversion Model
PSD	:	Particle Size Distribution
P_k	:	Weight fraction vector of fuel

R	:	Radius of particle (m)
R	:	gas constant (8.314 kJ/kmol K)
R_e	:	Reynolds numbers
r	:	Mean particle radius (m)
$r_c(k)$	:	Particle radius vector
r_{char}	:	Char combustion rate (kmole/s)
S_c	:	Sherwood numbers
S_h	:	Schmidt numbers
SCM	:	Shrinking-Core Model
T_b	:	Bed temperature (K)
t	:	Time (s)
$\hat{t}$	:	Residence time (s)
U	:	Gas velocity (m/s)
U_2	:	Superficial gas velocity
U_t	:	Terminal velocity
V	:	Reactor volume (m^3)
x_c	:	carbon fraction
Z_i	:	Distance for the ith above the lower region (m)
Z_{i-1}	:	Distance for the (i-1)th above the lower region (m)
ε_i	:	Void fraction in ith interval (dimensionless)
ε^*	:	Axial voidage at saturated condition
μ	:	Gas velocity (kg/m s)
ρ	:	Gas density (kg/m^3)
ρ_B	:	Solid molar density (kmole/m^3)
τ	:	Complete conversion time (s)
Φ	:	Slip factor (dimensionless)

CHAPTER 1

INTRODUCTION

1.1 Importance and reason for research

Coal is one of the important available energy sources. Because of coal is plentiful and cheap. However its have high pollution. Despite its pollutant that its cost, the demand of coal probably rising in next decay. Many countries which have large reserves of coal have been putting a great deal of effort in the development of nonpolluting, higher economy, power-generating systems that utilize coal as fuel. Thailand is certainly one of the nations possessing coal resources in a significant amount. Substantial portion of coal in Thailand is lignite, which is low grade coal containing high sulfur.

Traditionally, the use of coal combustion to generate heat or electricity creates a number of environmental challenges. Varies technology were developed to overcome the problems associated with the use of coal. Circulating fluidized bed combustors (CFBC) are considered as an improvement over the traditional methods associated with coal combustion. The CFBC has several advantages over conventional coal combustion method, particularly its can be used high sulfur coal. Operation of CFBC at industrial levels has confirmed many advantages that include flexibility, high combustion efficiency, low NO_x emissions and high sulfur capture efficiency and the long residence time of the fuel in the furnace. Long residence time also contributes to inherently low emissions of carbon monoxide. The CFBC has high flexibility on input fuel. It can be use to burn a combination of coal and biomass, as known as co-combustion. Some typical biomass fuels in co-firing studies are cattle manure, sawdust, sewage sludge, wood chip and agricultural residues. The combustion of coal with biomass can reduce the levels of pollutants in flue gas and also reduce consumption of coal. Therefore, using biomass in combination with coal can improve the environmental performance.

Technical knowledge about design and operation of CFBC is widely available for pilot plant and large scale units. However, little has been done in the field of mathematical modeling and simulation of combustion in CFBC. This might be attributed

to the fact that the combustion process occurring in a CFBC involves a number of complex phenomena including chemical reactions, heat and mass transfers, particle size reduction due to combustion, attrition, fragmentation, and so on.

1.2 Research objectives

The objectives of our research are to study the effect of operating parameters on emission gas and carbon combustion efficiency of circulating fluidized bed combustor system.

1.3 Scope of research

Our research focuses on the simulation of co-combustion between coal and biomass in circulating fluidized bed combustion using ASPEN PLUS and the study of the effect of operating parameters including bed temperature and ratio of mixing fuel on combustion efficiency and pollution emissions. We optimize the carbon combustion efficiency.

1.4 Contribution of Research

This research provides information of optimum operating condition on combustion efficiency with acceptable pollution emissions in the circulating fluidized bed combustion. The result of this study can be use to improve the energy management system of co-combustion between coal and biomass in circulating fluidized bed combustor.

1.5 Procedure Plan

1. The first step, we investigate the circulating fluidized bed combustion systems.
2. Various literatures related to the operation of co-firing on circulating fluidized bed combustion and its development, are studied.

3. We study ASPEN PLUS program and the several ASPEN PLUS unit operation blocks that are used to simulate the circulating fluidized bed combustion.

4. Developed the circulating fluidized bed on operating parameter and study the operating parameter that affect to emission and combustion efficiency.

5. Analyze the effect of operating parameters on pollution emissions and combustion efficiency.

6. Optimize the CFBC in other obtain the highest combustion efficiency with acceptable pollution emissions.

7. Finally, we conclude our research and write thesis.

1.6 Thesis organization

This thesis is organized into 6 chapters. Relevant results and detailed analysis are documents in the appendixes.

Chapter 1 introduces this research with the general background, the problem statement, research objective and the scope of study. Chapter 2 covers the basics of fluidization, theory of circulating fluidized bed combustor, combustion of solid fuels and pollution from combustion in circulating fluidized bed combustor. Combustion model and hydrodynamic behavior model were presented in Chapter 3. Chapter 4 presents a delicate procedure in the circulating fluidized bed combustor simulation. Chapter 5 illustrates simulative results and discusses. Chapter 6 finalizes of validated with conclusion of validated for further study are proposed.

CHAPTER 2

THEORY

Fluidization has received increasing importance as a national objective in the area of energy development the past years in many countries. Because of fluidization system was respond requirement to industrial by to reduce cost and increase efficiency of process. The principal application of gas-solid fluidization is in the following industries:

- Energy conversion
- Petrochemical processing
- Mineral processing
- Chemical and pharmaceutical
- Physical processing

2.1   Principles of Fluidization

Basic technical term

Bed   A place where an action or reactions take place between distributors to surface of particles.

Elutriation   The lifting out of the small element in a mixture of solid particles by a stream of high speed gas.

Fluidization   The state of suspending particles in a rapidly moving stream of gas or vapor, the particles are close enough together and interact in such a manner that they give the impression of a boiling liquid.

Dense phase   Gas-solid suspension that is sufficiently concentrated that there are significant particle-particle interactions and inter-particle contacts.

Dilute phase   Suspension sufficiently sparse that there are relatively few inter-particle contacts.

Voidage   Fraction by volume of a fluid-solid suspension occupied by the fluid.

2.2   The Phenomenon of Fluidization

In Fluidized bed combustion the packed bed consists of solid materials confined in a vessel, usually cylindrical in shape. The force of gravity causes the solid materials to pack together inside the vessel. The relative position of the packed material remains constant without the application of additional forces. The packing material rests on a distributor which, as the name implies, is employed to keep up flowing fluids (gases or liquids) evenly distributed inside the packed bed, and which supports the gravitational weight of the packed materials.

With changes in gas velocity, the solids move from one state or regime to another. Each of flow regimes has distinct characteristics. *Table 2.1* presents a comparison of some characteristic features of different gas-solid processes used in various types of boilers. These regimes, arranged in order of increasing velocities, are:

- Packed bed of fixed bed
- Bubbling bed
- Turbulent bed
- Fast bed (circulating fluidized bed)
- Transport bed (pneumatic or entrained bed)

Fluid is passed upward through a bed of fine particles as shown in *Figure 2.1*. At a low flow rate, fluid merely percolates through the void spaces between stationary particles. This is a fixed bed. With increases in flow rate, particles move apart and a few are seen to vibrate and move about in restricted regions. This is the expanded bed. At a still higher velocity, a point is reached when the particles are all just suspended in the upward flowing gas or liquid. At this point the frictional force between a particle and fluid counterbalances the weight of the particle, the vertical component of the compressive force between adjacent particles disappears, and the pressure drop through any section of the bed about equals the weight of fluid and particles in that section. The bed is considered to be just fluidized and is referred to as an incipiently fluidized bed or a bed at minimum fluidization.

Table 2.1   Comparison of principal Gas-Solid Contacting Processes

Property	Packed Bed	Fluidized Bed	Fast Bed	Pneumatic Transport
Application in boilers	Stoker fired	Bubbling fluidized	Circulating fluidized	Pulverized coal fired
Mean particle diameter (mm)	<300	0.03-3	0.05-0.5	0.02-0.08
Gas velocity through combustion zone (m/s)	1.0-3.0	0.5-2.5	4.0-6.0	15-30
Typical U/Ut	0.01	0.3	2	40
Gas motion	Up	Up	Up	Up
Gas mixing	Near plug flow	Complex two phases	Dispersed plug flow	Near plug flow
Solids motion	Static	Up and down	Mostly up, some down	Up
Solid-solid mixing	Negligible	Usually near perfect	Near perfect	Small
Overall voidage	0.4-0.5	0.5-0.85	0.85-0.99	0.98-0.998
Temperature gradient	Large	Very small	Small	Maybe significant
Typical bed-to-surface. Heat transfer coefficient (W/m^{2}K)	50-150	200-550	100-200	50-100

Source: Modified from Grace, J.R., *Can. J. Chem.Eng.*,64, 353-363,1986.
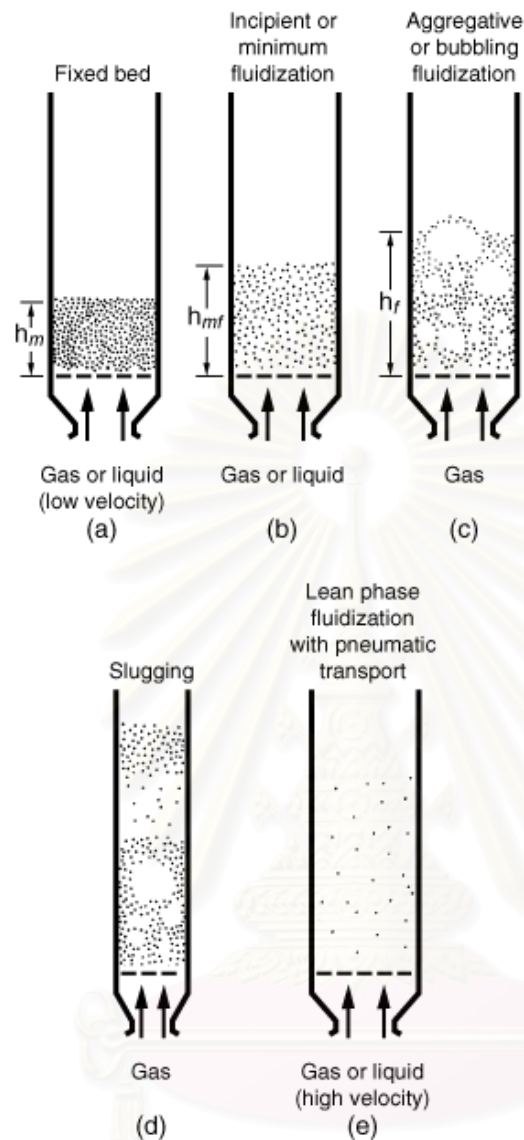
Figure 2.1 Various kinds of contacting of a batch of solids by fluid (Kunii and Levenspiel, 1991).

In gas-solid system, with an increase in flow rate beyond minimum fluidization, large instabilities with bubbling and channeling of gas are observed. At higher flow rates agitation becomes more violent and the movement of solids becomes more vigorous. In addition, the bed does not expand much beyond its volume at minimum fluidization. Such a bed is called an aggregative fluidized-bed, a heterogeneously fluidized-bed, a bubbling fluidized-bed, or simply a gas fluidized-bed, in a few rare cases liquid-solid systems will not fluidize smoothly and gas-solid systems will not bubble.

A fluidized-bed is considered to be dense-phase fluidized-bed as long as there is a fairly clearly defined upper limit or surface to the bed. However, at a sufficiently high fluid flow rate the terminal velocity of the solids is exceeded, the upper surface of the bed disappears, entrainment becomes appreciable, and solids are carried out of the bed with the fluid stream. In this state we have a disperse-, dilute-, or lean-phase fluidized-bed with pneumatic transport of solids. Consider briefly the quality of fluidization in a bubbling bed. Although the properties of solid and fluid alone will determine whether smooth or bubbling fluidization occurs, many factors influence the rate of solid mixing, the size of bubbles, and the extent of heterogeneity in the bed. These factors include bed geometry, gas flow rate, type of gas distributor, and vessel internal.

The slugging, a phenomenon strongly affected by the vessel geometry. Gas bubbles coalesce and grow as they rise, and in a deep enough bed may eventually become large enough to spread across the vessel. Thereafter the portion of the bed above the bubble is pushed upward, as by a piston. Particles rain down from the slug and it finally disintegrates. At about this time another slug forms and this unstable oscillatory motion is repeated. Slugging is usually undesirable since it increases the problems of entrainment and lowers the performance potential of the bed for both physical and chemical operations. Slugging is especially serious in long, narrow fluidized bed.

The creation of a special hydrodynamic condition, known as fast-bed is keys to the CFB process as it produces a high slip velocity between the gas and the solids shown in *Figure 2.2*. A unique combination of gas velocity, recirculation rate, solids characteristics, volume of solids, and geometry of the system gives rise to this special hydrodynamic condition.
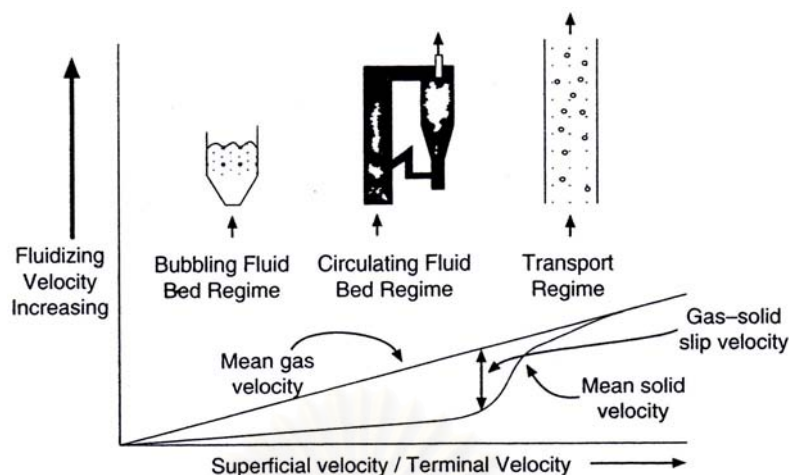
Figure 2.2 Motion of gas and solids resulting in a high slip velocity between particles.

2.3 Circulating fluidized bed

Nowadays, circulating fluidized bed (CFB) has found widespread applications in a variety of industrial processes. Some major applications for such systems are the fluid catalytic cracking (FCC), coal combustors and coal gasifiers. In the context of use in circulating fluidized bed combustor (CFBC), the fast fluidized bed may be defined as: A high velocity gas-solid suspension where particles, elutriated by the fluidizing gas above the terminal velocity of individual particles, are recovered and returned to the base of furnace at a rate sufficiently high to cause a degree of solid refluxing that will ensure a minimum level of temperature uniformity in the furnace.

A circulating fluidized bed combustor is shown schematically in *Figure 2.3*. The primary combustion air is injected through an air distributor or grate located at the furnace floor and the secondary air is injected from the sides at a certain height above the furnace floor. Fuel is fed into the lower region of the furnace, where it burns to generate heat. Limestone is fed into the bed in a similar manner. The fuel burns while it is mixed with the hot bed solids. Relatively coarse particles of sorbent and unburned char are captured in the gas-solid separator and recycled back near the base of the furnace. Finer solid residues (ash or spent sorbents) generated during combustion and desulfurization leave the furnace, escaping through the gas-solid separators, but are finally collected by a bag-house or electrostatic precipitator located further downstream.

2.3.1 Characteristics of circulating fluidized bed

As shown in *Figure 2.3*, the CFB is divided into two distinct coexisting regions, i.e., the lower dense region, which is located right above the distributor, and the upper region, which is located between the upper surface of the dense bed and the riser exit. The height of each region depends on the superficial gas velocity, solids mass flux and properties of solids and fluid. Upper region of the riser is assumed to be axially composed of three zones.

- The acceleration zone is at the bottom part of the upper region where the solids are accelerated to a constant upward velocity.
- The fully developed zone is located above the acceleration zone, where the flow characteristics are invariant with height.
- The deceleration zone is located above the fully developed zone, where the solids are decelerated depending on the exit geometry of the riser.

The circulating fluidized bed system has three compositions:

- Riser or furnace
- Gas-solid separator
- Down comer and return leg
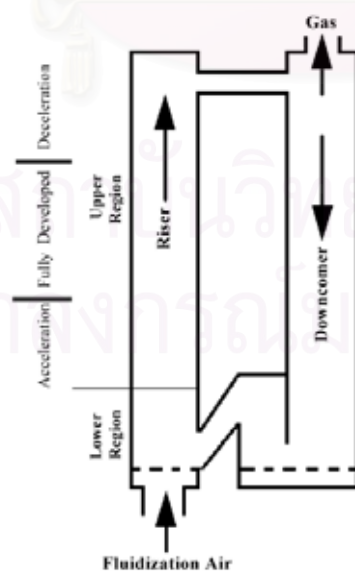
Figure 2.3   Schematic diagram of a circulating fluidized bed reactor.

The combustion process in a CFBC, whose furnace could be divided into three distinct zones from a combustion standpoint:

- Lower Zone (located below the secondary air level)
- Upper Zone (located above the secondary air level)
- Hot gas-solid separator

(i)   Lower Zone

The lower zone in the furnace is fluidized by primary combustion air, which constitutes about 40-80% of the stoichiometric quantity of air required for the coal feed. This section receives fresh coal from the coal feeder and unburned char from the hot cyclone. Char particles that are captured by the hot cyclone are returned to this section by means of a loop-seal or L-valve. Devolatilization and particle combustion occur in this zone, which is usually oxygen deficient. Therefore, to protect the boiler tubes from possible corrosion attack, this zone is refractory lined.

(ii)   Upper Zone

The secondary air is added at the interface between the lower and upper zones of the furnace. Sometimes, when staged combustion is not essential, as in the case of low-volatile coal, secondary air maybe added close to the grid.

In any case, the entire combustion air passes through the upper furnace. Char particles, transported to the upper zone, and are exposed to an oxygen-rich environment, where most of the combustion occurs. The upper zone is usually much taller than the lower zone. Char particles, transported upwards through the core, slide down the wall or through the core, often entrapped in falling solid clusters. The char particles could make many trips around the height of the furnace before they are finally entrained out through the top of the furnace.

(iii) Cyclone

Unburned char particles that are entrained out of the furnace go around the refractory-lined cyclone. The residence time of char particles within the cyclone is short and the oxygen concentration in it is low. Thus the total extent of combustion inside the cyclone is

expected to be small compared to that in the rest of the combustion loop. However, there could be exceptions.

2.3.2 Combustion of fuel in CFB furnaces

Fuel flexibility made circulating fluidized-bed (CFB) boilers a favorite choice especially in Asia and Eastern Europe. CFB boilers can burn even the worst grade of available fuels without any major performance penalty (Basu & Fraser, 1991). This fuel flexibility is attributed to a unique combustion and heat transfer environment offered by CFB furnaces. The riser of the CFB loop forms the furnace, where coal burns in a suspension of hot non-combustible granular solids. These solids are maintained in a fast-fluidized condition. Feeders drop the coal (crushed below 6-10 mm size) into the furnace from the side. Intense mixing in the CFB furnace helps the fresh coal particles mix immediately with the hot bed solids, which outnumber the coal particles by 98 to 2, or more. Thus, irrespective of the physical state or heat content of the fresh coal, the bed solids easily raise the coal particles above their ignition temperature without any significant drop in their own temperature. The ignited coal particles then begin to transfer back their combustion heat to the bed solids at the same high rate. A coal particle introduced into a combustion system passes through various stages as illustrated in *Figure 2.4*. A fuel particle fed into the bed undergoes the following sequence of events:

- Heating and drying,
- Devolatilization and volatile combustion,
- Swelling and fragmentation (for some types of coal),
- Combustion of char.
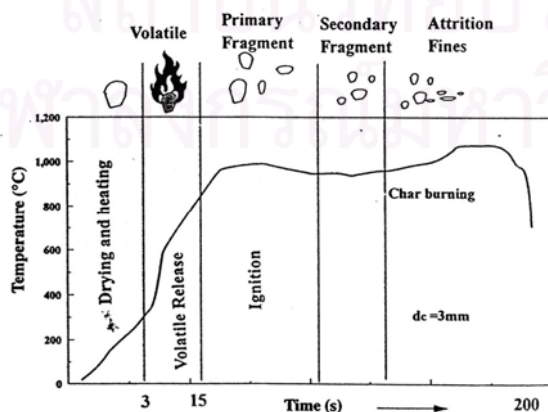
Figure 2.4 Stages of combustion of a coal particle (adapted from Howard, 1989).

2.3.2.1   Heating and Drying

Drying is essentially a process of simultaneous heat and mass transfer. Heat, necessary for evaporation, is supplied to the particles of material and moisture vapors are removed from the material into the drying medium. The combustible material generally constitutes around 0.5-5.0% by weight of the total solids in CFB combustor. The remaining solids, known as bed materials, fuel ash, sorbents or some other noncombustible solids; and they constitute 95-99.5% of the bed. Thus, when a fresh fuel particle is fed into a CFBC, it is immediately engulfed by a large body of noncombustible hot solids. These particles preheat the cold particle close to the bed temperature.

2.3.2.2   Devolatilization and volatile combustion

Devolatilization (or pyrolysis) is the process of release of a wide range of gaseous products of decomposition of fuel. The volatile matter comprises a number of hydrocarbons, which are releases in steps. The first steady release usually occurs at around 500-600 degree Celsius, and the second release occurs at around 800-1000 degree Celsius. Although the proximate analysis provides an estimate of the volatile matter, the actual yield of volatile matter and its composition may be affected by a number of factors. These include the rate of heating, the initial and final temperature, and the exposure time at the final temperature, the particle size, the type of coal, and the pressure.

2.3.2.3   Swelling and fragmentation

A large particle decreases in size through combustion and through a number of other communition processes, including fragmentation and attrition. The particle surface is, therefore, minimum at the onset of devolatilization, but gases released from the interior of the fuel particle cause it to swell. The volatile gases released inside non-porous fuel particles exert a high internal pressure that sometimes breaks the fuel into fragments. This phenomenon is called primary fragmentation. Here, a fuel particle is broken into several pieces that are smaller than the parent particle. The period time of char burns, the internal pores of the char increase, thus weakening the bridge connecting carbon piece inside the char. Once the bridge is too weak to withstand the hydrodynamic force on the char, it breaks loose a fragment. This process is called secondary fragmentation.

2.3.2.4 Combustion of char

The combustion of char generally starts after the evolution of volatile combustion. During the combustion of char particle, oxygen from the bulk stream of the furnace air is transported to the surface of the particle. The oxygen enters into an oxidation reaction with the carbon on the char surface to produce CO_2 and CO. The char, being a highly porous substance, has a large number of internal pores of varying sizes and tortuosity. Oxygen, under favorable conditions, diffuses into the pores and oxidizes the carbon on the inner walls of the pores. After the combustion of char, ash is the residual product, which takes no part in the combustion reaction. The combustion processes are similar in circulating, turbulent or bubbling fluidized beds, but the burning rates of char are different in these beds. The burning rate of char in turbulent fluidized beds is higher than that in bubbling fluidized beds due to higher mass transfer rate in the turbulent bed (Basu & Subbarao, 1986).

Reaction Product

The products of combustion on the carbon surface could be both carbon monoxide and carbon dioxide, according to the following equations:

$$C + O_2 \rightarrow CO_2$$
$$C + \frac{1}{2}O_2 \rightarrow CO$$
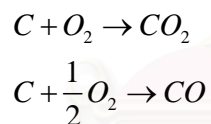
Regimes of Combustion

The combustion of char may occur inside its pores or on its external surface depending on the regime under which it is combustion. There are three regimes of combustion, depending upon the combustor operating condition, as well as on the char particle characteristics (Basu, 1999).

Regime I

The chemical kinetic rate is much slower than the diffusion rate. This regime would occur on the exterior surface of coarse nonporous particles at temperatures around $900^{\circ}C$. In porous coarse particles, it would not occur until the temperature is lower than

$600^{\circ}C$. For fine porous particles occur at $800^{\circ}C$. In porous chars, oxygen diffuses into the char and combustion occurs uniformly throughout the char. As a result, the density of the particle, rather than its diameter, decreases with combustion.

Regime II

The reaction rate and pore diffusion rate are comparable with each other. Thus there is limited penetration of oxygen into the char. Pores near the external surface consume most of the oxygen. This condition of combustion occurs for medium size char where mass transfer to the pores is comparable to the reaction rate, as in bubbling fluidized beds and also in some parts of the CFB.

Regime III

This condition occurs when the mass transfer rate is very slow compared to the kinetic rate. The kinetic rate is so fast that the limited amount of oxygen reaching the external surface of the char through the relatively slow mass transfer process is entirely consumed before it has a chance to enter the pores. This type of combustion is sometimes called diffusion controlled combustion. It occurs in large particles and where the mass transfer is small compared to the reaction rate.

2.3.3 Factors affecting combustion efficiency

The combustion efficiency of bubbling fluidized bed (BFB) combustor is typically up to 90% without fly-ash recirculation and could increase to 98-99% with recirculation (Oka, 2004). The efficiency of a circulating fluidized bed (CFB) combustor is generally higher due to its tall furnace and large internal solid recirculation. The efficiency depends to a great extent on the physical and chemical characteristics of the fuel as well as on the operating condition of the furnace. The following section discusses different factors that could influence the combustion efficiency. Factors affecting the combustion efficiency can be classified into three categories:

- Fuel characteristics (feed stock, fuel ratio, attrition, intrinsic reactivity, volatile matter and devolatilization, fuel particle size)

- Operational parameters (fluidizing velocity, excess air, combustion temperature)

- Design parameters (bed height, freeboard height, recirculation of unburnt solids, fuel feeding, secondary sir injection)

2.3.4 Combustion generated pollutants

The major gaseous effluents that affect the ecosystem are sulfur dioxide, nitrogen oxide, and the greenhouse gases. The combustion of fossil fuels is stationary and transportation systems are the main source of air pollution. In an environmentally conscious society, it is desirable, if not essential, to minimize the emission of the above pollution-causing gases from circulating fluidized bed combustor. In this present discusses the impact of two pollutants, i.e., SO_2 and NO_x.

2.3.4.1 Sulfur dioxide emission

Formation of sulfur dioxide

When fuel burns, the sulfur is oxidized primarily to sulfur dioxide.

$$S + O_2 \rightarrow SO_2$$
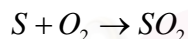
The rest of the sulfur dioxide escapes into the atmosphere. Part of the sulfur dioxide maybe converted into sulfur trioxide.

$$SO_2 + \frac{1}{2}O_2 \rightarrow SO_3$$
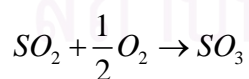
The formation of sulfur trioxide depends on gas residence time, temperature, excess air, and the presence of catalytic surfaces in the furnace. The formation of sulfur trioxide is favored by high temperature and pressure. Since the reaction is slow, only a small part of the sulfur dioxide has time to convert into sulfur trioxide (Burdett et al., 1983).

Retention of SO₂

One of the principal incentives for fluid bed combustion is the ability to capture sulfur dioxide in situ using low cost sorbents, limestones $(CaCO_3)$ and dolomites $(CaCO_3 \square MgCO_3)$, which are fed as solids to the combustion chamber. The first step is calcination; the limestone is decomposed into *CaO* and *CO₂* through an endothermic reaction according to:

$$CaCO_3 \rightarrow CaO + CO_2$$
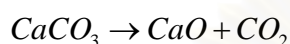
The second step in sulfur dioxide capture with limestone during fluidized bed combustion is sulfation, where the calcium oxide absorbs sulfur dioxide, forming calcium sulfate. Calcium sulfate is a relatively inert and stable solid that is disposed of easily. The overall reaction is as follows:

$$CaO + SO_2 + \frac{1}{2}O_2 \rightarrow CaSO_4$$
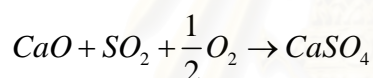
The direct reaction of calcium carbonate with sulfur dioxide at fluidized bed temperatures (800-900°C) is so slow that the sulfur dioxide absorbed through direct reaction with calcium carbonate is insignificant. Second reaction has to take place through the decomposition (calcination) of CaCO₃ to calcium dioxide (first reaction). The carbon dioxide released during the calcination creates and enlarges many pores in the limestone. Absorption of sulfur dioxide by sorbents is presented in *Figure 2.5*.
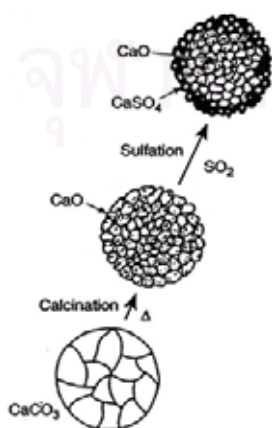
Figure 2.5 Illustration of formation of an impervious sulfate shell in sulfur capture (Shearer *et al.,* 1980).

2.3.4.2 Nitrogen oxide emission

Nitrogen oxides are some of the major air pollutions emitted by coal combustion. The symbol NO_x represents nitric oxide (NO), nitrogen dioxide (NO_2) and nitrous oxide (N_2O). Although the nitrogen of the combustion air does not oxidize to a significant extent at the low operating temperature 800-900°C of a CFB furnace, the fuel nitrogen does. Staged combustion remains an attractive method for reducing NOx emissions in various combustion systems. For staged combustion in a CFBC, the air used for the combustion is divided into two or more streams: the first one is supplied through the bottom air distributor and secondary air streams are injected in the upper region of the riser. NO_x formations in combustion processes result from a combustion of a thermal generation process and fuel nitrogen oxidation. At very high temperatures, thermal generation of NO_x from the air nitrogen becomes very important to emphasize the complexity involved in NO_x chemistry within the CFBC because of many catalytic reactions involving, for example, char, and ash and sorbents particles. Thermal generation. Three main reactions are used to represent this process in the model:

$$\frac{1}{2}N_2 + \frac{1}{2}O_2 \rightarrow NO$$

$$\frac{1}{2}N_2 + O_2 \rightarrow NO_2$$

$$N_2 + \frac{1}{2}O_2 \rightarrow N_2O$$
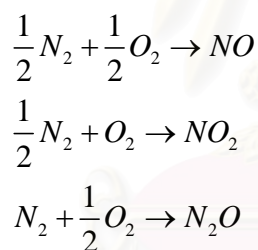
2.4 Advantages and Disadvantages of circulating fluidized bed system

Advantages

Wide applicability of fuel

- Suitable for burning mixtures of various fuels
- High adaptability to fuel property fluctuations
- High fuel drying ability

High combustion efficiency

- High thermal efficiency
- Low excess air combustion

Combustion with low environmental load

- Low SO_x combustion
- Low NO_x combustion

High equipment economics

- Reduces the initial investment
- Suited for distributed medium-scale power generation

Disadvantages

- Increased overall reactor height
- Added complexity in designing and operating recirculation loop
- Decreased suspension-to-wall heat transfer coefficients for given particles
- Somewhat more restricted range of particle properties

2.5 Biomass

About 12% of the world's energy comes from the use of biomass fuels, which include items as diverse as residential yard waste, manure, agricultural residues, and dedicated energy crops. In industrialized nations, bioenergy facilities typically use biomass fuels in large industrial cogeneration applications (pulp and paper production, sugar cane milling, etc.). Conversely, developing nations largely rely on biomass for rural cook stoves or small industries. Such applications are relatively inefficient and dirty. Increasing industrialization and household income are driving the economies of developing nations to implement cleaner and more efficient biomass technologies.

Environmental concerns may help make biomass an economically competitive fuel. Because biomass fuels are generally less dense, lower in energy content, and more difficult to handle than fossil fuels, they usually do not compare favorably to fossil fuels on an economic basis. However, biomass fuels have several important environmental advantages. Biomass fuels are renewable, and sustainable use is greenhouse gas neutral (biomass combustion releases no more carbon dioxide than absorbed during the plant's growth). Biomass fuels contain little sulfur compared to coal (reduced sulfur dioxide

emissions) and have lower combustion temperatures (reduced nitrogen oxide emissions). However, unless biomass is efficiently and cleanly converted to a secondary energy form, the environmental benefits are only partially realized, if at all. For this reason, efficient, modern biomass utilization must be favored over traditional applications.

The use of biomass as an energy source is widely practiced throughout Thailand industries, particularly in rural and agricultural areas. Major industrial users of biomass energy include sugar cane milling, rice milling, palm oil production, and the wood products industry.

2.5.1 Type of biomass

Rice Husk

Properties - small (less than 5mms long and 2mms thick), yellow, 15 per cent of moisture

Sources - rice mills

Utilizations - fuel, soil preparation before cultivation, chickens' litter

Strengths - low moisture, small size, suitable for using as fuel. Husk ash can sell

Weaknesses - 16-18 per cent of ash after incineration and transportation arguably may not be worth the expense due to its light weight (1 m^3 = 123 kg)

Table 2.2 Characteristics of rice husk

Source industry	Rice mills, ~40,500 mills in country
Source of biomass	Rice paddy
Source output, tonne/yr	25,000,000
Supply forecast	Slightly increase, 1 to 2 percent per year
Biomass production rate, percent of source	21
In process use, percent of source	negligible
Total biomass supply, percent of source	21
Biomass collectivity, tonne/yr	50-80
Total biomass avilability, tonne/yr	5,250,000
Higher heating value, kJ/kg	14,755
Fuel consumption, tonne/yr/MW	9,600
Aggregate power generation potential, MW	234-375
Price, Bath/tonne	50-100
Other uses	Soil conditioner, fuel, brick making

Source : www.dedp.go.th

Wood residues

Properties - Para wood trees' lifetime is 20-25 years and they need to be cut for recultivation. Divided into three parts: 1. Roots or stumps, 2. Stems, less than 3 inches in diameter, 3. Logs, 4 inches in diameter, to be cut to 1.05m length for sawmills and furniture factories, and of which to get the outside stabs, sawdust and wood shavings as wastes

Sources - Outside stabs cut from logs and sawdust are available at sawmills, wood shavings at furniture factories, roots and stems at the plantations

Utilizations - Sawdust can be used in mushroom plant nursery, to make incense and burn charcoals. Other wood wastes will be used in rubber curing, burning charcoals, making plywood, medium density boards and chipboards, and using as construction materials such as pilings, palates and wooden cases

Strengths - Root and branches not yet to be used to best potential

Weaknesses - big size and fresh wood wastes contain 50 per cent of moisture that is too high for combustion and therefore need the drying and chipping process before use.

Table 2.3   Characteristics of wood residues

Source industry	Sawmills, production plants
Source of biomass	Saw logs, parawood trees, processed wood
Source output, tonne/yr	250,000
Supply forecast	Fluctuating
Biomass production rate, percent of source	55
In process use, percent of source	negligible
Total biomass supply, percent of source	55
Biomass collectivity, tonne/yr	60
Total biomass availability, tonne/yr	1,800,000
Higher heating value, kJ/kg	10,365
Fuel consumption, tonne/yr/MW	19,700
Aggregate power generation potential, MW	118
Price, Bath/tonne	50-100
Other uses	Fuel, particle board, charcoal

Source : www.dedp.go.th

Bagasse

Properties - long, lean, cut and left in the farms during December-April, mostly await for open burning

Sources - sugar cane fields

Utilizations - tops can be made animals' food

Strengths - Leafs and tops are yet to be used to best potential

Weaknesses - Available only during December-April, hard to collect and machinery required

Table 2.4   Characteristics of bagasse

Source industry	Sugar mills
Source of biomass	Sugar mills
Source output, tonne/yr	50,000,000
Supply forecast	Stable
Biomass production rate, percent of source	28-30
In process use, percent of source	23
Total biomass supply, percent of source	5-7
Biomass collectivity, tonne/yr	90-100
Total biomass avilability, tonne/yr	14,000,000
Higher heating value, kJ/kg	9,243
Fuel consumption, tonne/yr/MW	17,600
Aggregate power generation potential, MW	160-248 (existing excess bagasse only)
Price, Bath/tonne	0-150
Other uses	Production of medium density fiber board, fuel

Source : www.dedp.go.th

2.5.2 Biomass Beneficiaries

- Growth of community economics. Biomass power plants help develop local extensive industries, increase employment in the area and the communities will gain extra income from the locality tax.

- Additional income for farmers. Besides the agricultural produce, they now can make money from the wastes.

- An alternative power generation which is friendly to the environment.

- Stability of the country's grid power system due to the sustainable supply from nationwide small power plants. No more power shortage in the far-end grids.

2.6 Literature Review

Circulating fluidized bed combustors (CFBCs) are considered as an improvement over the traditional methods associated with coal combustion. The CFBC has several advantages over conventional coal combustion method, particularly its can be used high sulfur coal. Operation of CFBCs at industrial levels has confirmed many advantages that include flexibility, high combustion efficiency, low NOx emissions and high sulfur capture

efficiency (Huilin, 1999). The flexibility of fuel, CFBC can be burn with the co-combustion. The different authors have proposed to study the co-combustion in a circulating fluidized bed such as Aysel and Topal (2004) study the co-combustion of olive cake with lignite coal in a CFB and Gayan (2004) study the co-combustion of coal and pine bark in CFBC. The benefits of co-firing to the electricity generation community are obvious: a low-cost–low-risk renewable energy, reduced airborne emissions, diversified fuel sources, generation of power that meets most renewable portfolio standards and that can and should be considered as green power (Aemesto and Bahillo, 2002). Renewable natural energy includes biomass, solar energy (photovoltaic power generation and solar thermal electric power generation), geothermal energy, wind energy, wave energy, tidal energy, ocean thermal energy, hydraulic energy (Yamamoto,2001). The most of fuel that is used co-combustion with coal are biomass. Biomass, as an important source of renewable energy, has been used to a great extent by several industrial countries. Biomass is one of the most promising sources of renewable energy. There are several works dealing with the effect of biomass addition on the gas emissions (Leckner and Karlsson, 1993). Dayton et al. (1999) investigated the interactions between biomass feedstock and coal to address the issues of gaseous emissions when co-combusting these fuels. They concluded that the levels of pollutants decreased with increasing the amount of biomass fuel added.

The most of work to study and develop the performance of circulating fluidized bed combustor. Armesto (2003),Gayan (2004) study the effect of different parameters such as furnace temperature, share of mixture and excess air ratio) on the emissions and combustion efficiency. Aysel (2003) study the result of combustion between only coal and olive cake combustion with coal. The combustion efficiency increase the excess air ratio and furnace temperature increase. And the emission decrease when the share of biomass in the mixture increases. So, biomass is renewable energy that can be burn mix with coal, reduce emission to the air and conserve fossil fuel resources.

Technical knowledge about design and operation of CFBC is widely available for pilot plant and large scale units. However, little has been done in the field of mathematical modeling and simulation of combustion in CFBCs. This might be attributed to the fact that the combustion process occurring in a CFBC involves complex   phenomena including chemical reactions, heat and mass transfer, particle size reduction due to combustion, attrition, fragmentation and other mechanisms, gas and solid flow structure, etc (Sotudeh-gharebaagh, 1998). Gharebaagh R.S. *et al.* (1998) presents the details of the modeling

approaches taken to obtain a process simulation program for coal combustion in a CFBC. A model was developed for the combustion of coal in a circulating fluidized bed using the ASPEN PLUS simulator. Wang and Luo (1997) developed a mathematical model for describe physical and chemical process. Basu et al. (1987) developed a CFBC model in which a plug flow regime for both the gas and solids is assumed. Lee and Hypanen (1989) presented a CFBC model which considers the riser as a plug flow reactor for the gas phase and a CSTR reactor for the solid phase. The model also considers the feed particle size distribution and the attrition phenomena. Using a lumped-modeling approach, Arena *et al.* (1991) introduced the means for predictive calculation by dividing the CFBC riser into four blocks, each corresponding to a separate reactor. Three of these blocks related to the CFBC riser. The hydrodynamic parameters were considered uniform within each section and were used in various kinetic models to predict char conversion. Chen and Xiaolong (2006) presented a modeling method for a large scale CFB boiler for simulate the axial distribution of solid and gas particles in the bed and uses core-annulus construction to describe the radial distributions of solid particles. Adanez (2001) simulate and optimize the behavior of a CFB reactor, and study the effect of operating conditions such as temperature, excess air, air velocity, Ca/S molar on carbon combustion efficiency and sulfur retention. Moreover, Todd (1996) predict hydrodynamic model for circulating fluidized bed risers. The results show that the model is capable of predicting the complete performance of CFB boiler.

Circulating fluidized bed combustion for optimize the operating conditions to achieve the highest boiler combustion efficiency. Zhou Hao. (2003) optimize pulverized coal combustion performance based on artificial neural network (ANN) and genetic algorithms (GA) is suggested for modeling the carbon burnout behavior in a tangentially fired utility boiler and optimizing the operating conditions to achieve the highest boiler heat efficiency consecutively. A genetic algorithm is employed to perform a search to determine the optimum solution of the neural network model, identifying appropriate set point for the current operating conditions.

In this research, study the effect of operating parameters on emission and combustion efficiency in order to the co-combustion on circulating fluidized bed complete and available. To optimize the carbon combustion efficiency so that the maximize combustion efficiency.

CHAPTER 3

MODELLING

3.1 Mechanism of combustion

A char particle may take 1-10 s (depending upon the riser height) to pass through the furnace once. However, as the particle is likely to make many trips around the CFB loop, the total residence time could be as much as 10,000 s (Stenseng et al., 1997), depending on the solid inventory, feed rate, coal size, etc. The total residence time of a char particle in the riser should exceed its burn out time. If that does not happen, the residual part of the char leaves the furnace unburnt. Thus an adequate description of the burning of char particles in the CFB furnace is important. The combustion of char, in its simplest form, has three major steps that were considered in the model (Soutdeh-Gharebaagh et.al., 1998).

$$C + \frac{1}{2}O_2 \rightarrow CO$$
$$CO + \frac{1}{2}O_2 \rightarrow CO_2$$
$$C + CO_2 \rightarrow 2CO$$
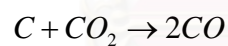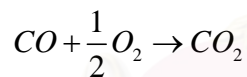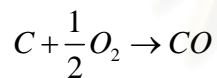
The first and third reactions are heterogeneous reaction and the second reaction is homogeneous reaction. Temperatures that use to simulate in this model are 750-900°C. Since the temperature of the burning fuel in the CFBC is not sufficiently high, the effect of the third reaction on the combustion rate is low (LaNauze R.D., 1985), and this reaction is neglected in the model. For the remaining two reactions, the reaction rate expressions must be developed.

Combustion rate

For the first reaction is a gas-solid reaction. The following expression for the char combustion rate, to form *CO,* per one particle (Selcuk *et.al.*,1997).

$$r_{char} = 4\pi r^2 k_r C_{o_2} \tag{3.1}$$

where, r is mean particle radius, k_r is the kinetic rate constant, is generally given by an Arrhenius relation and C_{o_2} is oxygen concentration. The frequency factor and the activation energy vary with the origin of the fuel from which the char is formed. For example, the kinetic rate constant k_r for a lignite coal burning in a fast fluidized bed was measured as (Adanez J., 1992).

$$k_r = k_0 T_b \exp\left(\frac{-E_a}{RT_b}\right) \tag{3.2}$$

where k_0 =   frequency factor for lignite (m/K.s)

            T_b =   bed temperature (K)

            E_a =   activation energy (J/kmol)

            R =   gas constant (8.314 kJ/kmol .K)

The kinetic rate constant k_r for a biomass burning was measured as (Gaur and Reed, 1998).

$$k_r = k_0 \exp\left(\frac{-E_a}{RT_b}\right) \tag{3.3}$$

where k_0 =   frequency factor for biomass (m/s)

Because of, particles shrink in size during reaction. The following equation is used to calculate the mean particle radius based on the particle size distribution (Grace *et.al.*, 1997)

$$r_c = \frac{1}{\sum \dfrac{P_k(r_c(k))}{r_c(k)}}$$

(3.4)

where r_c is mean particle radius, $r_c(k)$ is particle radius vector, and P_k is weight fraction vector of fuel.

For the second reaction, carbon monoxide produced during the heterogeneous combustion of char reacts with oxygen in the homogeneous gas phase reaction to form CO_2. Factor contributing to CO emission levels are the bed temperature, CO, O2and H2O concentration. The following expression is used for the CO combustion rate in the model (Robinson, W.D., 1986).

$$r_{CO,i} = 1.18*10^{13} f_{CO} f_{O_2}^{0.5} f_{H_2O}^{0.5} \left(\frac{P}{R_1 T_b} \right) \exp\left(-\frac{25000}{RT_b} \right) C\varepsilon_i$$

(3.5)

where, f is the mole fraction of CO, O_2 and H_2O, P is bed pressure, T_b is bed temperature, R_1 and R is universal gas constant, C is combustion gas concentration and ε_i is void fraction.

Fluid-Particle Reaction

Heterogeneous reactions in which a gas or liquid contacts a solid, reacts with it, and transforms it into product. Such reactions may be represented by

A(fluid) + bB(solid) $\longrightarrow$ fluid products

$\longrightarrow$ solid products

$\longrightarrow$ fluid and solid products
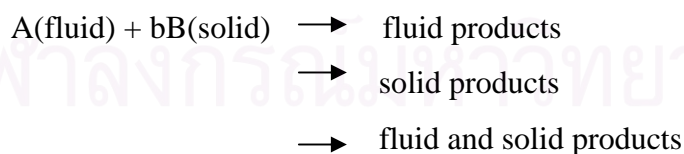
For the noncatalytic reaction of particles with surrounding fluid, there are two simple models, the progressive-conversion model and the shrinking core model.

- Progressive-Conversion Model (PCM). The reactant gas enters and reacts throughout the particle at all times, most likely at different rates at different locations

within the particle. Thus, solid reactant is converted continuously and progressively throughout the particle.

- Shrinking-Core Model (SCM). The reaction occurs first at the outer skin of the particle. The zone of reaction then moves into the solid, leaving behind completely converted material and inert solid, refer to these as ash. Thus, at any time there exists an unreacted core of material which shrinks in size during reaction.

In the first reaction is a gas-solid reaction and during reaction, the particle size shrinks to finally disappearing. So, the shrinking particle model (Levenspiel, 1999) is more applicable here. Both mass transfer of oxygen and the chemical reaction rate of combustion govern this rate. For a reaction of this kind, there are three steps occurring in succession: (a) the diffusion of reactant through the gas film around the char particle to surface of solid, (b) reaction on the surface between reactant (gas or liquid) and solid, and (c) the diffusion of reactant products from the surface of the solid through the gas film back into the main body of gas. In this case, the ash layer is absent and does not contribute any resistance. Also, effect of the resistances must be considered: diffusion through gas film controls and chemical reaction controls.

Gas Film Diffusion Controls

Film resistance at the surface of a particle is dependent on numerous factors, such as the relative velocity between particle and fluid, size of particle, and fluid properties. These have been correlated for various ways of contacting fluid with solid, such as packed beds, fluidized beds, and solids in free fall. For a single sphere of diameter moving with relative velocity through a fluid, the mass transfer coefficient at the surface is given by (Froessling, 1938):

$$Sh = 2 + 0.6 \, \text{Re}^{1/2} \, Sc^{1/3} \tag{3.6}$$

The Sherwood, Reynolds, and Schmidt numbers are used in forced convection mass transfer correlations.

Sherwood number
$$Sh = \frac{k_c d_p}{D_A} \qquad (3.7)$$

Schmidt number
$$Sc = \frac{\mu}{\rho D_A} \qquad (3.8)$$

Reynolds number
$$Re = \frac{\rho d_p U}{\mu} \qquad (3.9)$$

Replace in equation (3.5),

$$\frac{2Rk_c}{D_A} = 2 + 0.6 \left(\frac{2R\rho U}{\mu} \right)^{1/2} \left(\frac{\mu}{\rho D_A} \right)^{1/3} \qquad (3.10)$$

Rearrange equation (3.9) to estimate k_c

$$k_c = \frac{D_A}{R} + 0.3 D_A \frac{\left(\frac{2\rho U}{\mu} \right)^{1/2} \left(\frac{\mu}{\rho D_A} \right)^{1/3}}{R^{1/2}} \qquad (3.11)$$

$$k_c = \frac{K_1}{R} + \frac{K_2}{R^{1/2}} \qquad (3.12)$$

by $\qquad K_1 = D_A \qquad$ and $\qquad K_2 = 0.3 D_A \left(\frac{2\rho U}{\mu} \right)^{1/2} \left(\frac{\mu}{\rho D_A} \right)^{1/3}$

where k_c is mass transfer coefficient of reactant A, D_A is diffusion coefficient of reactant A, ρ is gas density, μ is gas viscosity, U is gas velocity and R is radius of particle.

During reaction a particle change in size; hence k_c also varies. So, size of particle was considered to calculate mass transfer coefficient. For small particles, particle has radius less than 5 mm or equal 5 mm. For large particle, particle has radius more than

5 mm (Kunii, Daizo, 1999). In general k_c rises for an increase in gas velocity and for smaller particles.

$$k_c \propto \frac{1}{2R} \qquad \text{For small } R \text{ and } u \qquad (3.13)$$

$$k_c \propto \frac{u^{1/2}}{(2R)^{1/2}} \qquad \text{For large } R \text{ and } u \qquad (3.14)$$

The time for complete conversion of a particle is τ. Then by taking radius of particle is zero. The time for complete can be calculated using the following equations (Levenspiel, 1999):

Small particles $$\tau = \frac{\rho_B R_0^2}{2bC_{Ag}K_1} \qquad (3.15)$$

Large particles $$\tau = \frac{\rho_B R^{3/2}}{3bC_{Ag}K_2} \qquad (3.16)$$

The residual radius of particle after the combustion can be calculated using the following equations:

Small particles $$r_c = \sqrt[3]{R^3 - \frac{2bC_{Ag}D_A R \hat{t}}{\rho_B}} \qquad (3.17)$$

Large particles $$r_c = \sqrt[3]{R^3 - \frac{0.9 \hat{t} b C_{Ag} D_A R^{3/2} \left(\frac{2U\rho}{\mu}\right)^{1/2} \left(\frac{\mu}{\rho D_A}\right)^{1/3}}{\rho_B}} \qquad (3.18)$$

The mean residence time for mixed flow in the reactor is:

$$\hat{t} = \frac{V(1-\varepsilon)}{F} \tag{3.19}$$

where V is reactor volume, F is volumetric flow rate of solid and ε is void fraction

Chemical Reaction Controls

Chemical reaction control when the chemical kinetic rate is slower than the diffusion rate. The reaction occurs on the surface of solid between reactant and solid. The rate is proportional to the available surface of unreacted core.

The time for complete can be calculated using the following equations (Levenspiel, 1999):

$$\tau = \frac{\rho_B R}{b k_1 C_{Ag}} \tag{3.20}$$

$$k_1 = k_0 \exp\left(-\frac{E_a}{R_g T}\right) \tag{3.21}$$

where k_1 is first order reaction rate constant base on unit surface, k_0 is frequency factor, E_a is activation energy, R_g is universal gas constant and T is bed temperature.

The residual radius of particle after the combustion can be calculated using the following equations:

$$r_c = R - \frac{\hat{t} b k_1 C_{Ag}}{\rho_B} \tag{3.22}$$

The unconverted fraction of the reactant was given by the following equation (Levenspiel, 1999). Often the feed consists of particles of different sizes; hence the overall mean of B unconverted in all these sizes is

$$\begin{pmatrix} \text{mean value for} \\ \text{fraction of B} \\ \text{unconverted} \end{pmatrix} = \sum_{\text{all sizes}} \begin{pmatrix} \text{fraction unconverted} \\ \text{in particles of size } R_i \end{pmatrix} \begin{pmatrix} \text{fraction of exit or} \\ \text{entering stream consisting} \\ \text{of particles of size } R_i \end{pmatrix}$$

or in symbols

$$1 - \overline{\overline{X}}_B = \sum_{R=0}^{R_m} \left[1 - X_B(R_i) \right] \frac{F(R_i)}{F} \tag{3.23}$$

For film diffusion control

$$1 - \overline{\overline{X}}_B = \sum_{}^{R_m} \left\{ \frac{1}{2!} \frac{\tau(R_i)}{\bar{t}} - \frac{1}{3!} \left[\frac{\tau(R_i)}{\bar{t}} \right]^2 + \dots \right\} \frac{F(R_i)}{F} \tag{3.24}$$

For chemical reaction control

$$1 - \overline{\overline{X}}_B = \sum_{}^{R_m} \left\{ \frac{1}{4} \frac{\tau(R_i)}{\bar{t}} - \frac{1}{20} \left[\frac{\tau(R_i)}{\bar{t}} \right]^2 + \dots \right\} \frac{F(R_i)}{F} \tag{3.25}$$

where $\tau(R_i)$ is the time for complete reaction of particles of size R_i

Carbon combustion efficiency

The carbon combustion efficiency was calculated considering the carbon feed inlet and the carbon losses in the different solid streams (flue gas, fly ash and bottom stream).

$$\% E_c = \left(\frac{\text{Total rate of carbon losses}}{\text{Total rate of carbon in the feed stream}} \right) * 100$$

or

$$\%E_c = \frac{F_A x_{cA} - (F_{fg} x_{c,fg} + F_{fa} x_{c,fa} + F_{bt} x_{c,bt})}{F_A x_{cA}} \times 100 \qquad (3.26)$$

Where F_A is fuel flow rate in the feed (kg/s), F_{fg} is flow rate of flue gas, F_{fa} is flow rate of fly ash, F_{bt} is flow rate of bottom ash, x_c is carbon fraction.

3.2 Hydrodynamic model

The hydrodynamic characteristics of the CFB, the CFB is divided into two distinct coexisting regions, i.e., the dense lower region with a constant suspension density, which is located above the distributor, and the dilute upper region with a decaying suspension density with height, which is located between the upper surface of the dense bed and the riser exit. The height of each region depends on the superficial gas velocity, solids mass flux and properties of solids and fluid. Upper region of the riser of the riser is assumed to be axially composed of three zones (Sabbaghan *et.al.*, 2004) as shown in Figure 2.3

1. The acceleration zone is at the bottom part of the upper region where the solids are accelerated to a constant upward velocity.
2. The fully developed zone is located above the acceleration zone, where the flow characteristics are invariant with height.
3. The deceleration zone is located above the fully developed zone, where the solids are decelerated depending on the exit geometry of the riser.

Details related to the gas-solid structures chosen to represent two regions of the riser are:

3.2.1 Lower region of the CFBC

The lower region is fluidized by the primary air supply. The mean voidage of the dense region is considered constant and may be obtained using the correlation proposed by Kunii and Levenspiel (1991) as shown in Figure 3.1.
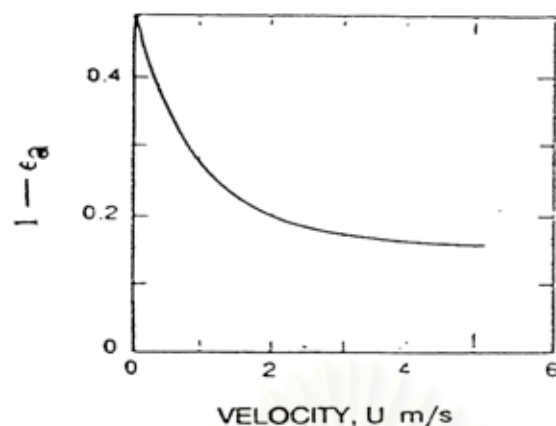
Figure 3.1 Mean void of the dense bed as a function of superficial gas velocities.

3.2.2 Upper region of the CFBC

The upper region is suspended both by the combustion gases from the lower region and the secondary air supply which determines the boundary between the two regions. Hydrodynamic model, as proposed in most CFBC literature regarding the upper region, are classified into three broad groups (Berruti *et.al.*, 1995): (1) those predicting the axial profile of the solids suspension density but failing to predict the radial variation, (2) those assuming two or more regions considering either the core annulus or the cluster models to predict the radial variation, (3) those applying the fundamental equations of fluid mechanics to model gas-solid flow structure.

For simulation purposes, chose to apply the type1 model to predict the mean voidage profile in the upper region of the CFBC because can be easily coupled with reaction models to simulate CFBC reactors. This region consists of two zones: an acceleration zone and a fully developed zone.

In the acceleration zone, the axial voidage decreases with the vertical position along the riser (Kunii and Levenspiel, 1991):

$$\frac{\varepsilon^* - \varepsilon(z)}{\varepsilon^* - \varepsilon_1} = e^{-aZ} \tag{3.27}$$

where ε^* is axial voidage at saturated condition, ε_1 is mean voidage of lower region, $\varepsilon(Z)$ is axial voidage in the acceleration zone, a is decay constant.

For the decay factor a, proposed the following correlation of Lewis *et al.*, (1962):

$$aU_0 = \begin{cases} 2\text{ - }5 & \text{s}^{-1} & (d_p < 70 \text{ } \mu\text{m}) \\ 4\text{ - }12 & \text{s}^{-1} & (d_p > 88 \text{ } \mu\text{m}) \end{cases} \tag{3.28}$$

Or the decay constant was obtained using the correlation of Kunii and Levenspile as shown in *Figure 3.2* (Basu and Fraser, 1991).
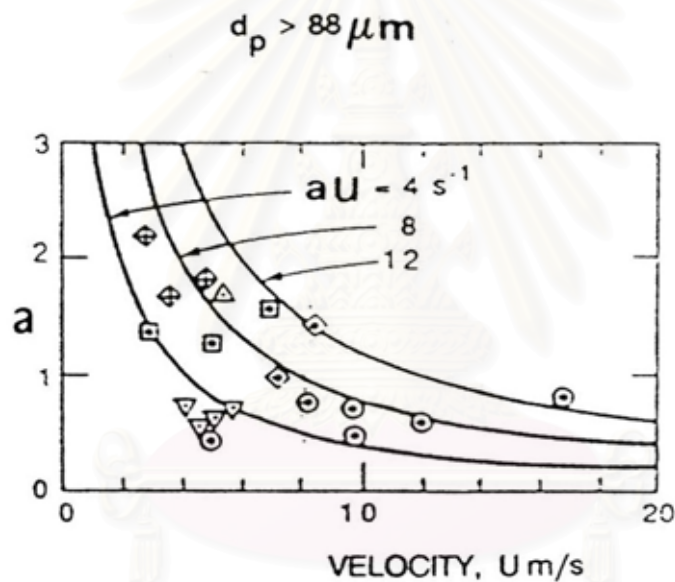
Figure 3.2 Decay constant in an axial bed density profile.

In the lumped modeling approach used in this work, the riser will be divided into a discrete number of intervals. Based on the void fraction variation in the acceleration zone given by equation (3.27), the mean value of voidage in a certain riser interval between height Z_{i-1} and Z_i can be calculated using the expression proposed by Kunii and Levenspiel (1991):

$$\varepsilon_i = \varepsilon^* - \frac{1}{a\Delta L}(\varepsilon_1 - \varepsilon^*)(\exp^{-aZ_i} - \exp^{-aZ_{i-1}}) \text{ } i=2,3 \tag{3.29}$$

In the fully developed zone, the mean axial voidage is estimated by the following equation:

$$\varepsilon_4 = \frac{1}{1 + \dfrac{\Phi G_s}{U_2 \rho_s}} \tag{3.30}$$

where the slip factor Φ is:

$$\Phi = 1 + \frac{5.6}{F_r} + 0.47 F_{rt}^{0.41} \tag{3.31}$$

where Froude number (F_r) and particle Froude number (F_{rt})

$$F_r = \frac{U_2}{\sqrt{gD_r}} \tag{3.32}$$

$$F_{rt} = \frac{U_t}{\sqrt{gD_r}} \tag{3.33}$$

where U_2 is superficial gas velocity, U_t is terminal velocity, g is gravity force, and D_r is diameter of riser.

Terminal velocity for irregularly shaped particles of sphericity, ϕ_s (Levenspiel,1999).

$$U_t = \left[\frac{18}{(d_p^*)^2} + \frac{2.335 - 1.744 \phi_s}{(d_p^*)^{1/2}} \right]^{-1} \tag{3.34}$$

and dimensionless equation

$$d_p^* = d_p \left[\frac{\rho_g (\rho_s - \rho_g) g}{\mu^2} \right]^{1/3} \tag{3.35}$$

CHAPTER 4

THE CFBC SIMULATION

4.1 General hypotheses of the reaction model

1. The fuels, primary air and limestone are fed into the bottom of the bed at a uniform temperature. The secondary air and tertiary air are fed above lower region in order of bed.

2. The time required for volatile combustion is very short, the devolatilization process is considered instantaneous and to take place at the bottom of the bed.

3. Char combustion is slower, it is assumed to occur after all the volatile products have been burned.

4. Burning fuel and gas temperatures are considered constant and equal to the bed temperature.

5. Uniform pressure, atmospheric pressure.

6. There is perfect mixing of solids (individual ash, char particles and sorbents) in the lower region and in each zone of the upper region.

4.2 CFBC simulation

The process simulation program for a CFBC was developed using four ASPEN PLUS reactor blocks to represent the phenomena identified in the fuel combustion process. A detailed description of the ASPEN PLUS reactors blocks along with their requirement is given in the ASPEN PLUS user manuals. *Table 4.1* present the reactor model parameters required for the simulation.

Considering the reaction and hydrodynamic models, there are several complete FORTRAN programs and an external subroutine for the kinetic and hydrodynamic models were used in the simulation. The FORTRAN codes were used:
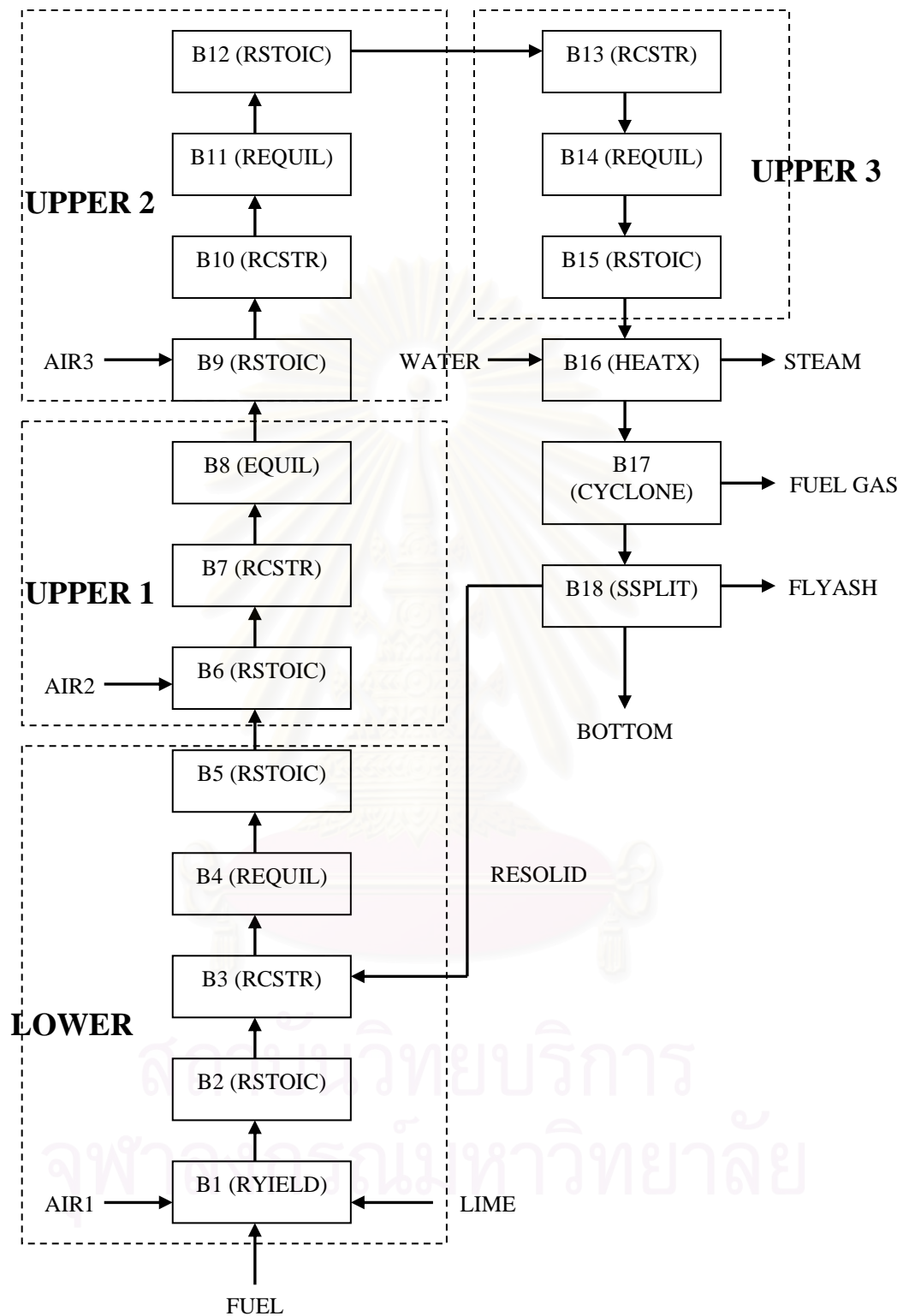
Figure 4.1 Simulation diagram of the CFBC.

KINETIC, is the external kinetic subroutine developed for both heterogeneous gas-solid and homogeneous gas phase reactions. HYDRO, is inserted into the ASPEN PLUS input file to calculate the mean void fraction in each section of the dense zone in lower region and the upper region of the riser.

Table 4.1 The reactor models description utilized in the simulation

Reactor block	Description
RYIELD	To simulate a reactor by specifying yield distribution data or correlation when reaction stoichiometry and kinetics are unknown
RSTOIC	To simulate a reactor with the unknown or unimportant reaction kinetic and known stoichiometry by specifying the extent of reaction or the fractional component of the key component To handle any number of simultaneous or series reactions
REQUIL	To calculate simultaneous phase chemical equilibrium by solving stoichiometric chemical and phase equilibrium equation To be convenient to the known reaction stoichiometry when only a few reactions approach equilibrium
RCSTR	To model CSTR reactors with known reaction kinetic To require user supplied kinetics subroutine when solids, such as char, are participiting in the reactions

The modeling procedure

For simulation purposes, the combustion of fuel particles can be modeled using the following reactions (Soutdeh-Gharebaagh *et al.,* 1998):

1. Devolatilization and volatile combustion
2. Char combustion
3. NO_x formation
4. SO_2 absorption

These reaction steps occur in the different region of the riser therefore can be divided into a number of individual reactors. To simulate the CFBC using ASPEN PLUS, reactor blocks were used and combined in a program flow sheet representing the CFBC is presented in *Figure 4.1*. The CFBC riser is divided into two regions: lower region and upper region. Each region used reactors block: RYIELD, RSTOIC, REQUIL

and RCSTR. The lower region is represented by a single CSTR (continuous stirred tank reactor). The upper region is represented by three CSTR. The number of CSTR in series is determined based on the hydrodynamic behavior of the upper. The use of four CSTR reactors in ASPEN PLUS is justified. *Figure 4.2* shows the mean solid fraction (1-εi) corresponding to the four reactors (lower region and three sections of the upper region).
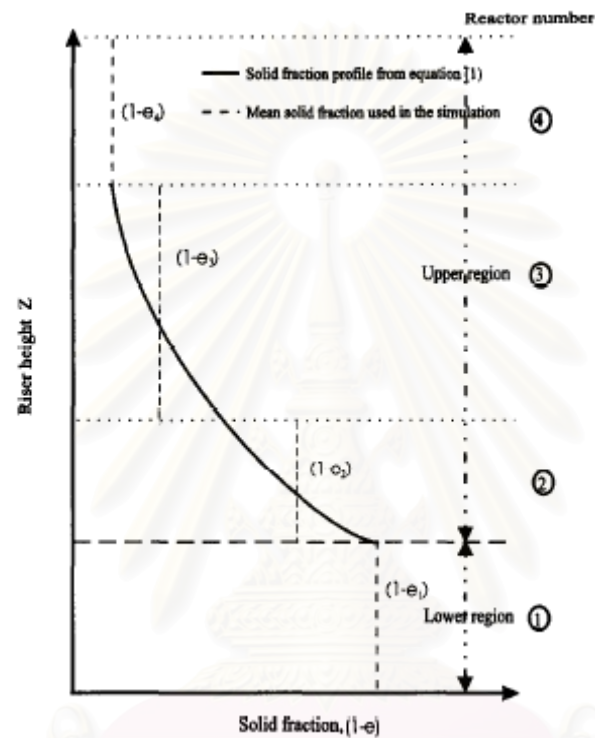
Figure 4.2   Variation of void fraction with height in the riser (Gharebaagh R., 1998).

4.2.1 Devolatilization and volatile combustion

Fuel was fed into CFBC, it decomposes into two parts: hydrogen-rich volatile and char. The char remains in the bed and burns slowly in combustor.

RYIELD (ASPEN PLUS yield reactor) was used to simulate decomposition process. Fuel is converted into its constituting components such as carbon, hydrogen, nitrogen, oxygen, sulfur and ash (by specifying the distribution vector according to the ultimate analysis).

RSTOIC (ASPEN PLUS stoichiometric reactor) was used to simulate volatile combustion. Three reactions are considered in the model:

$$C + \frac{1}{2}O_2 \rightarrow CO$$
$$S + O_2 \rightarrow SO_2$$
$$H_2 + \frac{1}{2}O_2 \rightarrow H_2O$$
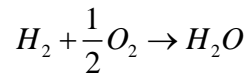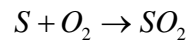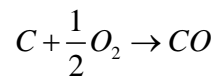
(i) Considering that the volatile matter (VM) in the coal, (obtained from a proximate analysis) consists exclusively of carbon, hydrogen and sulfur. This supposes that the entire hydrogen content of the coal is found in the volatile matter. The volatile carbon fraction reacts to form CO only during the volatile combustion process because of the oxygen depletion in the lower region of the riser.

(ii) The coal hydrogen content is entirely consumed during the volatile combustion process.

(iii) The coal sulfur content is assumed to be converted completely to SO_2 during the volatile combustion process.

In the devolatilization and volatile combustion process occurs in the lower region reactor only.

Physical properties of fuel
Proximate analysis

A typical proximate analysis includes the moisture, ash, volatile matter, and fixed carbon contents.

Table 4.2 Proximate analysis of fuel

Proximate analysis (wt.%)	Lignite[1]	Bagasse[2]	Bark[1]	Rice husk[2]
Moisture	19.86	35.48	39.66	9.50
Fixed carbon	34.85	7.71	9.09	14.68
Volatile matter	34.84	55.23	48.85	57.48
Ash	10.45	1.57	2.04	18.34

Ultimate analysis

The ultimate analysis gives the composition of the fuel in wt% of carbon, hydrogen and oxygen (the major components) as well as sulfur, nitrogen and ash.

Table 4.3   Ultimate analysis of fuel

Ultimate analysis (wt.%)	Lignite[1]	Bagasse[2]	Bark[1]	Rice husk[2]
Ash	13.04	2.44	2.82	15.26
Carbon	68.15	48.64	48.40	42.83
Hydrogen	5.09	5.87	6.72	6.05
Nitrogen	1.24	0.16	0.19	0.54
Sulfur	0.59	0.07	0.01	0.05
Oxygen	11.89	42.82	41.87	35.27

Source: 1. Siam Kraft Industry Co., Ltd.
*   2. Jenkins B.M. (1998).*

4.2.2   Char combustion

RCSTR (ASPEN PLUS continuous stirred tank reactor) was used to simulate char combustion. The char particles resulting from the devolatilization process consist of the remaining carbon fraction and ash only. These particles are then burned to produce a mixture of CO and CO_2. There are two main reactions for char combustion are considered:

$$C + \frac{1}{2}O_2 \rightarrow CO$$

$$CO + \frac{1}{2}O_2 \rightarrow CO_2$$
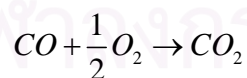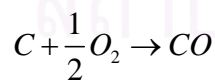
These reactions occur in the entire riser. This block requires the knowledge of the reaction kinetic model. The first reaction is heterogeneous reaction (gas-solid reaction). The rate of reaction of the first reaction was calculated by shrinking particle model and hydrodynamics model subroutine that explain in section 3.1 and 3.2.

Table 4.4 Physical and chemical properties of fuels

Fuel	Activation energy	Frequency factor	Reference
Lignite	$1.492*10^8$ J/kmole	59600 m/s K	Yamsakuna, 2000
Bagasse	$1.246*10^7$ J/kmole	210870 m/s	Gaur and Reed, 1998
Bark	$4.207*10^7$ J/kmole	86560 m/s	Gaur and Reed, 1998
Rice husk	$4.495*10^7$ J/kmole	185290 m/s	Gaur and Reed, 1998

4.2.3 NOx formation

REQUIL (ASPEN PLUS equilibrium reactor) is used to predict the amount of thermal NO_x formed during coal combustion based on equilibrium conditions considering the nitrogen present in the riser. Thermal generation NO_x, Three main reactions are used to represent this process in the model:

$$\frac{1}{2}N_2 + \frac{1}{2}O_2 \rightarrow NO$$

$$\frac{1}{2}N_2 + O_2 \rightarrow NO_2$$

$$N_2 + \frac{1}{2}O_2 \rightarrow N_2O$$
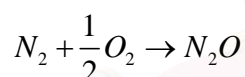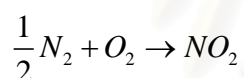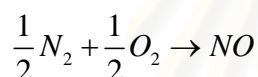
4.2.4 SO$_2$ absorption

RSTOIC (ASPEN PLUS stoichiometric reactor) was used to simulate SO_2 absorption. The sulfur dioxide was captured by limestone can be presented by the below reactions:

$$CaCO_3 \rightarrow CaO + CO_2$$

$$CaO + SO_2 + \frac{1}{2}O_2 \rightarrow CaSO_4$$
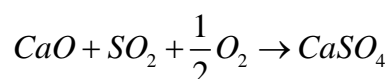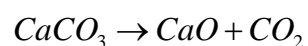
Since $CaCO_3$ is unstable under CFBC conditions, the calcinations process is assumed to occur instantaneously and completely in the lower region of the bed. The

second reaction, representing the SO_2 capture in the riser, is considered to occur in both the lower and the upper regions.

Sulfur retention

For calculating the sulfur retention only combustible sulfur was considered. The sulfur retention was determined taking into account the inlet sulfur, the gas outlet flow rate and the SO_2 concentration by the following equation (Adanez *et.al*., 2001):

$$R_s = \frac{(F_{0,fuel} x_s / M_s) - QC_s}{F_{0,fuel} x_s / M_s} \times 100$$

where R_s is sulfur retention, $F_{0,fuel}$ is flow rate feed, x_s is sulfur content in the fuel, M_s is molecular weight of sulfur, Q is volumetric gas flow rate, and C_s is SO_2 concentration at the outlet of the bed.

4.2.5 Heat exchanger

The duty of heat exchanger is to exchange the heat from the wall of combustor to the wall tubes for steam producing. The shell and tube heat exchanger was used to simulate the heat exchange between hot gas from combustion and water. The model was used to simulate the operation of a CFBC that produced 110 ton/hr of steam at 510°C and 110 barg.

4.2.6 Cyclone

Cyclone separated an inlet gas stream containing solids into a solids stream and a gas stream carrying the residual solids. Use cyclone to simulate cyclone separators in which solid particles are removed by the centrifugal force of a gas vortex.

In this case, simulation mode is used to simulate the cyclone. In simulation mode, cyclone calculates the separation efficiency and pressure drop from a user-

specified cyclone diameter. In simulation, used medium efficiency and the efficiency of cyclone was calculated by Leith-Licht model at diameter of cyclone was 5 meter.

4.2.7 Separator

SSplit combines material streams and divides the resulting stream into two or more streams. Use SSplit to model a splitter where the split of each substream among the outlet streams can differ.

In this case, SSplit was used to simulate separation between fly ash, bottom and resolid stream. Substream in the outlet streams have the same composition, temperature, and pressure as the corresponding substream in the mixed inlet stream. Only the substream flow rates differ.

CHAPTER 5

RESULTS AND DISCUSSION

In this thesis study the effect of operating parameters on emission gas and carbon combustion efficiency in circulating fluidized bed combustor system. The operating parameters studied were combustion temperature (750-900°C), flow rate of primary air, flow rate of secondary air, ratio of mixed fuel. Fuels included in the experiment were lignite and biomass (bagasse, rice husk and bark). Moreover, study effects of Ca/S on the sulfur retention were the Ca/S molar ratio (0.5-2.0).

Effect of combustion temperature

In this case, study single fuel was lignite 4 kg/s. Lignite was fed into the circulating fluidized bed combustor at atmospheric pressure by varies bed temperature between 750-900°C. The combustion temperature is maintained in the range of 750-900°C for the following reasons: ash does not fuse at this temperature; sulfur capture reaction is optimum at around 800-900°C and alkali metals from the coal are not vaporized at such low temperature.
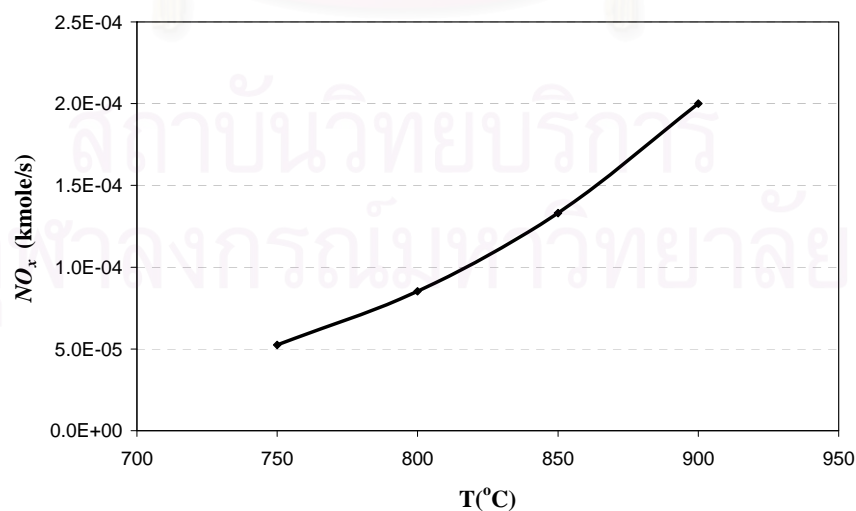
Figure 5.1 Effect of combustion temperature on the amount load of NO_x.

Combustion temperature has the dominant effect on the emission of *NOx*. In *Figure 5.1*, show the effect of the combustion temperature on *NOx* emission. Then increase in the combustion temperature increase *NOx* emission. Since high temperature is favorable to the thermal decomposition of *NOx*, so at high temperature one finds a rise in *NOx* emission.

Combustion is an exothermic oxidation process occurring at a relatively high temperature. When increase combustion temperature, the char combustion rate of carbon to carbon monoxide and the reaction rate of carbon monoxide to carbon dioxide are better. So, the amounts of carbon monoxide emission are increase. Shown in *Figure 5.2,* shows the effect of the combustion temperature on carbon monoxide emission. And the amounts of carbon dioxide are increase too. Shown in *Figure 5.3,* shows the effect of the combustion temperature on carbon dioxide.

During the combustion of a char particle, oxygen from the bulk stream is transported to the surface of the particle. When increase combustion temperature, the rate of reaction is better. The oxygen then undergoes an oxidation reaction with the carbon on the char surface to produce *CO* and *CO$_2$*. So, the oxygen concentration is decrease. Shown in *Figure 5.4,* shows the effect of the combustion temperature on the amount of oxygen.
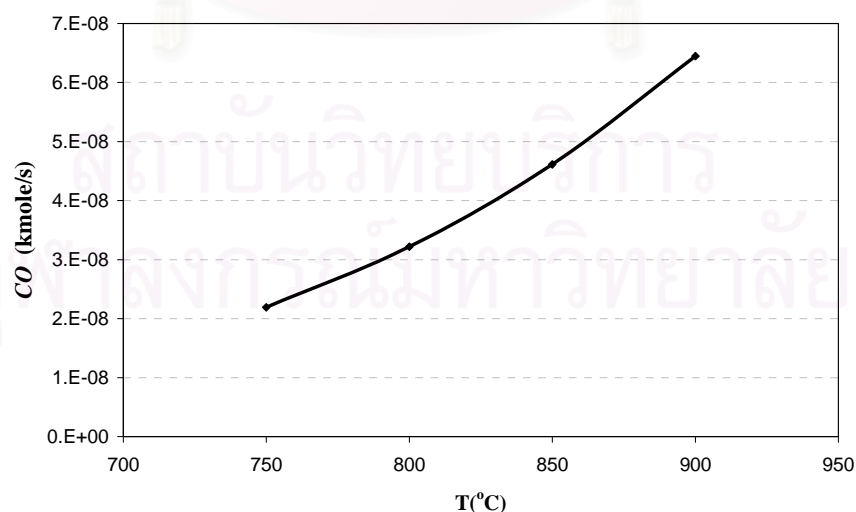
Figure 5.2 Effect of combustion temperature on the amount load of *CO*.
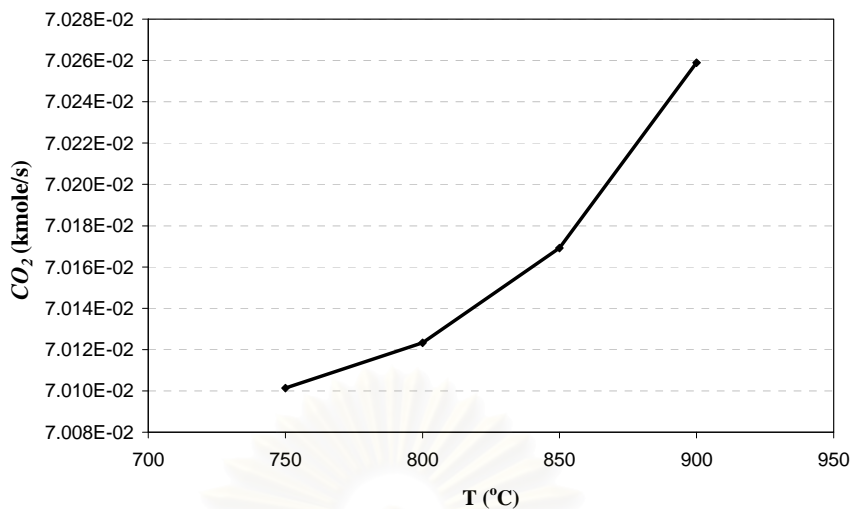
Figure 5.3 Effect of combustion temperature on the amount load of CO_2.
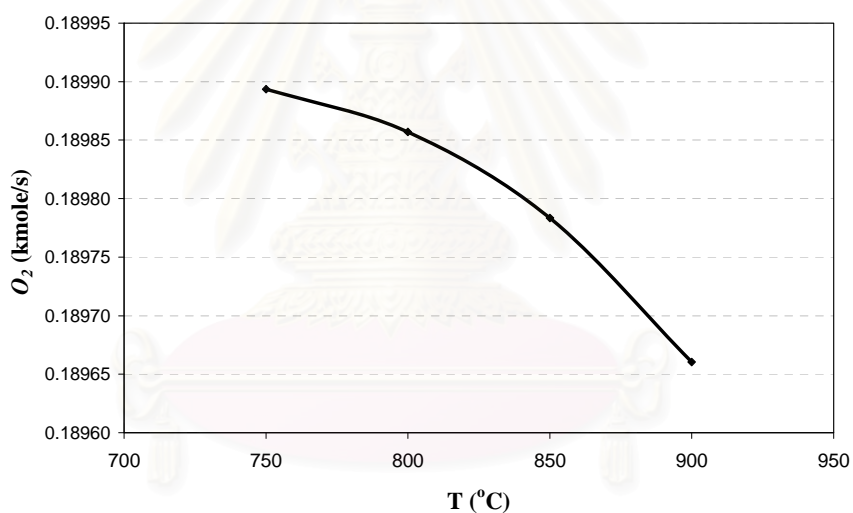
Figure 5.4 Effect of combustion temperature on the amount load of O_2.

The effect of combustion temperature on the amount load of SO_2 emission is shown in *Figure 5.5*. The combustion temperature has not any significant effect on the load of SO_2 emission.
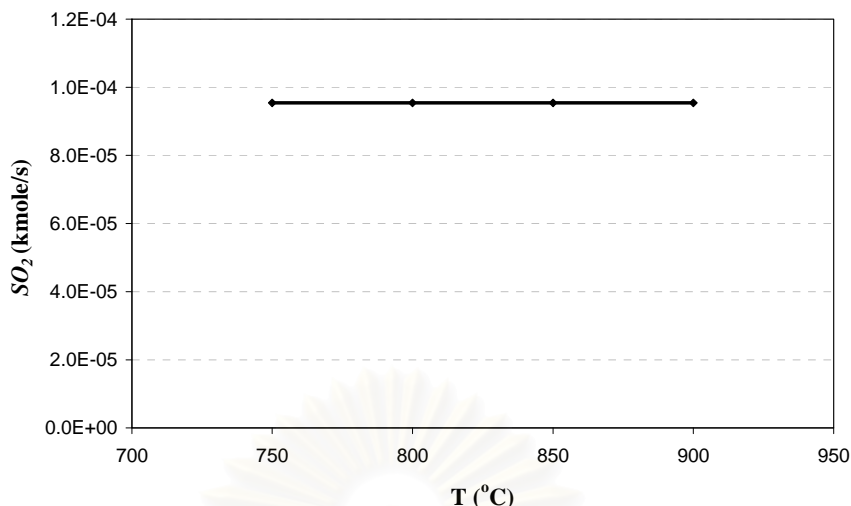
Figure 5.5 Effect of combustion temperature on the amount load of SO₂.

An increase in the combustion temperature from 750-900°C increased the carbon combustion efficiency and decreased the carbon concentration due to the increase in the reaction rates. As seen in *Figure 5.6,* show the effect of the combustion temperature on *%Ec*. The highest of carbon combustion efficiency is 98.824% at 900°C. The temperature between 750-850°C, the carbon combustion efficiency is rapid increase. Reactivity increase with temperature, the reaction rate increases quickly. At 750°C, the carbon combustion efficiency is 98.522% and at 850°C is 98.822%. But an increase of the temperature from 850 to 900°C gave a small increase of the carbon combustion efficiency from 98.822% to 98.824%. The high temperature, the change in carbon combustion efficiency was smaller. Because of the heat loss to surrounding was increase, the high combustion temperature.

Table 5.1   Effect of combustion temperature on carbon combustion efficiency

Temperature (^{o}C)	% Ec
750	98.521766
800	98.740893
850	98.822476
900	98.823693
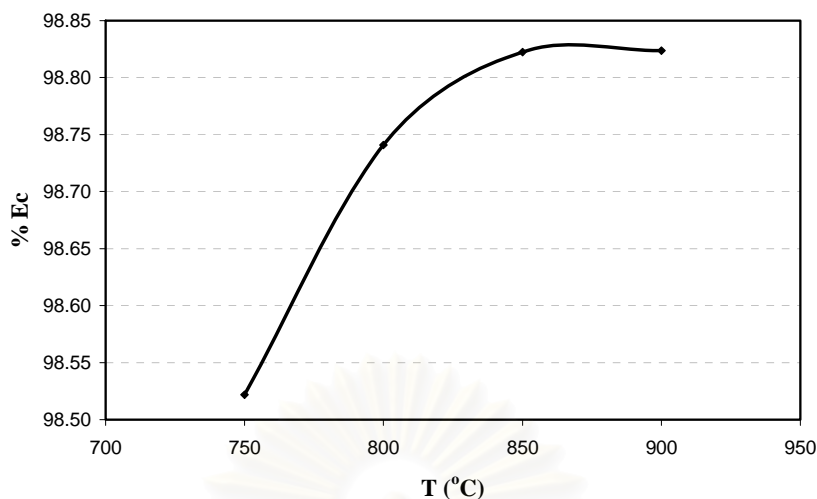
Figure 5.6 Effect of combustion temperature on the carbon combustion efficiency.

Effect of primary air and secondary air flow rate

The 4 kg/s of lignite was fed into the circulating fluidized bed combustor at atmospheric pressure, temperature 900°C. Vary primary air flow rate (22-25 m^3/s) at secondary air flow rate is 10 m^3/s and secondary air flow rate (10-14 m^3/s) at primary air flow rate is 22 m^3/s.

From the results, effects of the both primary air flow rate and secondary air flow rate on NO_x emission have the similar trend. Increase air flow rate increase the oxidation rate of nitrogen species and nitrogen was the component of air (~79 % by mole) when increase air increase nitrogen too. So, the NO_x emission is reduced significantly when the air flow rate is reduced. Shown in *Figure 5.7*, shows the effect of the primary air flow rate on the amount load of NO_x emission and *Figure 5.8* shows the effect of the secondary air flow rate on the amount load of NO_x emission.
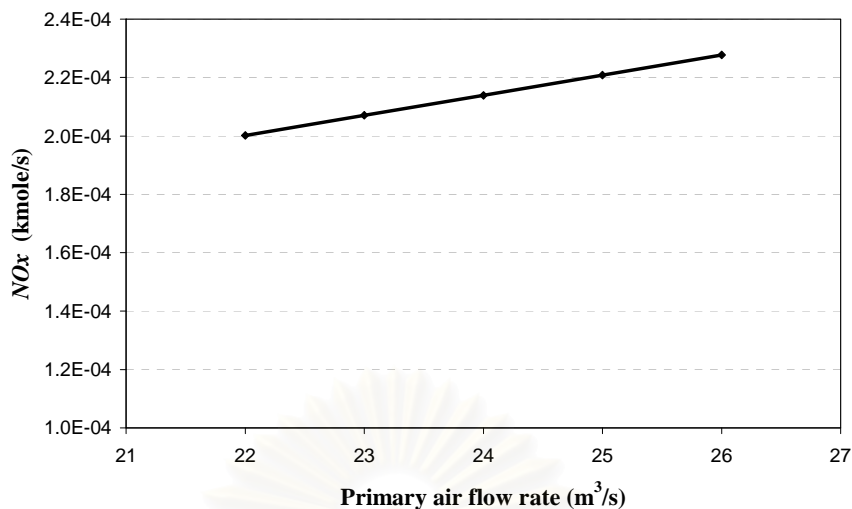
Figure 5.7 Effect of primary air flow rate on the amount load of NO_x.
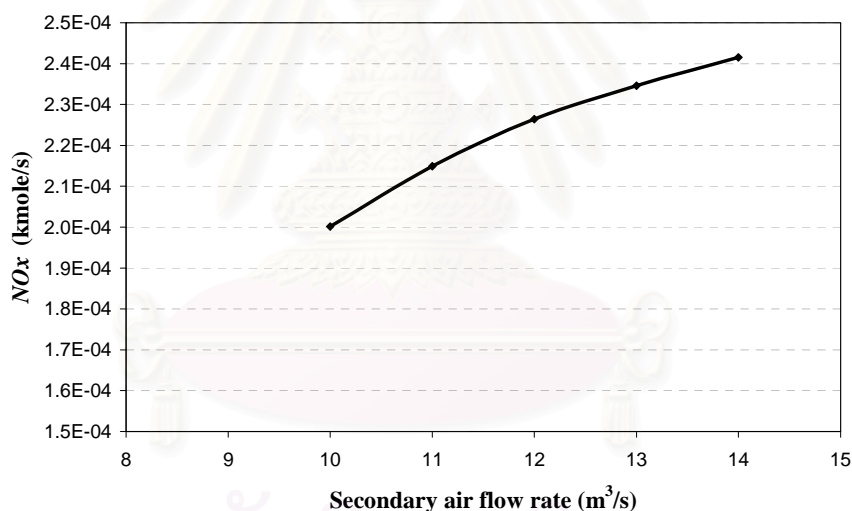
Figure 5.8 Effect of secondary air flow rate on the amount load of NO_x.

An increase in the primary air flow rate reduces the carbon combustion efficiency. Because of the air flow rate was more increase, the gas velocity was increase too. So the reaction time between char particles and oxygen were short, produced CO and CO_2 emissions were decrease. *Figure 5.9* show effect of the primary air flow rate on the amount load of CO emission and *Figure 5.10* show effect of the primary air flow rate on the amount load of CO_2 concentration.
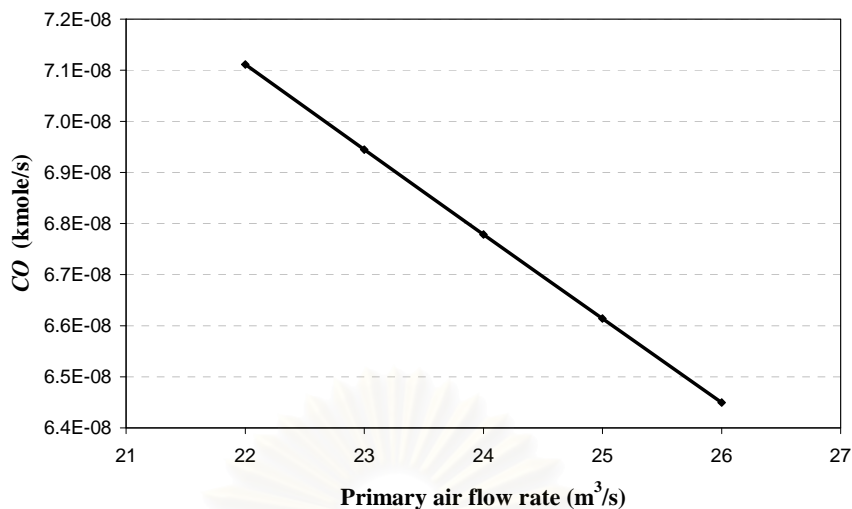
Figure 5.9 Effect of primary air flow rate on the amount load of *CO*.
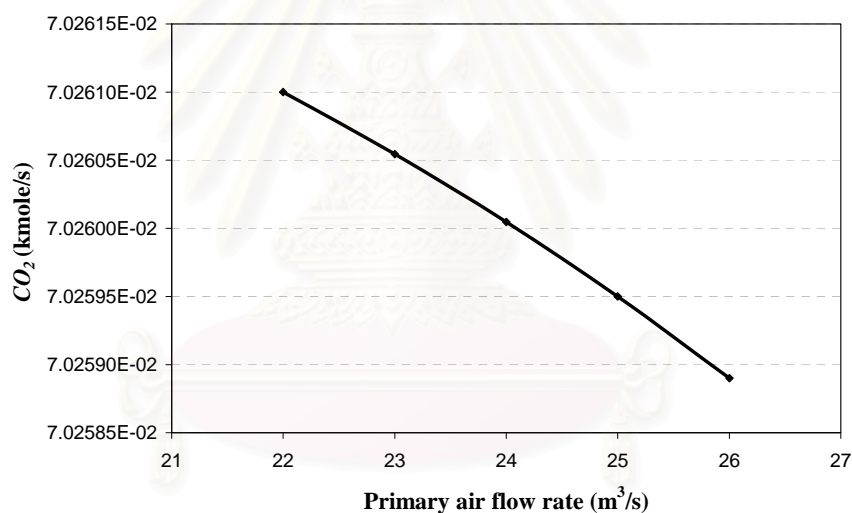
Figure 5.10 Effect of primary air flow rate on the amount load of CO_2.

And an increase in the secondary air flow rate reduced the amount load of carbon monoxide and carbon dioxide emission that same trend with increasing primary air flow rate. Shown in *Figure 5.11*, show the effect of secondary air flow rate on the amount load of *CO* emission and *Figure 5.12,* show the effect of secondary air flow rate on the amount load of CO_2.
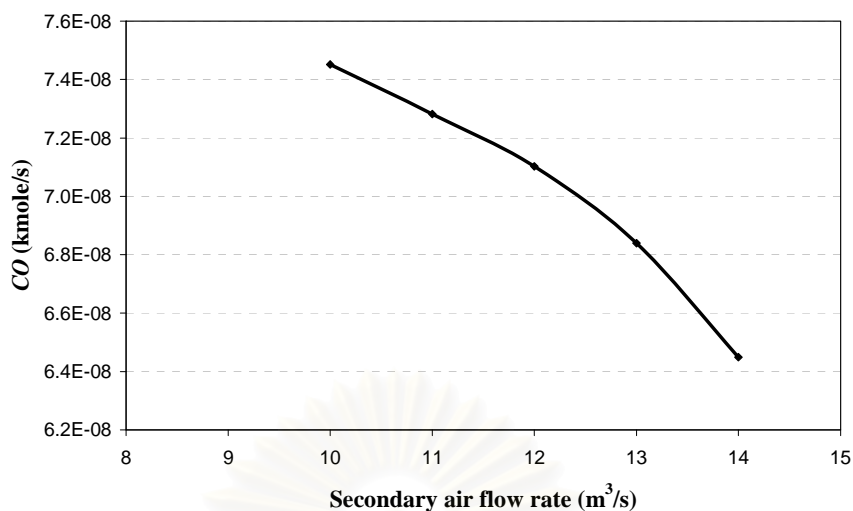
Figure 5.11 Effect of secondary air flow rate on the amount load of CO emission.
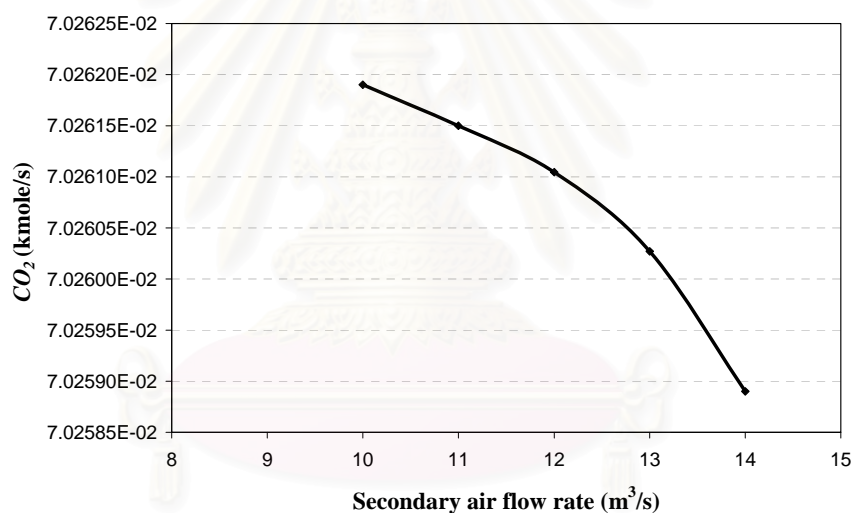
Figure 5.12 Effect of secondary air flow rate on the amount load of CO_2.

But an increase of the secondary air flow rate gave a small decrease of the combustion efficiency. These results can be explained taking into account the fact that an increase in the secondary air flow rate produces a decrease in the oxygen concentration in the lower part of the combustor and therefore a decrease in the char combustion rate. Therefore, char particles were oxidized by oxygen to CO is better than the reaction of CO to CO_2 because the oxygen concentration is not enough in the CO combustion reaction. *Figure 5.1*3 show the effect of secondary air flow rate on the amount of CO emission. So the CO emission is increase when the flow rate of secondary air is increase, but the CO_2

concentration is decrease. Shown in *Figure 5.14*, shows the effect of secondary air flow rate on the amount of CO_2 concentration.
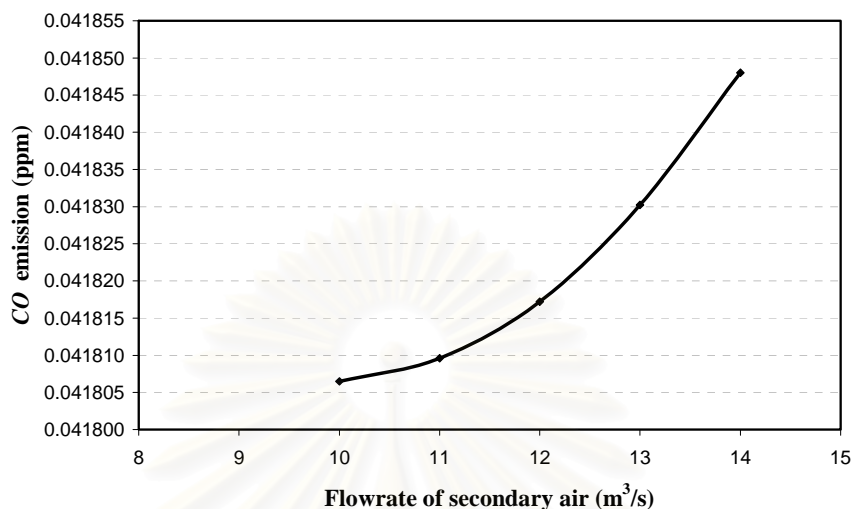
Figure 5.13 Effect of secondary air flow rate on the amount of CO concentration.
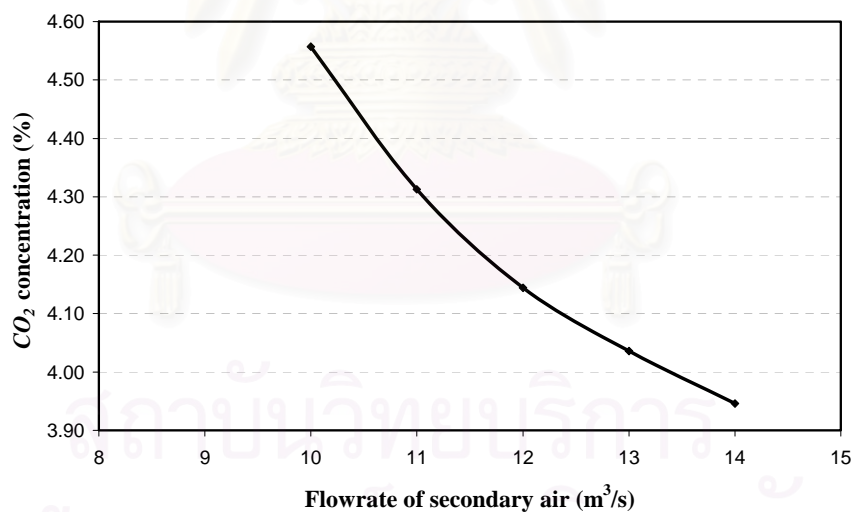
Figure 5.14 Effect of secondary air flow rate on the amount of CO_2 concentration.

An increase air flow rate has not any significant effect on the amount load of SO_2 emission. Shown in *Figure 5.15,* shows the effect of primary air flow rate on the amount load of SO_2 emission and *Figure 5.16* shows the effect of secondary air flow rate on the amount load of SO_2 emission.
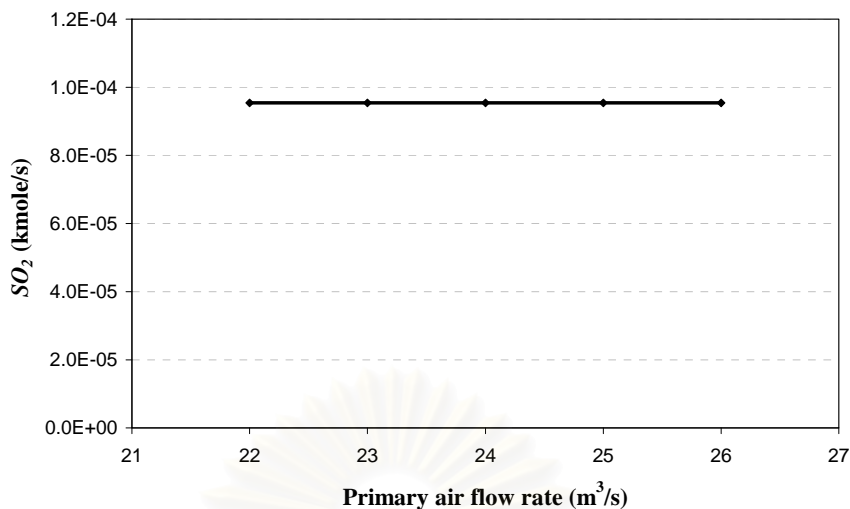
Figure 5.15 Effect of primary air flow rate on the amount load of SO_2 emission.
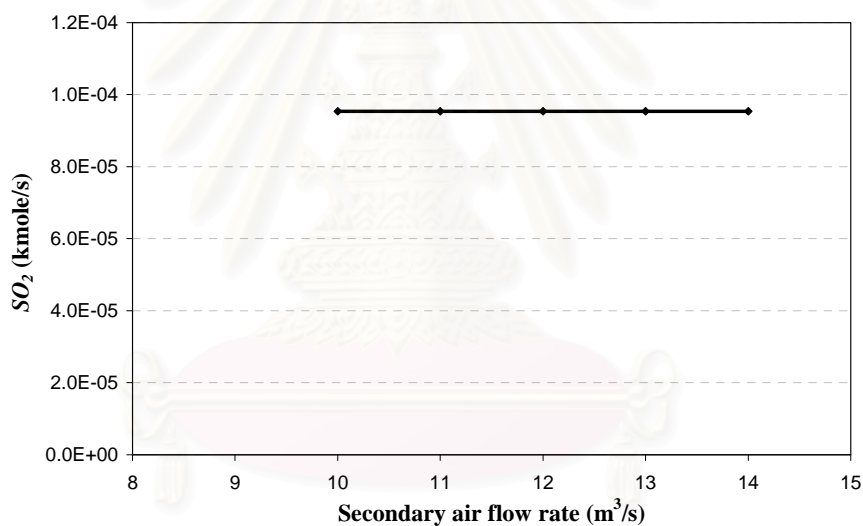
Figure 5.16 Effect of secondary air flow rate on the amount load of SO_2 emission.

But an increase air flow rate decrease the amount concentration of SO_2 emission. Shown in *Figure 5.17,* shows the effect of primary air flow rate on the amount concentration of SO_2 emission and *Figure 5.18* shows the effect of secondary air flow rate on the amount concentration of SO_2 emission. Because of the amount of sulfur in fuel uniform but concentration of oxygen is increase so the amount of SO_2 concentration are decrease too.
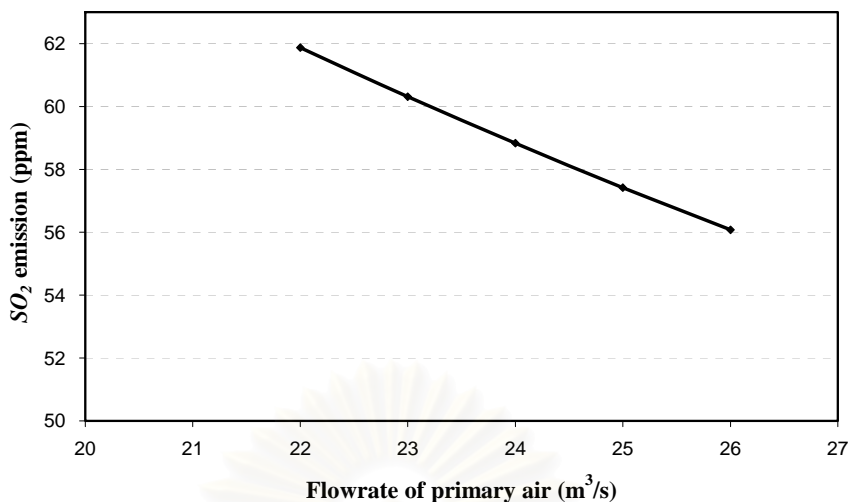
Figure 5.17 Effect of primary air flow rate on the amount of SO_2.
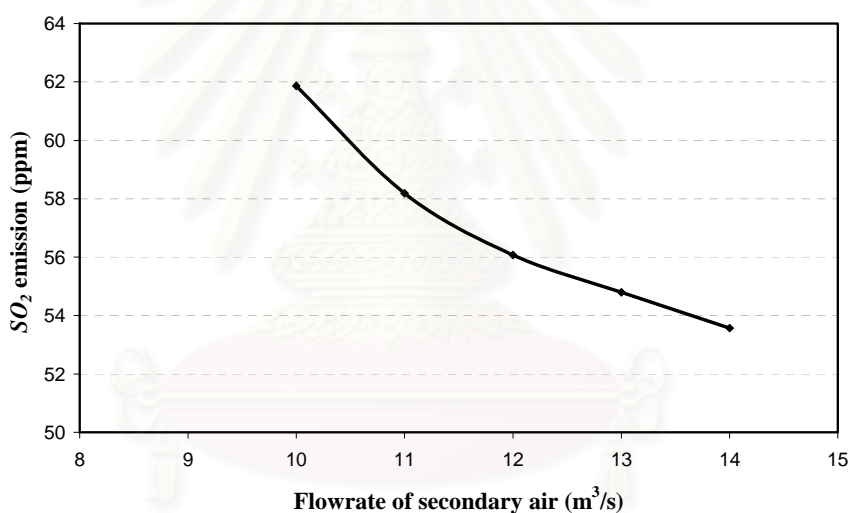
Figure 5.18 Effect of secondary air flow rate on the amount of SO_2.

Effect of air flow rate (primary air and secondary air) on the carbon combustion efficiency shown in *Figure 5.19* and *5.20* with constant temperature ($900^{o}C$). These results suggest that an increase in the air flow rate reduces the carbon combustion efficiency. An increase in air flow rate at temperature constant, these effects mainly affects the mean residence time of char particles in the bed. Since their combustion time is always much shorter than the mean residence time of char particles in the bed. And the solids circulation flow rate increases and so the flow rate of solids losses by the cyclone increased.
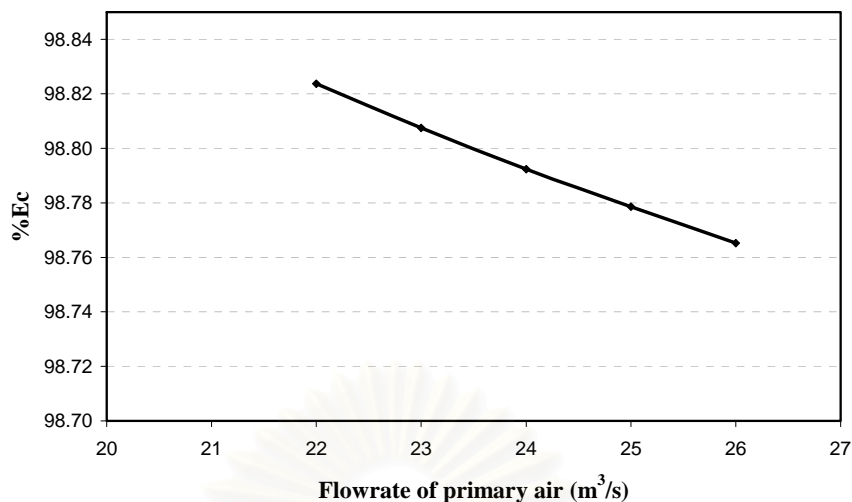
Figure 5.19 Effect of primary air flow rate on the carbon combustion efficiency.
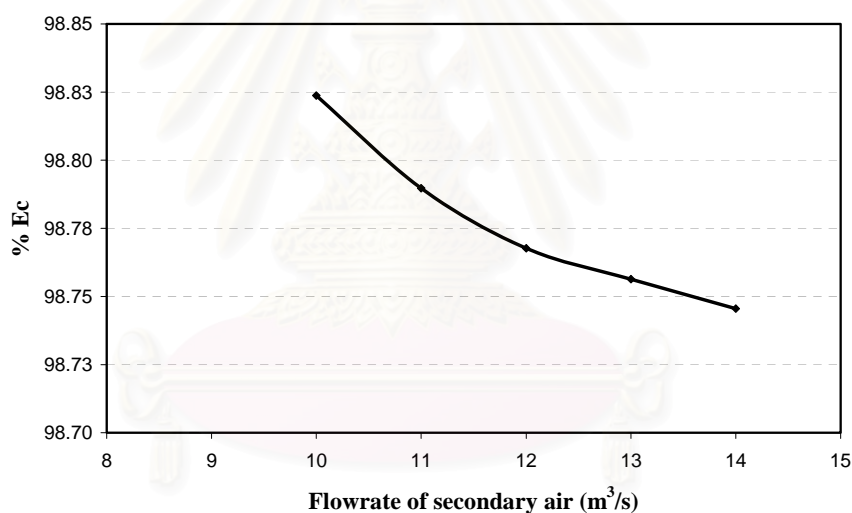
Figure 5.20 Effect of secondary air flow rate on the carbon combustion efficiency.

Effect of ratio of mixed fuel

In this case, the mixed fuels between lignite and biomass (bagasse, bark and rice husk) by vary combustion temperature (750-900°C). In each experimental, biomass was fed increase 10% of flow rate. The amounts of mixed fuel were shown in Table 5.2. In case of a single fuel, 4 kg/s of lignite was fed into the combustor. When

mixed biomass with lignite, the flow rate of biomass was increased 10% by keeping the amount of carbon inlet constant.

Table 5.2 The amount of mixed fuel between lignite and bagasse

Ratio of mixed fuel	Lignite (kg/s)	Bagasse (kg/s)
100% coal	4.0	0
90% coal + 10% bagasse	3.6	0.6
80% coal + 20% bagasse	3.2	1.13
70% coal + 30% bagasse	2.8	1.68
60% coal + 40% bagasse	2.4	2.24
50% coal + 50% bagasse	2.0	2.80
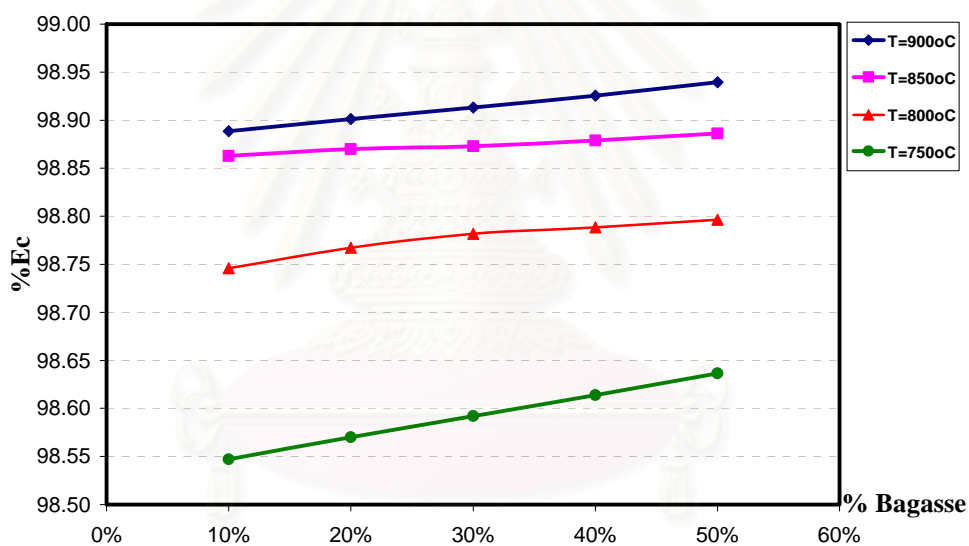
Figure 5.21 Effect of percentage of bagasse added in the lignite on the carbon combustion efficiency at temperature 750°C to 900°C.

Table 5.3 The amount of mixed fuel between lignite and bark

Ratio of mixed fuel	Lignite (kg/s)	Bark (kg/s)
100% coal	4.0	0
90% coal + 10% bark	3.6	0.56
80% coal + 20% bark	3.2	1.13
70% coal + 30% bark	2.8	1.69
60% coal + 40% bark	2.4	2.25
50% coal + 50% bark	2.0	2.82
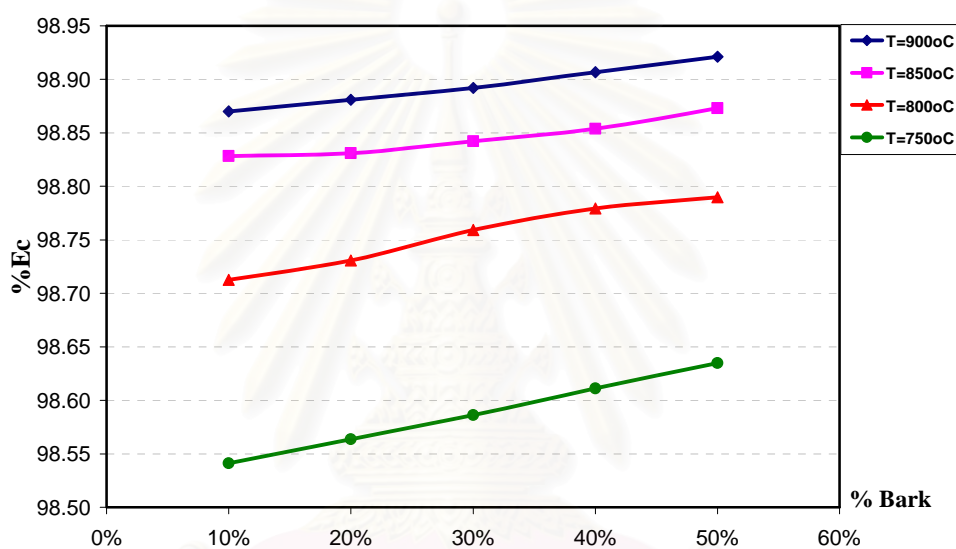
Figure 5.22 Effect of percentage of bark added in the lignite on the carbon combustion efficiency at temperature 750°C to 900°C.

Table 5.4 The amount of mixed fuel between lignite and rice husk

Ratio of mixed fuel	Lignite (kg/s)	Rice husk (kg/s)
100% coal	4.0	0
90% coal + 10% rice husk	3.6	0.64
80% coal + 20% rice husk	3.2	1.27
70% coal + 30% rice husk	2.8	1.91
60% coal + 40% rice husk	2.4	2.55
50% coal + 50% rice husk	2.0	3.18
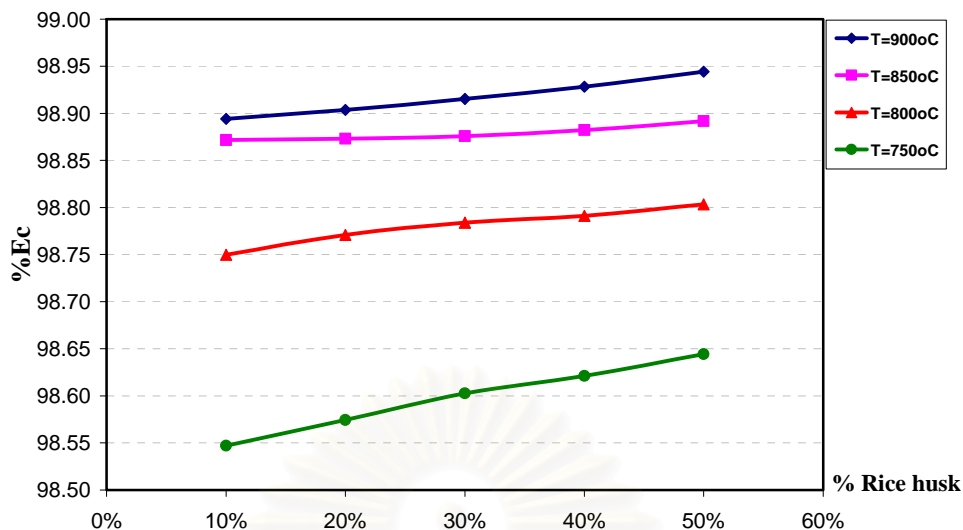
Figure 5.23 Effect of percentage of rice husk added in the lignite on the carbon combustion efficiency at temperature 750°C to 900°C.

In this case, the mixed fuels between lignite and biomass (bagasse, bark and rice husk) at combustion temperature 900°C, 1 atm. In each experimental, biomass was fed increase 10% of flow rate.
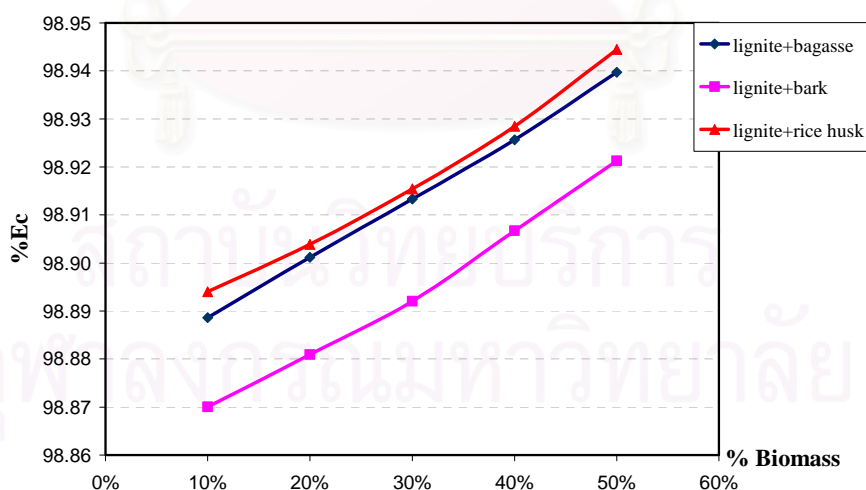
Figure 5.24 Effect of percentage of biomass added in the lignite on the carbon combustion efficiency at temperature 900°C.

Figure 5.21-5.23 shows the effect of the percentage of biomass added in the feed on the carbon combustion efficiency by vary combustion temperature 750-900°C. The results of the three type of biomass (bagasse, bark and rice husk) have the similar trend. As can be seen, the carbon combustion efficiency increased when the percentage of biomass increased. At 900°C, the carbon combustion efficiency is highest due to an increase in the combustion temperature increase in the reaction rates.

Figure 5.21-5.24 shows the effect of the percentage of biomass added in the feed on the carbon combustion efficiency for mixing lignite and three kinds of biomass. As can be seen, the carbon combustion efficiency increase when the percentage of biomass increase. At 50% of biomass is present in the lignite and biomass mixture. These results were expected because the particle size distributions of the lignite had great amount of fines, being part of these fine particles lost in the cyclone system. Moreover in biomass has the volatile matter content been high so the combustion occurs easily.

The effect of biomass type on the carbon combustion efficiency is very strong. This behavior can be explained according to the differences on the volatile matter content and the moisture content for the three type of biomass. In general, when the moisture content of the fuel increases devolatilization time is greater caused by the increased moisture content in the fuel which delays the gas evolution from the fuel during the devolatilization process (Wildegger-Gaismaier, 1990). The volatile matter content is an important property in combustion applications, providing a suitable indication of the reactivity or combustibility of fuel. An important step in the combustion is the devolatilization, ignition and burning of the volatile. Therefore, volatile matter is one of the factors governing the reactivity and burnout efficiency of fuel. In general, when the volatile matter content is low the reactivity is too low and the combustion of this fuel is more difficult (Carpenter AM., 1988). In this study, the rice husk reactivity is highest that the bagasse and bark reactivity. Because of the volatile matter content in rice husk is 57.48% wt., bagasse is 55.23% wt. and bark is 48.85% wt. and the moisture content is 9.50%, 35.48% and 39.66% respectively due to the carbon combustion efficiency of mixed fuel between lignite and rice husk is highest at 50% of rice husk is 98.945%. The mixed fuel between lignite and bagasse is 98.939% and between lignite and bark is 98.921% at 900°C.
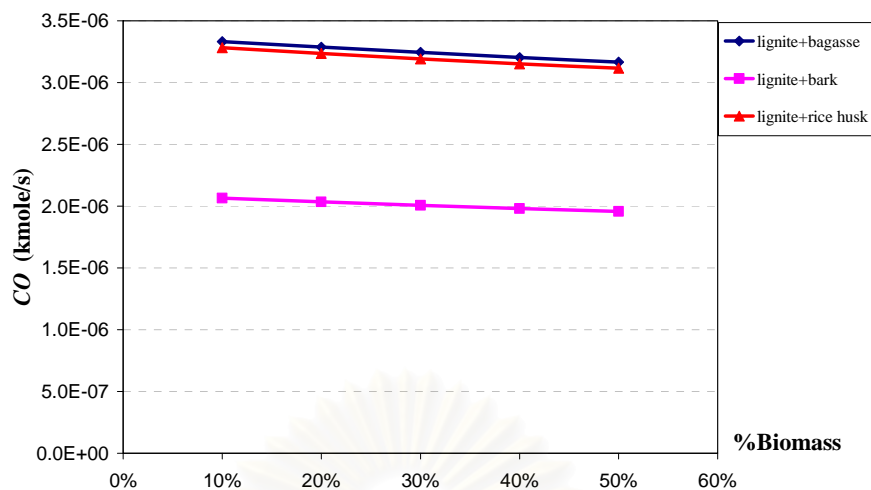
Figure 5.25 Effect of percentage of biomass added in the lignite on the carbon monoxide emission at temperature 900^oC.
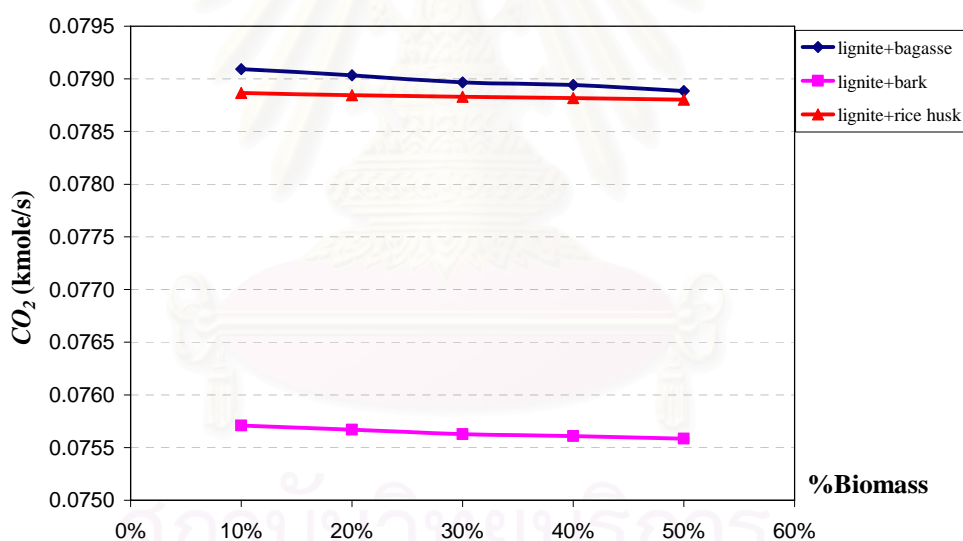
Figure 5.26 Effect of percentage of biomass added in the lignite on the carbon dioxide emission at temperature 900^oC.

The adding of biomass in the mixed fuel are increases, the amount of CO and CO_2 emission are decrease. From *Figure 5.25* show effect of percentage of biomass added in the lignite on the carbon monoxide emission and *Figure 5.26* Effect of percentage of biomass added in the lignite on the carbon dioxide emission at temperature

900°C. Because of the biomass has lower carbon content in comparison to lignite. In during the char combustion to produced CO and CO_2 are decrease.

The carbon content of bark is lower than bagasse so the CO and CO_2 emission are lower. Although the carbon content of rice husk is lower than bark but the volatile matter is much higher and in the bark has the moisture content higher, the combustion occurs not better. Therefore, the reaction rate of mixture between rice husk and lignite is better, the CO and CO_2 emission in flue gas are increase.
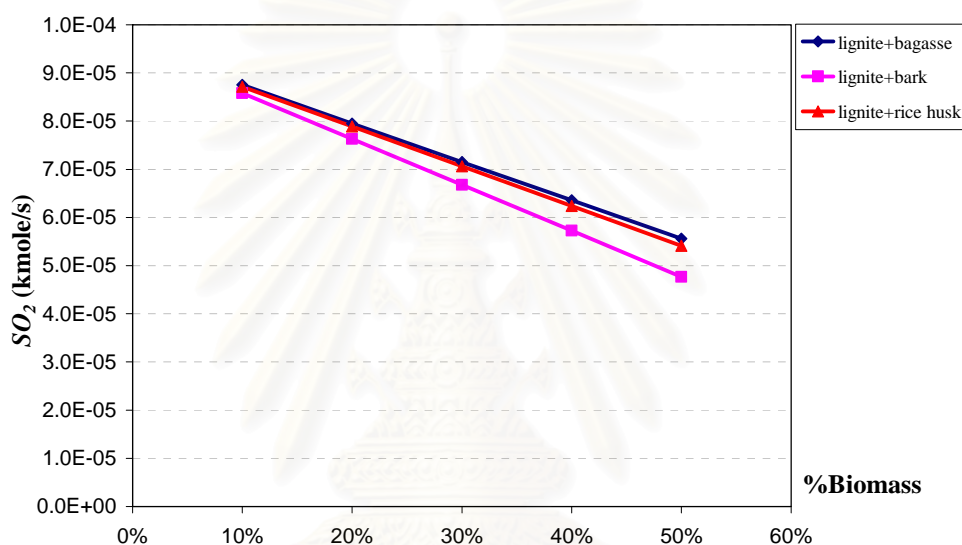
Figure 5.27 Effect of percentage of biomass added in the lignite on the sulfur dioxide emission at temperature 900°C.

The effect of the percentage of biomass added in the feed on the SO_2 emission is shown in the *Figure 5.27.* An increase of the biomass in the mixed fuel causes a decrease on the SO_2 emission. This is due to the fact that biomass has lower sulfur content in comparison to lignite. The sulfur content of the lignite is 1.75% and the sulfur content of the bark, rice husk and bagasse are 0.01%, 0.05% and 0.07% respectively. So, SO_2 emissions are lower when the biomass shares in the lignite. Because of the sulfur content of the bark is lower than that of the rice husk and bagasse. The SO_2 emission from flue gas of mixed fuel between lignite and bark is lower. In consequence, not only, the feeding limestone in during the combustion is decrease SO_2 emission, but decreasing of

SO_2 emissions in combustion can be clearly larger than reduction of sulfur content of the feedstock after mixing biomass to lignite.

Effect of ratio of Ca/S to the sulfur retention

In this case, study single fuel was lignite 4 kg/s. Lignite was fed into the circulating fluidized bed combustor at atmospheric pressure, temperature 900°C. Vary ratio of calcium to sulfur between 0.5-2.0. The flow rate of $CaCO_3$ was fed in the combustor shown in *Table 5.3*.

Table 5.5   Vary mole ratio of Ca/S (100% coal)

Ca/S	Flow rate of $CaCO_3$ (kg/s)
0.5	0.092185
1.0	0.184375
1.5	0.276555
2.0	0.368750

Table 5.6   Sulfur retention efficiency

Ca/S	%Rs
0.5	99.7517683
1.0	99.7519166
1.5	99.7521650
2.0	99.7522134

Figure 5.28 shows effect of Ca/S molar ratio on the sulfur retention at temperature 900°C. The Ca/S molar ratio ranged between 0.5 and 2. As can be seen in the figure an increase in the Ca/S molar ratio gives a significant increase in the sulfur retention reached in the combustion. Sulfur capture of 99.75% is usually achieved at molar ratios of calcium to sulfur of 2.
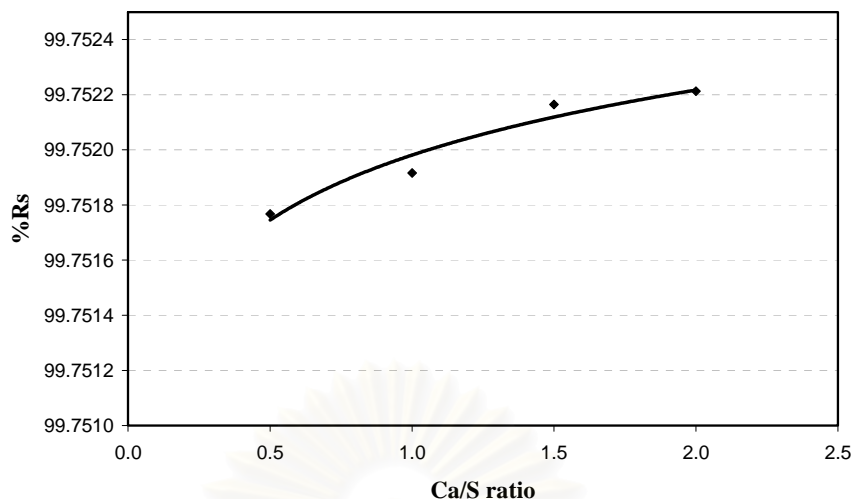
Figure 5.28 Effect of Ca/S mole ratio on the sulfur retention at temperature 900°C.

When coal burns, the sulfur is oxidized primarily to sulfur dioxide. Limestone and dolomite are two principle sorbents used for the absorption of sulfur dioxide in circulating fluidized bed combustor. *Figure 5.29* show Effect of Ca/S mole ratio on the sulfur dioxide emission at temperature 900°C. Increase molar ratios of calcium to sulfur, the sulfur capture are better. The amounts of sulfur dioxide are decrease. But the amounts of CO_2 concentration are increase because the calcination, where the limestone decomposes into CaO and CO_2 are increase. *Figure 5.30* show the effect of Ca/S mole ratio on the carbon dioxide emission at temperature 900°C.
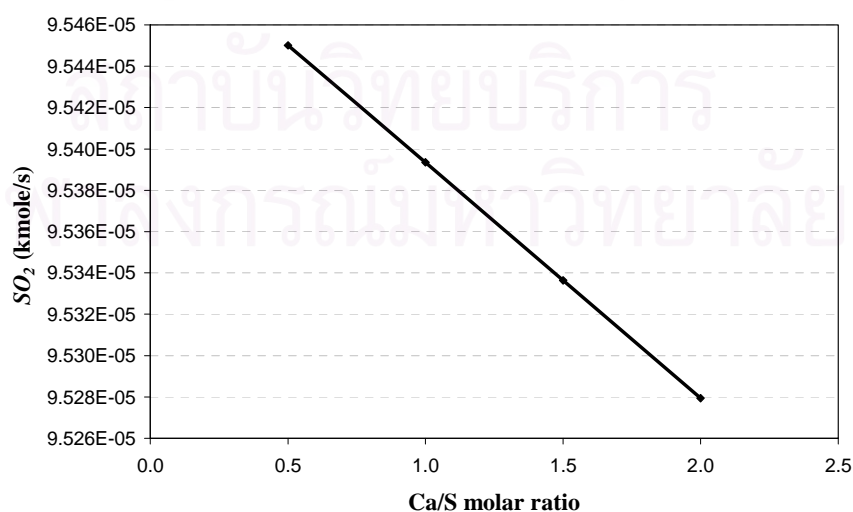
Figure 5.29 Effect of Ca/S mole ratio on the SO_2 emission at temperature 900°C.
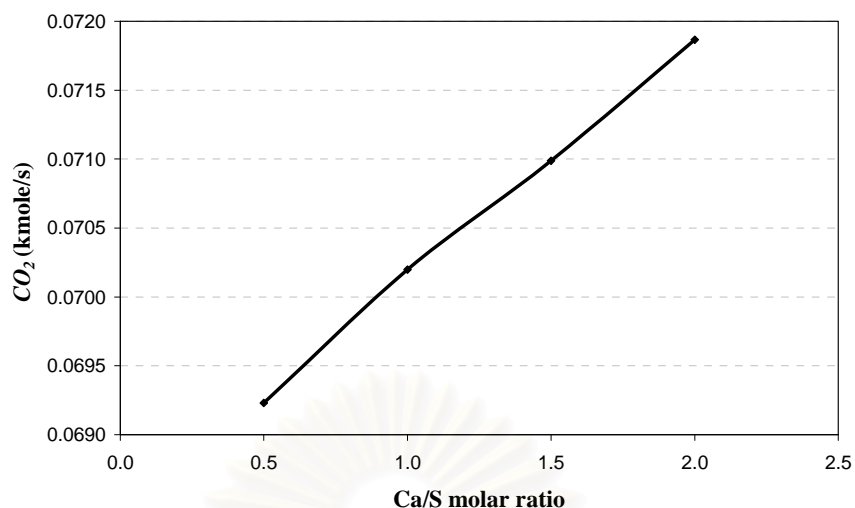
Figure 5.30 Effect of Ca/S mole ratio on the CO_2 emission at temperature 900°C.
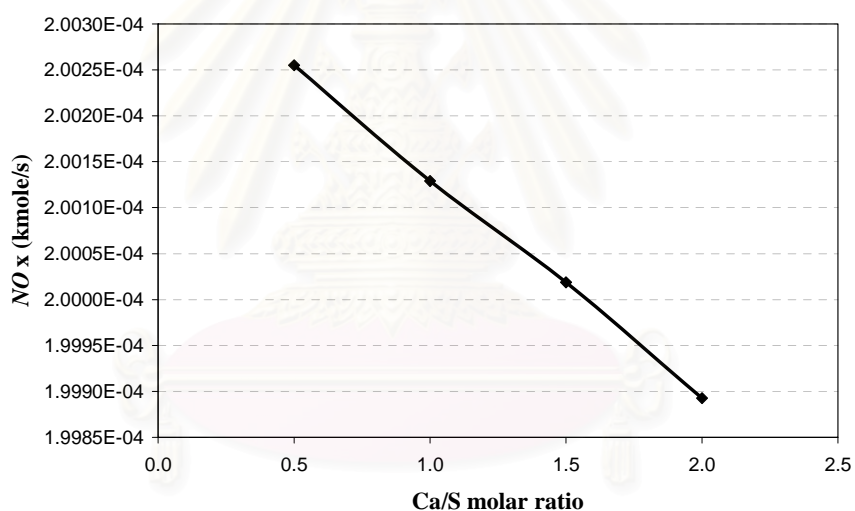
Figure 5.31 Effect of Ca/S mole ratio on the NO_x emission at temperature 900°C.

The effect of calcium to sulfur ratio on the NO_x emission was shown in *Figure 5.31*. Limestone has a complex role in NO_x formation and destruction. While it catalyses the production of NO_x from ammonia, formed from volatile nitrogen, it also catalyses the reduction of NO_x by CO. The relative importance of these effects appears to be a function of fuel reactivity as discussed by Lyngleft and Leckner (1989). For reactive fuels such as bituminous or sub-bituminous coals, the oxidation of volatile nitrogen dominates and limestone addition tends to increase NO_x emission. But the result in *Figure*

5.31, NO$_x$ emission are small decrease when increase ratio of Ca/S. From this result was supported by Grace J.R. (1997) that for low volatile fuels such as petroleum cokes, the catalytic can be dominant. In that case limestone addition is beneficial to *NO$_x$* emission. The amount *NO$_x$* emission is strongly dependent upon the combustion temperature.

CHAPTER 6

CONCLUSIONS AND RECOMMENDATIONS

6.1 Conclusions

In this research proposed a model for simulating the co-combustion of lignite coal and biomass (bagasse, bark and rice husk) in a circulating fluidized bed combustor. A mathematical model was used for the prediction of carbon combustion efficiencies and sulfur retentions in CFBC. The model allows prediction of the effect of the main operating conditions, such as combustion temperature, primary and secondary air flow rate, percentage of biomass in the feed, biomass type and Ca/S molar ratio on the carbon combustion efficiency and the emission levels of CO, SO_2 and NO_x, and O_2 and CO_2 concentration.

- An increase in the combustion temperature increases the carbon combustion efficiency due to the increase in the reaction rates so the CO and CO_2 emission load are increases. At high combustion temperature also has its advantages. The combustible loss is primarily due to the unburned carbon fines that escape through the cyclone before they can complete their combustion. So a high temperature may help reduce the burn time and hence the combustible loss. The carbon combustion efficiency is highest about 98.824% at 900°C. But then increase in the combustion temperature increase NOx emission load. Since high temperature is favorable to the thermal decomposition of NOx.

- An increase in the primary and secondary air flow rate reduces the carbon combustion efficiency. The carbon combustion efficiency is highest about 98.824% at 900°C, primary air flow rate 22 m^3/s and secondary air 10 m^3/s.

- The carbon combustion efficiency increase when the percentage of biomass increases. The type of biomass has signification on carbon combustion efficiency because of the volatile matter and moisture content in component of biomass is different. Rice husk has the volatile matter content is highest so the combustion occur the better. The carbon combustion efficiency of mixed fuel between lignite and rice husk is highest

at 50% of rice husk is 98.945%. The mixed fuel between lignite and bagasse is 98.939% and between lignite and bark is 98.921% at 900°C.

- SO_2 emissions correlate quite well with lignite sulfur content. As could be expected when the percentage of biomass was added in the mixture increases the SO_2 emissions decrease and CO, CO_2 emission decrease too.

- An increase in the Ca/S molar ratio gives a significant increase in the sulfur retention reached in the combustion. The sulfur capture of 99.75% is usually achieved at molar ratios of calcium to sulfur of 2. But the rate of sulfation of calcium oxide particles through the reaction is found to decrease exponentially with time. But the amounts load of CO_2 concentration are increase because the calcination reaction.

6.2 Recommendations

A future study in the circulating fluidized bed combustor simulation should be performed in the following areas:

- Because of the combustion temperature changed with along the height of riser but in this simulation assumed constant combustion temperature throughout the height of riser. Therefore, should be considered combustion temperature on the each bed height.

- The emissions gas from the circulating fluidized bed combustor in this simulation were considered in the series reactions but the real reactions was took place in the network reactions. Thus the complex models should be developed.

- The future study should modify type of mixed fuels.

- The future study should consider operation at high temperature.

References

Adanez J., Abanades J.C. (1992). Modeling of lignite combustion in atmospheric fluidized bed combustion. *Ind. Eng. Chem. Res.* 31:2286-2292.

Adanez J., de Diego L.F., and Gayan P. (1995). A model for prediction of carbon combustion efficiency in circulating fluidized bed combustors. *Fuel* 74:1049-1056.

Adanez J., de Diego L.F., and Gayan P. (2001). Circulating fluidized bed combustion in the turbulent regime: modeling of carbon combustion efficiency and sulphur retention. *Fuel* 80:1405-1414.

Agarwal, P. K. (1986).A single particle model for the evolution and combustion of coal volatiles. *Fuel 65*: 803-810.

Arena, U. (1991). Modelling of circulating fluidized bed combustion of a char. *Can. J. Chem.Eng.*69: 860.

Aspen Technology Inc., *Aspen Plus 11.1 Unit Operation Models.* U.S.A.: Cambridge, September 2001.

Aysel T., Topal H. (2003). Co-combustion of olive cake with lignite coal in a circulating fluidized bed. *Fuel* 83:859-867.

Basu P. (1999). Combustion of coal in circulating fluidized bed boiler:a review. *Chemical Engineering Science* 54:5547-5557.

Basu, P., Fraser, S.A. (1991).Circulating Fluidized bed boilers. *Design and operations* (Chapter 4), 95-126.

Basu, P., Subbarao, D. (1986).An experimental investigation of burning rate and mass transfer in a turbulent fluidized bed. *Combustion and Flame 66*: 261-269.

Basu, P., & Yan, Z. (1993). Characterization of the fine char particle combustion in circulating fluidized beds. In L. Rubow, *Proceedings of the 12th international conference on fluidized bed combustion.* San Diego: ASME, 283-288.

Berruti F., Chaouki J. (1995). The hydrodynamics of circulating fluidized beds. *a review. Can. J. Chem. Engng* 73: 579.

Brereton, C. (1997). Combustion performance. In A. Avidan, J. R.Grace, & T. Knowlton, *Circulating fluidized beds*. London:Blackie Academic & Professional, 388.

Burdett, N.A., Gliddon, and Hotchkiss R.S. (1983).SO_3 in coal-fired fluidized bed combustions. *J. Inst.Energy* 56: 119-124.

Chen Y. and Xiaolong G. (2006).Dynamic modeling and simulation of a 410 t/h Pyroflow CFB boiler.*Computer and Chemical engineering*.

Dayton D.C., Belle-Oudry D. (1999). Effect of coal minerals on chlorine and alkali metals released during biomass/coal co-firing. *Energy Fuel* 13:1203-1211.

Froessling N., Gerland B. (1938). *Geophysical* 52:170.

Gaur, S., Reed T.B. (1998). *Thermal Data for Natural and Synthetic Fuels*. New York, Marcel Dekker.

Gayan P., Adanez J. (2003). Circulating fluidized bed co-combustion of coal and biomass. *Fuel* 83: 277-286.

Gharebaagh R.S., Legros R. (1998). Simulation of circulating fluidized bed reactors using ASPEN PLUS. *Fuel* 77: 327-337.

Grace J.R., Avaidan A.A., and Knowlton T.M. (1997). Circulating fluidized beds. *Blackie Academic and Professional.*

Hao Z. and Qian X. (2003). Optimizing pulverized coal combustion performance based on ANN and GA. *Fuel Processing Technology* 85:113-124.

Howard, J.R. (1989). *Fluidized Bed Technology,* Bristol, UK: Adam Hilger.

Huilin L., Guangbo Z.,and Gidaspow D. (2000).A coal combustion model for circulating fluidized bed boilers. *Fuel* 79:165-172.

Jenkins B.M., Baxter L.L. (1998). Combustion properties of biomass. *Fuel Processing Technology* 54:17-46.

Kunii, D, and Levenspiel, O. (1991). *Fluidization Engineering*. New York: Wiley.

Kunii, Daizo. (1999). *Fluidization Engineering*. New York: Wiley.

LaNauze R.D. (1985). *Fundamentals of Coal Combustion, Fluidization, 2nd ed.*, Acadamic, New York, 631-674.

Leckner B., Kaelsson M. (1993). Emissions from circulating fluidized bed combustion of mixtures of wood and coal. *Proceedings of the 12th International Conference on FBC*, New York:ASME, 109-115.

Lee Y.Y. and T. Hyppanen (1989). *FBC Technology for today*, New York:A.M. Manager. ASME, 738-742.

Levenspiel, O. (1999). *Chemical reaction engineering (3rd ed.),* New Delhi:Wiley Eastern Ltd., 368.

Lewis W.K., Gilliland E.R. (1962). Entrainment from fluidized beds. *Chemical Engineering Progress Symposium Series* 58: 38.

Ngampradit N. (2004). *Modeling and Simulation of size reduction of fuels in Circulating Fluidized bed Combustor by considering attrition and fragmentation.* Ph.D.'s thesis, Department of Chemical Technology, Graduate School, Chulalongkorn University.

Oka, S.N. (2004). *Fluidized Bed Combustion*, New York: Marcel Dekker, 331-334.

Pillai, K.K. (1981).The influence of coal type on devolatilization and combustion in fluidized beds. *Journal of Institute of Energy 54*: 142-150.

Robinson W.D. (1986). *The solid Waste Handbook.* A Practical Guide. Wiley, NewYork.

Sabbaghan H., Sotudeh-Gharebagh R. (2004). Modeling the acceleration zone in the riser of circulating fluidized beds. *Powder technology* 142:129-135.

Selcuk N., Degirmenci E. (1997). Evaluation of an improved code for the performance of AFBCs. *Journal of the Institute of Energy,* 70, 31-50.

Sotudeh-Gharebaagh. (1998).Simulation of circulating fluidized bed reactor using ASPEN PLUS. *Fuel* 77: 327-337.

Stenseng, M., Lin, W., Johnsson, J. E., & Johansen, K. D. (1997). Modeling of devolatilization in CFB combustion. In F. D. S. Preto,*Proceedings of the 14th international conference on fluidized bed combustion*, vol. 1 New York: ASME., 117-124.

Todd S. Pugsley, Franco Berruti (1996).A predictive hydrodynamic model for circulating fluidized bed risers. *Power Technology* 89:56-69.

Wang Q., Luo Z., and Li X. (1997). A mathematical model for a circulating fluidized bed (CFB) boiler. *Energy* 24: 633-653.

Wu, S., & Basu, P. (1993). Surface reaction rates of coarse bituminous char particles in the temperature range of 600-1340 K. *Fuel 72*:1429-1433.

Yamamoto K. (2001). Biomass Power Generation by CFB Boiler. *NKK technology review,* 85.

Yamsakulna S. (2000). *Energy management system design for stream power plant.* Master's thesis, Department of Chemical Technology, Graduate School, Chulalongkorn University.
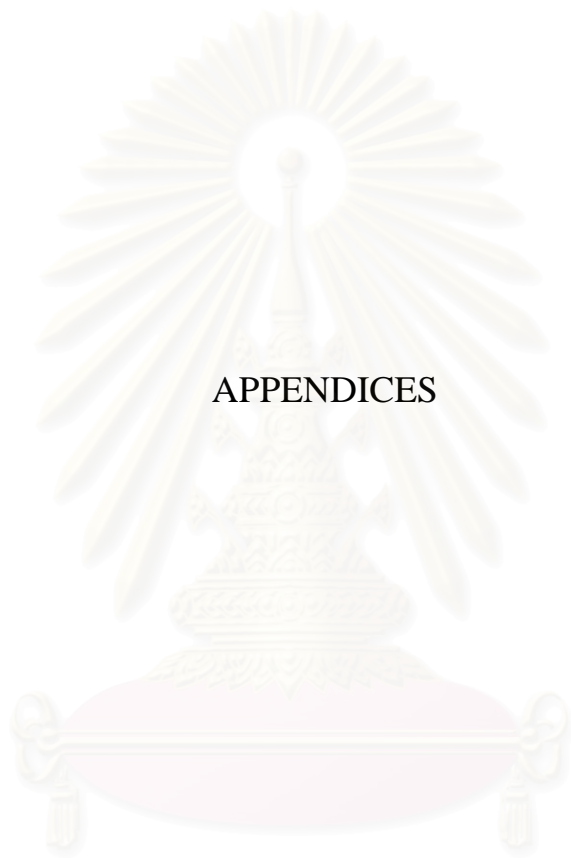
APPENDICES

Appendix A

DIMENSION OF THE CFBC
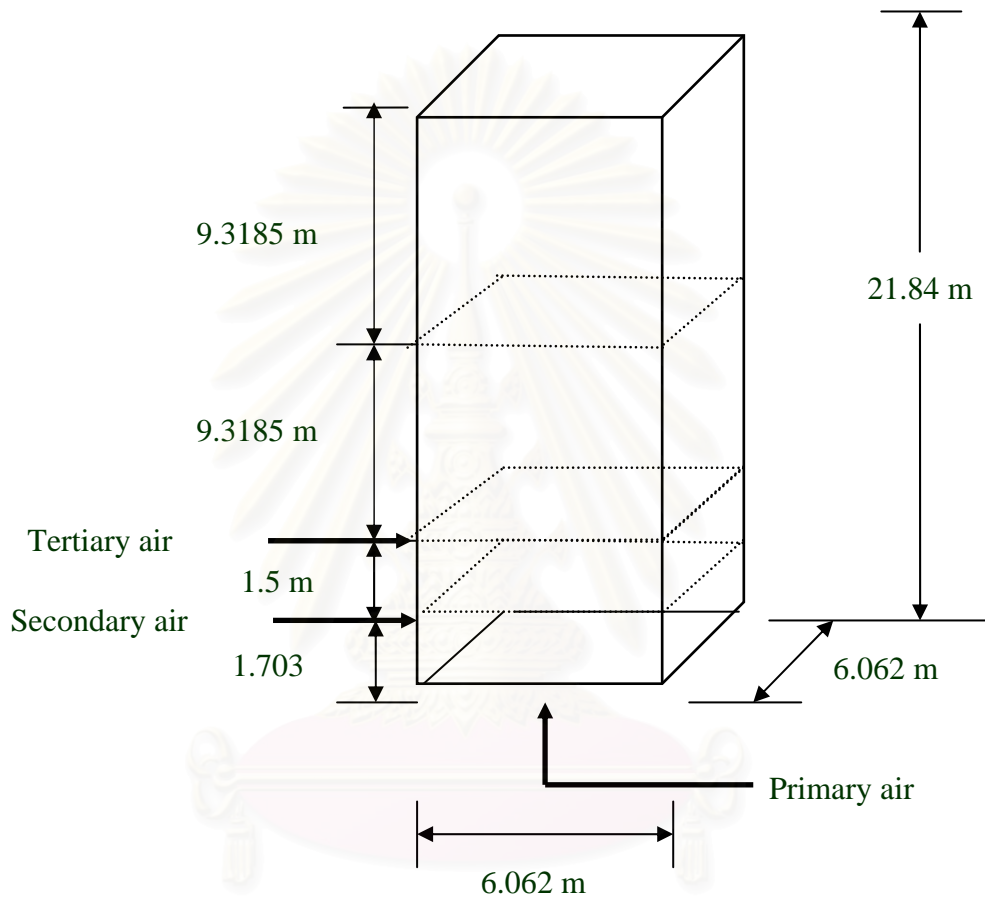
Figure A-1 Dimension of a circulating fluidized bed combustor

Reactor volume of lower region	=	6.062*6.062*1.703	=	62.582	m^3
Reactor volume of first upper region	=	6.062*6.062*1.5	=	55.122	m^3
Reactor volume of second upper region	=	6.062*6.062*9.3185	=	342.435	m^3
Reactor volume of third upper region	=	6.062*6.062*9.3185	=	342.435	m^3
Total reactor volume	=	6.062*6.062*21.84	=	802.574	m^3

Table A-1   Ratio of mixed fuel

Ratio of mixed fuel	Lignite (kg/s)	Bagasse (kg/s)	Volume (m^3)
100% coal	4.0	0	0.0050
90% coal + 10% bagasse	3.6	0.60	0.0095
80% coal + 20% bagasse	3.2	1.13	0.0134
70% coal + 30% bagasse	2.8	1.68	0.0175
60% coal + 40% bagasse	2.4	2.24	0.0216
50% coal + 50% bagasse	2.0	2.80	0.0258
40% coal + 60% bagasse	1.6	3.36	0.0300
30% coal + 70% bagasse	1.2	3.92	0.0342
20% coal + 80% bagasse	0.8	4.48	0.0383
10% coal + 90% bagasse	0.4	5.04	0.0425

Ratio of mixed fuel	Lignite (kg/s)	Rice hush (kg/s)	Volume (m^3)
100% coal	4.0	0	0.0050
90% coal + 10% rice hush	3.6	0.64	0.0087
80% coal + 20% rice hush	3.2	1.27	0.0124
70% coal + 30% rice hush	2.8	1.91	0.0162
60% coal + 40% rice hush	2.4	2.55	0.0200
50% coal + 50% rice hush	2.0	3.18	0.0237
40% coal + 60% rice hush	1.6	3.82	0.0274
30% coal + 70% rice hush	1.2	4.45	0.0312
20% coal + 80% rice hush	0.8	5.09	0.0349
10% coal + 90% rice hush	0.4	5.72	0.0386

Ratio of mixed fuel	Lignite (kg/s)	Bark (kg/s)	Volume (m^3)
100% coal	4.0	0	0.0050
90% coal + 10% bark	3.6	0.56	0.0057
80% coal + 20% bark	3.2	1.13	0.0065
70% coal + 30% bark	2.8	1.69	0.0072
60% coal + 40% bark	2.4	2.25	0.0080
50% coal + 50% bark	2.0	2.82	0.0087
40% coal + 60% bark	1.6	3.37	0.0095
30% coal + 70% bark	1.2	3.94	0.0102
20% coal + 80% bark	0.8	4.50	0.0110
10% coal + 90% bark	0.4	5.06	0.0117

THE EMISSION GAS

Table B-1 The emissions load of flue gas (combustion of lignite), vary combustion temperature.

Emission Load	Temperature (^{o}C)			
	750	800	850	900
C (kg/s)	0.040296636	0.034323246	0.032099280	0.032066113
O_2 (kmole/s)	0.189893600	0.189856900	0.189783400	0.189660400
N_2 (kmole/s)	1.110606000	1.110591000	1.110564000	1.110531000
SO_2 (kmole/s)	0.000095383	0.000095383	0.000095383	0.000095383
CO (kmole/s)	0.000000022	0.000000032	0.000000046	0.000000064
CO_2 (kmole/s)	0.070101400	0.070123300	0.070169100	0.070258900
NOx (kmole/s)	0.000052446	0.000085272	0.000133094	0.000200122
CaO (kg/s)	0.076133920	0.076133920	0.076133940	0.076133970
$CaSO_4$ (kg/s)	0.087212120	0.087212070	0.087212140	0.087212090
Ash (kg/s)	0.521599963	0.521600026	0.521600055	0.521600033

Table B-2 The emissions load of flue gas (combustion of lignite), vary primary air flow rate at 900°C.

Emission load	Volumetric flow rate of primary air (m^3/s)				
	22	23	24	25	26
C (kg/s)	0.032066113	0.032508298	0.032918501	0.033294585	0.033657834
O2 (kmole/s)	0.189660400	0.197821500	0.205582600	0.213543800	0.221505000
N2 (kmole/s)	1.110531000	1.140496000	1.170462000	1.200428000	1.230393000
SO2 (kmole/s)	0.000095383	0.000095383	0.000095383	0.000095383	0.000095383
CO (kmole/s)	0.000000071	0.000000069	0.000000068	0.000000066	0.000000064
CO2 (kmole/s)	0.070261000	0.070260500	0.070260000	0.070259500	0.070258900
NOx (kmole/s)	0.000200122	0.000207039	0.000213946	0.000220844	0.000227733
CaO (kg/s)	0.076133970	0.076133950	0.076133940	0.076133900	0.076133940
CaSO4 (kg/s)	0.087212090	0.087212080	0.087212060	0.087212090	0.087212060
Ash (kg/s)	0.521600033	0.521600000	0.521599977	0.521599975	0.521600036

Table B-3 The emissions load of flue gas (combustion of lignite), vary secondary air flow rate at 900°C.

Emission load	Volumetric flow rate of secondary air (m^3/s)				
	10	11	12	13	14
C (kg/s)	0.032066113	0.033163214	0.033593933	0.033901053	0.034197689
O2 (kmole/s)	0.189660400	0.213543700	0.221504900	0.229466200	0.237427400
N2 (kmole/s)	1.110531000	1.200428000	1.230393000	1.260359000	1.290325000
SO2 (kmole/s)	0.000095383	0.000095383	0.000095383	0.000095383	0.000095383
CO (kmole/s)	0.000000075	0.000000073	0.000000071	0.000000068	0.000000064
CO2 (kmole/s)	0.070261900	0.070261500	0.070261045	0.070260270	0.070258900
NOx (kmole/s)	0.000200122	0.000214900	0.000227733	0.000234616	0.000241491
CaO (kg/s)	0.076133970	0.076133900	0.076133940	0.076133940	0.076133800
CaSO4 (kg/s)	0.087212090	0.087212090	0.087212060	0.087212140	0.087212120
Ash (kg/s)	0.521600033	0.521599975	0.521600036	0.521600050	0.521600005

Table B-4 The emissions load of flue gas, vary the percentage of bagasse added in lignite at 900°C.

Emission load	% Bagasse				
	10%	20%	30%	40%	50%
C (kg/s)	0.03029571	0.02995423	0.02962344	0.02928660	0.02890400
O2 (kmole/s)	0.18830000	0.18990000	0.19150000	0.19339000	0.19534000
N2 (kmole/s)	1.11038900	1.11024200	1.11009500	1.10994900	1.10980300
SO2 (kmole/s)	0.00008754	0.00007950	0.00007152	0.00006357	0.00005561
CO (kmole/s)	0.00000333	0.00000329	0.00000324	0.00000320	0.00000317
CO2 (kmole/s)	0.07909200	0.07903500	0.07896800	0.07894300	0.07888600
NOx (kmole/s)	0.00019883	0.00019978	0.00020064	0.00020179	0.00020274
CaO (kg/s)	0.07908698	0.08211451	0.08512080	0.08775642	0.09111200
CaSO4 (kg/s)	0.08004301	0.07269276	0.06539430	0.05812162	0.05084904
Ash (kg/s)	0.48407993	0.44485519	0.40611194	0.36761588	0.32911982

Table B-5   The emissions load of flue gas**,** vary the percentage of bagasse added in lignite at 850°C.

Emission load	% Bagasse				
	10%	20%	30%	40%	50%
C (kg/s)	0.03100041	0.03080651	0.03072578	0.03056720	0.03036680
O2 (kmole/s)	0.18585870	0.18925640	0.19238700	0.19538400	0.19838110
N2 (kmole/s)	1.11042200	1.11027400	1.11012800	1.10998200	1.10983700
SO2 (kmole/s)	0.00008754	0.00007950	0.00007152	0.00006357	0.00005561
CO (kmole/s)	0.00000359	0.00000354	0.00000350	0.00000346	0.00000342
CO2 (kmole/s)	0.07703650	0.07666660	0.07653980	0.07653450	0.07652910
NOx (kmole/s)	0.00013162	0.00013283	0.00013392	0.00013497	0.00013600
CaO (kg/s)	0.07908694	0.08211450	0.08512076	0.08734360	0.09111202
CaSO4 (kg/s)	0.08004296	0.07269271	0.06539398	0.05780260	0.05084911
Ash (kg/s)	0.48407992	0.44485198	0.40611192	0.36007511	0.32911992

Table B-6   The emissions load of flue gas**,** vary the percentage of bagasse added in lignite at 800°C.

Emission load	% Bagasse				
	10%	20%	30%	40%	50%
C (kg/s)	0.03418100	0.03360363	0.03321352	0.03303110	0.03280760
O2 (kmole/s)	0.18775390	0.19115390	0.19428460	0.19728170	0.20027890
N2 (kmole/s)	1.11044800	1.11030100	1.11015500	1.11001000	1.10986400
SO2 (kmole/s)	0.00008754	0.00007950	0.00007152	0.00006357	0.00005561
CO (kmole/s)	0.00000394	0.00000389	0.00000384	0.00000379	0.00000374
CO2 (kmole/s)	0.07516840	0.07479640	0.07466960	0.07466420	0.07465890
NOx (kmole/s)	0.00008477	0.00008554	0.00008625	0.00008691	0.00008757
CaO (kg/s)	0.07908692	0.08211453	0.08512080	0.08811645	0.09111201
CaSO4 (kg/s)	0.08004293	0.07269276	0.06539425	0.05812171	0.05084904
Ash (kg/s)	0.48407994	0.44485183	0.40611190	0.36761585	0.32911980

Table B-7 The emissions load of flue gas, vary the percentage of bagasse added in lignite at 750°C.

Emission load	% Bagasse				
	10%	20%	30%	40%	50%
C (kg/s)	0.03960768	0.03897804	0.03837520	0.03778970	0.03716600
O2 (kmole/s)	0.18920260	0.19260060	0.19573140	0.19872870	0.20172600
N2 (kmole/s)	1.11046300	1.11031600	1.11017000	1.11002500	1.10987900
SO2 (kmole/s)	0.00008754	0.00007950	0.00007152	0.00006357	0.00005561
CO (kmole/s)	0.00000439	0.00000433	0.00000428	0.00000423	0.00000418
CO2 (kmole/s)	0.07373410	0.07336430	0.07323750	0.07323220	0.07322680
NOx (kmole/s)	0.00005234	0.00005281	0.00005325	0.00005366	0.00005406
CaO (kg/s)	0.07908695	0.08211455	0.08512077	0.08811644	0.09111199
CaSO4 (kg/s)	0.08004298	0.07269274	0.06539431	0.05812171	0.05084911
Ash (kg/s)	0.48407990	0.44485191	0.40611190	0.36761587	0.32911994

Table B-8 The emissions load of flue gas, vary the percentage of bark added in lignite at 900°C.

Emission load	% Bark				
	10%	20%	30%	40%	50%
C (kg/s)	0.03080245	0.03060625	0.03020328	0.02980350	0.02940680
O2 (kmole/s)	0.18598430	0.18752910	0.18923040	0.19093180	0.19247640
N2 (kmole/s)	1.11039200	1.11025400	1.11011400	1.10997500	1.10983600
SO2 (kmole/s)	0.00008584	0.00007631	0.00006677	0.00005723	0.00004769
CO (kmole/s)	0.00000207	0.00000203	0.00000201	0.00000198	0.00000196
CO2 (kmole/s)	0.07571050	0.07566840	0.07562850	0.07560890	0.07558320
NOx (kmole/s)	0.00019812	0.00019893	0.00019982	0.00020071	0.00020150
CaO (kg/s)	0.07972623	0.08331857	0.08691088	0.09050322	0.09409545
CaSO4 (kg/s)	0.07849091	0.06976971	0.06104844	0.05232724	0.04360598
Ash (kg/s)	0.48523190	0.44914588	0.41277794	0.37640988	0.33989391

Table B-9   The emissions load of flue gas**,** vary the percentage of bark added in lignite at 850°C.

Emission load	% Bark				
	10%	20%	30%	40%	50%
C (kg/s)	0.03193700	0.03186590	0.03156370	0.03124100	0.03072140
O2 (kmole/s)	0.18745660	0.18900140	0.19070280	0.19240430	0.19394930
N2 (kmole/s)	1.11042500	1.11028600	1.11014700	1.11000800	1.10986900
SO2 (kmole/s)	0.00008584	0.00007631	0.00006677	0.00005723	0.00004769
CO (kmole/s)	0.00000227	0.00000223	0.00000220	0.00000217	0.00002146
CO2 (kmole/s)	0.07415800	0.07424000	0.07420110	0.07416230	0.07424400
NOx (kmole/s)	0.00013220	0.00013273	0.00013332	0.00013391	0.00013444
CaO (kg/s)	0.07972626	0.08331853	0.08691085	0.09050318	0.09409538
CaSO4 (kg/s)	0.07849084	0.06976966	0.06104846	0.05232720	0.04360603
Ash (kg/s)	0.48523198	0.44914581	0.41277791	0.35110938	0.34032389

Table B-10   The emissions load of flue gas**,** vary the percentage of bark added in lignite at 800°C.

Emission load	% Bark				
	10%	20%	30%	40%	50%
C (kg/s)	0.03509110	0.03459706	0.03382521	0.03327060	0.03299140
O2 (kmole/s)	0.18868340	0.19016560	0.19186820	0.19357010	0.19511500
N2 (kmole/s)	1.11045200	1.11031300	1.11017400	1.11003500	1.11098960
SO2 (kmole/s)	0.00008584	0.00007631	0.00006677	0.00005723	0.00004769
CO (kmole/s)	0.00000248	0.00000249	0.00000246	0.00000243	0.00000240
CO2 (kmole/s)	0.07295860	0.07310320	0.07306320	0.07302390	0.07310590
NOx (kmole/s)	0.00008499	0.00008532	0.00008569	0.00008607	0.00008641
CaO (kg/s)	0.07972623	0.08331851	0.08691088	0.09050319	0.09409544
CaSO4 (kg/s)	0.07849090	0.06976963	0.06104844	0.05257905	0.04360606
Ash (kg/s)	0.48523187	0.44914584	0.41277787	0.37640981	0.34032394

Table B-11 The emissions load of flue gas, vary the percentage of bark added in lignite at 750°C.

Emission load	% Bark				
	10%	20%	30%	40%	50%
C (kg/s)	0.03976999	0.03915047	0.03854270	0.03785610	0.03721560
O2 (kmole/s)	0.18952080	0.19106570	0.19276740	0.19446910	0.19601400
N2 (kmole/s)	1.11046700	1.11032800	1.11018900	1.11005000	1.10991100
SO2 (kmole/s)	0.00008584	0.00007631	0.00006677	0.00005723	0.00004769
CO (kmole/s)	0.00000288	0.00000284	0.00000280	0.00000276	0.00000273
CO2 (kmole/s)	0.07213570	0.07221770	0.07217870	0.07213980	0.07222180
NOx (kmole/s)	0.00005259	0.00005275	0.00005283	0.00005306	0.00005327
CaO (kg/s)	0.07972627	0.08331856	0.08691087	0.09050313	0.08870885
CaSO4 (kg/s)	0.07849093	0.06976970	0.06104841	0.05232726	0.04360602
Ash (kg/s)	0.48523187	0.44914591	0.41277795	0.37640992	0.34032388

Table B-12 The emissions load of flue gas, vary the percentage of rice husk added in lignite at 900°C.

Emission load	% Rice husk				
	10%	20%	30%	40%	50%
C (kg/s)	0.03014829	0.02988049	0.02956454	0.02920940	0.02877370
O2 (kmole/s)	0.18215920	0.18337360	0.18444090	0.18550830	0.18672270
N2 (kmole/s)	1.11047900	1.11042300	1.11036900	1.11031500	1.11025900
SO2 (kmole/s)	0.00008714	0.00007887	0.00007063	0.00006238	0.00005412
CO (kmole/s)	0.00000328	0.00000324	0.00000319	0.00000315	0.00000312
CO2 (kmole/s)	0.07886580	0.07884680	0.07883120	0.07881650	0.07880300
NOx (kmole/s)	0.00019606	0.00019670	0.00019727	0.00019783	0.00019847
CaO (kg/s)	0.07923911	0.08235195	0.08545718	0.08856245	0.09167522
CaSO4 (kg/s)	0.07967337	0.07211623	0.06457763	0.05703893	0.04948173
Ash (kg/s)	0.56710390	0.61108197	0.65658585	0.70208987	0.74606710

Table B-13 The emissions load of flue gas, vary the percentage of rice husk added in lignite at 850°C.

Emission load	% Rice husk				
	10%	20%	30%	40%	50%
C (kg/s)	0.03076151	0.03071956	0.03064420	0.03046670	0.03021150
O2 (kmole/s)	0.18451610	0.18573060	0.18679820	0.18786550	0.18908000
N2 (kmole/s)	1.11051100	1.11045500	1.11040100	1.11034700	1.11029100
SO2 (kmole/s)	0.00008714	0.00007887	0.00007063	0.00006238	0.00005412
CO (kmole/s)	0.00000356	0.00000351	0.00000346	0.00000342	0.00000338
CO2 (kmole/s)	0.07654090	0.07647170	0.07650940	0.07654730	0.07647820
NOx (kmole/s)	0.00013114	0.00013157	0.00013194	0.00013232	0.00013274
CaO (kg/s)	0.07923919	0.08235201	0.08545719	0.08856238	0.09167526
CaSO4 (kg/s)	0.07967343	0.07211625	0.06457754	0.05703890	0.04948181
Ash (kg/s)	0.56710393	0.61108186	0.65658591	0.70208980	0.74606783

Table B-14 The emissions load of flue gas, vary the percentage of rice husk added in lignite at 800°C.

Emission load	% Rice husk				
	10%	20%	30%	40%	50%
C (kg/s)	0.03407873	0.03350530	0.03314788	0.03295500	0.03261580
O2 (kmole/s)	0.18646840	0.18746330	0.18865470	0.18972220	0.19093670
N2 (kmole/s)	1.11053800	1.11048200	1.11042800	1.11037400	1.11031900
SO2 (kmole/s)	0.00008714	0.00007887	0.00007063	0.00006238	0.00005412
CO (kmole/s)	0.00000384	0.00000397	0.00000381	0.00000377	0.00000372
CO2 (kmole/s)	0.07461570	0.07476610	0.07468000	0.07471780	0.07464860
NOx (kmole/s)	0.00008448	0.00008470	0.00008497	0.00008520	0.00008547
CaO (kg/s)	0.07923914	0.08235193	0.08545718	0.08856243	0.09167525
CaSO4 (kg/s)	0.07967345	0.07211628	0.06457754	0.05703893	0.04948171
Ash (kg/s)	0.56710397	0.61108186	0.65658588	0.70208983	0.74606793

Table B-15   The emissions load of flue gas**,** vary the percentage of rice husk added in lignite at 750°C.

Emission load	% Rice husk				
	10%	20%	30%	40%	50%
C (kg/s)	0.03960600	0.03886570	0.03808520	0.03758970	0.03695530
O2 (kmole/s)	0.18779570	0.18901040	0.19007790	0.19114560	0.19236020
N2 (kmole/s)	1.11055200	1.11049600	1.11044300	1.11038900	1.11033300
SO2 (kmole/s)	0.00008714	0.00007887	0.00007063	0.00006238	0.00005412
CO (kmole/s)	0.00000440	0.00000434	0.00000428	0.00000423	0.00000418
CO2 (kmole/s)	0.07330270	0.07323340	0.07327120	0.07330900	0.07323980
NOx (kmole/s)	0.00005214	0.00005231	0.00005245	0.00005260	0.00005276
CaO (kg/s)	0.07923913	0.08235202	0.08545720	0.08856244	0.09167524
CaSO4 (kg/s)	0.07967343	0.07211629	0.06457761	0.05703889	0.04948172
Ash (kg/s)	0.56710377	0.61108201	0.65658597	0.70208997	0.74606802

Table B-16   The emissions load of flue gas**,** vary Ca/S molar ratio at 900°C.

Ca/S (mole ratio)	Emission load of fluegas					
	O$_2$ (kmole/s)	CO$_2$ (kmole/s)	CO (kmole/s)	SO$_2$ (kmole/s)	NOx (kmole/s)	C (kg/s)
0.5	0.18979299	0.06923013	0.00000006447	0.00009545	0.0002003	0.03213893
1.0	0.18967959	0.07019919	0.00000006451	0.00009539	0.0002001	0.03218441
1.5	0.18956634	0.07098865	0.00000006455	0.00009534	0.0002000	0.03221029
2.0	0.18945319	0.07186642	0.00000006459	0.00009528	0.0001999	0.03223609

Appendix C

ASPEN PLUS input file

TITLE 'Mixed coal and bagasse'

IN-UNITS SI

DEF-STREAMS CONVEN ALL

SIM-OPTIONS
  IN-UNITS ENG
  SIM-OPTIONS FLASH-MAXIT=500

ACCOUNT-INFO ACCOUNT=2 PROJECT-ID=2 PROJECT-NAME="2" &
    USER-NAME="2"

RUN-CONTROL MAX-FORT-ERR=200

DESCRIPTION"
  In block RCSTR

  REAL (1)   = Total volumetric flow rate to RCSTR
  REAL (2-6)   = Radius of particle lignite input stream (m)
  REAL (7-11)   = Radius of particle bagasse input stream (m)
  REAL (15)   = Oxygen concentration
  REAL (16-20) = Radius of particle recycle stream of lignite (m)
  REAL (21-25) = Radius of particle recycle stream of bagasse (m)
  REAL (26-30) = Mean radius of mixed particle for lignite (m)
  REAL (31-35) = Mean radius of mixed particle for bagasse (m)
  REAL (36)   = Maximum error tolerance for mass balance
  REAL (37)   = Tolerance for mass balance
  REAL (38)   = Molar density in mixed stream
  REAL (39)   = Viscosity of mixed stream
  "
DATABANKS PURE11 / AQUEOUS / SOLIDS / INORGANIC / &
  NOASPENPCD

PROP-SOURCES PURE11 / AQUEOUS / SOLIDS / INORGANIC
COMPONENTS
  C C /
  O2 O2 /
  N2 N2 /
  CO CO /
  CO2 CO2 /
  H2 H2 /
  H2O H2O /

```
    S S /
    SO2 O2S /
    NO NO /
    N2O N2O /
    NO2 NO2 /
    CACO3 CACO3 /
    CAO CAO /
    CASO4 CASO4 /
    ASH /
    LIGNITE /
    BAGASSE
FLOWSHEET
    BLOCK B2 IN=LIGNITE OUT=S1
    BLOCK B3 IN=S1 AIR1 LIME S2 OUT=S3
    BLOCK B1 IN=BAGASSE OUT=S2
    BLOCK B4 IN=S3 RESOLID OUT=S4
    BLOCK B5 IN=S4 OUT=S5 S6
    BLOCK B6 IN=S5 S6 OUT=S7
    BLOCK B7 IN=S7 AIR2 OUT=S8
    BLOCK B8 IN=S8 OUT=S9
    BLOCK B9 IN=S9 OUT=S10 S11
    BLOCK B10 IN=S10 S11 AIR3 OUT=S12
    BLOCK B11 IN=S12 OUT=S13
    BLOCK B12 IN=S13 OUT=S14 S15
    BLOCK B13 IN=S14 S15 OUT=S16
    BLOCK B14 IN=S16 OUT=S17
    BLOCK B15 IN=S17 OUT=S18 S19
    BLOCK B16 IN=S18 S19 OUT=S20
    BLOCK B17 IN=S20 WATER OUT=S21 STEAM
    BLOCK B18 IN=S21 OUT=FLUEGAS S22
    BLOCK B19 IN=S22 OUT=BOTTOM FLYASH RESOLID


PROPERTIES SYSOP0


NC-COMPS ASH PROXANAL ULTANAL SULFANAL


NC-PROPS ASH ENTHALPY HCOALGEN / DENSITY DCOALIGT


NC-COMPS LIGNITE PROXANAL ULTANAL SULFANAL


NC-PROPS LIGNITE ENTHALPY HCOALGEN / DENSITY DCOALIGT


NC-COMPS BAGASSE PROXANAL ULTANAL SULFANAL


NC-PROPS BAGASSE ENTHALPY HCOALGEN / DENSITY DCOALIGT


DEF-SUBS-ATTR PSD PSD
    IN-UNITS ENG
    INTERVALS 5
    SIZE-LIMITS 0.0 <meter> / 5E-005 <meter> / 0.0001 <meter> /  &
        0.0002 <meter> / 0.0005 <meter> / 0.001 <meter>
```

DEF-SUBS-ATTR PSD1 PSD
  INTERVALS 5
  SIZE-LIMITS 0. <mm> / 1. <mm> / 40. <mm> / 75. <mm> / &
    76. <mm> / 77. <mm>

DEF-SUBS-ATTR PSD2 PSD
  INTERVALS 5
  SIZE-LIMITS 0. <mm> / 3.175 <mm> / 4. <mm> / 5. <mm> / &
    6. <mm> / 7. <mm>

DEF-SUBS CISOLID CISOLID

DEF-SUBS-CLA CISOLID
  DEF TYPE=CISOLID ATTR=PSD

DEF-SUBS CIPSD1 CIPSD1

DEF-SUBS-CLA CIPSD1
  DEF TYPE=CISOLID ATTR=PSD1

DEF-SUBS NCPSD1 NCPSD1

DEF-SUBS-CLA NCPSD1
  DEF TYPE=NC ATTR=PSD1

DEF-SUBS CIPSD2 CIPSD2

DEF-SUBS-CLA CIPSD2
  DEF TYPE=CISOLID ATTR=PSD2

DEF-SUBS NCPSD2 NCPSD2

DEF-SUBS-CLA NCPSD2
  DEF TYPE=NC ATTR=PSD2

DEF-STREAM-C CONVEN MIXED CISOLID CIPSD1 NCPSD1 CIPSD2 NCPSD2

PROP-SET PS-1 MUMX SUBSTREAM=MIXED PHASE=V

STREAM AIR1
  SUBSTREAM MIXED TEMP=306. PRES=1. <atm> VOLUME-FLOW=24.
  MOLE-FRAC O2 0.2 / N2 0.7525 / H2O 0.0475

STREAM AIR2
  SUBSTREAM MIXED TEMP=306. PRES=1. <atm> VOLUME-FLOW=12.
  MOLE-FRAC O2 0.2 / N2 0.7525 / H2O 0.0475

STREAM AIR3
  SUBSTREAM MIXED TEMP=306. PRES=1. <atm> VOLUME-FLOW=5.

MOLE-FRAC O2 0.2 / N2 0.7525 / H2O 0.0475

STREAM BAGASSE
  SUBSTREAM NCPSD2 TEMP=306. PRES=1. <atm>
  MASS-FLOW BAGASSE 1E-012
  COMP-ATTR BAGASSE PROXANAL (35.49 7.71 55.23 1.57)
  COMP-ATTR BAGASSE ULTANAL (2.44 48.64 5.87 0.16 0. &
    0.07 42.82)
  COMP-ATTR BAGASSE SULFANAL (0. 0. 0.)
  SUBS-ATTR PSD2 (0.8 0.2 0. 0. 0.)

STREAM LIGNITE
  SUBSTREAM NCPSD1 TEMP=306. PRES=1. <atm>
  MASS-FLOW LIGNITE 4.
  COMP-ATTR LIGNITE PROXANAL (19.86 34.85 34.84 10.45)
  COMP-ATTR LIGNITE ULTANAL (13.04 68.15 5.09 1.24 0. &
    0.59 11.89)
  COMP-ATTR LIGNITE SULFANAL (0. 0. 0.)
  SUBS-ATTR PSD1 (0.08 0.52 0.4 0. 0.)

STREAM LIME
  SUBSTREAM CISOLID TEMP=306. PRES=1. <atm>
  MASS-FLOW CACO3 0.2
  SUBS-ATTR PSD (0.02 0.07 0.45 0.405 0.055)

STREAM RESOLID
  SUBSTREAM CISOLID TEMP=880.0049 PRES=1. <atm>
  MASS-FLOW CAO 0.0088631 / CASO4 0.00717517
  SUBS-ATTR PSD (0.0139674 0.0636379 0.4464362 0.4187024 &
    0.0572559)
  SUBSTREAM CIPSD1 TEMP=880.0049 PRES=1. <atm>
  MASS-FLOW C 1.470247
  SUBS-ATTR PSD1 (1. 0. 0. 0. 0.)
  SUBSTREAM CIPSD2 TEMP=880.0049 PRES=1. <atm>
  MASS-FLOW C 0.6808252
  SUBS-ATTR PSD2 (0.0288329 0.971167 0. 0. 0.)

STREAM WATER
  SUBSTREAM MIXED TEMP=406. PRES=106.6 <barg>
  MASS-FLOW H2O 30.6

BLOCK B17 HEATX
  PARAM T-COLD=510. CALC-TYPE=RATING TYPE=COCURRENT &
    PRES-HOT=1. <atm> PRES-COLD=100. <barg> U-OPTION=FILM-COEF &
    F-OPTION=GEOMETRY CALC-METHOD=DETAILED
  FEEDS HOT=S20 COLD=WATER
  PRODUCTS HOT=S21 COLD=STEAM
  EQUIP-SPECS ORIENTATION=VERTICAL SHELL-DIAM=6.8
  TUBES TOTAL-NUMBER=272 TUBE-TYPE=FINNED LENGTH=15. &
    INSIDE-DIAM=52.32 <mm> OUTSIDE-DIAM=63.3 <mm> &

PITCH=88. <mm>

FINS HEIGHT=5. <mm> THICKNESS=5.

SEGB-SHELL NBAFFLE=268 BAFFLE-CUT=0.005

HOT-SIDE H-OPTION=GEOMETRY SHELL-TUBE=TUBE DP-OPTION=CONSTANT

COLD-SIDE H-OPTION=GEOMETRY DP-OPTION=CONSTANT

BLOCK B3 RSTOIC

PARAM TEMP=1173. PRES=1. <atm> NPHASE=1 PHASE=V

STOIC 1 CIPSD1 C -2. / MIXED O2 -1. / CO 2.

STOIC 2 CIPSD1 S -1. / MIXED O2 -1. / SO2 1.

STOIC 3 CIPSD2 C -2. / MIXED O2 -1. / CO 2.

STOIC 4 CIPSD2 S -1. / MIXED O2 -1. / SO2 1.

STOIC 5 MIXED H2 -2. / O2 -1. / H2O 2.

CONV 1 CIPSD1 C 0.3

CONV 2 CIPSD1 S 1.

CONV 3 CIPSD2 C 0.3

CONV 4 CIPSD2 S 1.

CONV 5 MIXED H2 1.

BLOCK-OPTION FREE-WATER=NO

BLOCK B6 RSTOIC

PARAM TEMP=1173. PRES=1. <atm> NPHASE=1 PHASE=V

STOIC 1 CISOLID CACO3 -1. / CAO 1. / MIXED CO2 1.

STOIC 2 CISOLID CAO -2. / MIXED SO2 -2. / O2 -1. / &

CISOLID CASO4 2.

CONV 1 CISOLID CACO3 1.

CONV 2 MIXED SO2 0.4

BLOCK-OPTION FREE-WATER=NO

BLOCK B7 RSTOIC

PARAM TEMP=1173. PRES=1. <atm> NPHASE=1 PHASE=V

STOIC 1 CIPSD1 S -1. / MIXED O2 -1. / SO2 1.

STOIC 2 CIPSD2 S -1. / MIXED O2 -1. / SO2 1.

STOIC 3 MIXED H2 -2. / O2 -1. / H2O 2.

CONV 1 CIPSD1 S 1.

CONV 2 CIPSD2 S 1.

CONV 3 MIXED H2 1.

BLOCK-OPTION FREE-WATER=NO

BLOCK B10 RSTOIC

PARAM TEMP=1173. PRES=1. <atm> NPHASE=1 PHASE=V

STOIC 1 CISOLID CAO -1. / MIXED SO2 -1. / O2 -0.5 / &

CISOLID CASO4 1.

CONV 1 MIXED SO2 0.4

BLOCK-OPTION FREE-WATER=NO

BLOCK B13 RSTOIC

PARAM TEMP=1173. PRES=1. <atm> NPHASE=1 PHASE=V

STOIC 1 CISOLID CAO -1. / MIXED SO2 -1. / O2 -0.5 / &

CISOLID CASO4 1.

    CONV 1 MIXED SO2 0.4
    BLOCK-OPTION FREE-WATER=NO

BLOCK B16 RSTOIC
    PARAM TEMP=1173. PRES=1. <atm> NPHASE=1 PHASE=V
    STOIC 1 CISOLID CAO -1. / MIXED SO2 -1. / O2 -0.5 / &
        CISOLID CASO4 1.
    CONV 1 MIXED SO2 0.4
    BLOCK-OPTION FREE-WATER=NO

BLOCK B1 RYIELD
    PARAM TEMP=1173. PRES=1. <atm> NPHASE=1 PHASE=V
    MASS-YIELD CIPSD2 C 0.4864 / MIXED H2 0.0587 / N2 &
        0.0016 / CIPSD2 S 0.0007 / MIXED O2 0.4282 / NCPSD2 &
        ASH 0.0244
    BLOCK-OPTION FREE-WATER=NO
    COMP-ATTR NCPSD2 ASH PROXANAL (0. 0. 0. 100.)
    COMP-ATTR NCPSD2 ASH ULTANAL (100. 0. 0. 0. 0. 0. 0. &
)
    COMP-ATTR NCPSD2 ASH SULFANAL (0. 0. 0.)
    SUBS-ATTR 1 CIPSD2 PSD2 (0.8 0.2 0. 0. 0.)

BLOCK B2 RYIELD
    PARAM TEMP=1173. PRES=1. <atm> NPHASE=1 PHASE=V
    MASS-YIELD CIPSD1 C 0.6815 / MIXED H2 0.0509 / N2 &
        0.0124 / CIPSD1 S 0.0059 / MIXED O2 0.1189 / NCPSD1 &
        ASH 0.1304
    BLOCK-OPTION FREE-WATER=NO
    COMP-ATTR NCPSD1 ASH PROXANAL (0. 0. 0. 100.)
    COMP-ATTR NCPSD1 ASH ULTANAL (100. 0. 0. 0. 0. 0. 0. &
)
    COMP-ATTR NCPSD1 ASH SULFANAL (0. 0. 0.)
    SUBS-ATTR 1 CIPSD1 PSD1 (0.08 0.52 0.4 0. 0.)

BLOCK B5 REQUIL
    PARAM NREAC=3 TEMP=1173. PRES=1. <atm> NPHASE=1 PHASE=V
    STOIC 1 N2 -0.5 * / O2 -0.5 * / NO 1. *
    STOIC 2 N2 -1. * / O2 -0.5 * / N2O 1. *
    STOIC 3 N2 -0.5 * / O2 -1. * / NO2 1. *
    TAPP-SPEC 1 0.0 / 2 0.0 / 3 0.0
    FRAC CISOLID
    FRAC CIPSD1
    FRAC NCPSD1
    FRAC CIPSD2
    FRAC NCPSD2

BLOCK B9 REQUIL
    PARAM NREAC=3 TEMP=1173. PRES=1. <atm> NPHASE=1 PHASE=V
    STOIC 1 N2 -0.5 * / O2 -0.5 * / NO 1. *
    STOIC 2 N2 -1. * / O2 -0.5 * / N2O 1. *

```
    STOIC 3 N2 -0.5 * / O2 -1. * / NO2 1. *
    TAPP-SPEC 1 0.0 / 2 0.0 / 3 0.0
    FRAC CISOLID
    FRAC CIPSD1
    FRAC NCPSD1
    FRAC CIPSD2
    FRAC NCPSD2


BLOCK B12 REQUIL
    PARAM NREAC=3 TEMP=1173. PRES=1. <atm> NPHASE=1 PHASE=V
    STOIC 1 N2 -0.5 * / O2 -0.5 * / NO 1. *
    STOIC 2 N2 -1. * / O2 -0.5 * / N2O 1. *
    STOIC 3 N2 -0.5 * / O2 -1. * / NO2 1. *
    TAPP-SPEC 1 0.0 / 2 0.0 / 3 0.0
    FRAC CISOLID
    FRAC CIPSD1
    FRAC NCPSD1
    FRAC CIPSD2
    FRAC NCPSD2


BLOCK B15 REQUIL
    PARAM NREAC=3 TEMP=1173. PRES=1. <atm> NPHASE=1 PHASE=V
    STOIC 1 N2 -0.5 * / O2 -0.5 * / NO 1. *
    STOIC 2 N2 -1. * / O2 -0.5 * / N2O 1. *
    STOIC 3 N2 -0.5 * / O2 -1. * / NO2 1. *
    TAPP-SPEC 1 0.0 / 2 0.0 / 3 0.0
    FRAC CISOLID
    FRAC CIPSD1
    FRAC NCPSD1
    FRAC CIPSD2
    FRAC NCPSD2

BLOCK B4 RCSTR
    USER-VECS NREAL=40
    REAL VALUE-LIST=* 0.0005 0.0205 0.0575 * * 0.0015875  &
        0.0035875
    PARAM VOL=61.84 TEMP=1173. PRES=1. <atm> MB-MAXIT=500
    CONVERGENCE SOLVER=NEWTON
    REACTIONS RXN-IDS=R-1

BLOCK B8 RCSTR
    USER-VECS NREAL=40
    PARAM VOL=54.75 TEMP=1173. PRES=1. <atm> MB-MAXIT=500
    CONVERGENCE SOLVER=NEWTON
    REACTIONS RXN-IDS=R-2

BLOCK B11 RCSTR
    USER-VECS NREAL=40
    PARAM VOL=338.4 TEMP=1173. PRES=1. <atm> MB-MAXIT=500
```

```
    CONVERGENCE SOLVER=NEWTON
    REACTIONS RXN-IDS=R-3


BLOCK B14 RCSTR
    USER-VECS NREAL=40
    PARAM VOL=338.4 TEMP=1173. PRES=1. <atm> MB-MAXIT=500
    CONVERGENCE SOLVER=NEWTON
    REACTIONS RXN-IDS=R-4


BLOCK B19 SSPLIT
    FRAC MIXED BOTTOM 0. / FLYASH 1.
    FRAC CISOLID BOTTOM 0.1 / FLYASH 0.8
    FRAC CIPSD1 BOTTOM 0. / FLYASH 0.
    FRAC NCPSD1 BOTTOM 0.2 / FLYASH 0.8
    FRAC CIPSD2 BOTTOM 0. / FLYASH 0.
    FRAC NCPSD2 BOTTOM 0.2 / FLYASH 0.8


BLOCK B18 CYCLONE
    PARAM TYPE=MEDIUM
    SIMULATION DIAM=5.


EO-CONV-OPTI


CALCULATOR C-1
F    COMMON/USER4/VFTOT,CONO2,VIS,VVOID,DPSD,FMOLE,VAIR1,BEDVV
F    COMMON/USER5/FCPSD,FCRPS,WFPSD,RWFPSD
F
F
F    REAL*8 VVOID(4),DPSD(2),WFPSD(5,2),WFRPSD(5,2), FRAC(3),
F    +    FCPSD(2),FCRPS(2),FMOLE(2),BEDVV(4)
F
F    DATA BEDW/6.026/
    DEFINE MFPSD1 STREAM-VAR STREAM=S3 SUBSTREAM=CIPSD1 &
        VARIABLE=MASS-FLOW
    DEFINE MFPSD2 STREAM-VAR STREAM=S3 SUBSTREAM=CIPSD2 &
        VARIABLE=MASS-FLOW
    DEFINE MFLIME STREAM-VAR STREAM=LIME SUBSTREAM=CISOLID &
        VARIABLE=MASS-FLOW
    DEFINE MFAIR1 STREAM-VAR STREAM=AIR1 SUBSTREAM=MIXED &
        VARIABLE=MASS-FLOW
    DEFINE MFNC1 STREAM-VAR STREAM=S3 SUBSTREAM=NCPSD1 &
        VARIABLE=MASS-FLOW
    DEFINE MFNC2 STREAM-VAR STREAM=S3 SUBSTREAM=NCPSD2 &
        VARIABLE=MASS-FLOW
    DEFINE MFC1 MASS-FLOW STREAM=S3 SUBSTREAM=CIPSD1 &
        COMPONENT=C
    DEFINE MFC2 MASS-FLOW STREAM=S3 SUBSTREAM=CIPSD2 &
        COMPONENT=C
    DEFINE MFCR1 MASS-FLOW STREAM=RESOLID SUBSTREAM=CIPSD1 &
        COMPONENT=C
```

```
DEFINE MFCR2 MASS-FLOW STREAM=RESOLID SUBSTREAM=CIPSD2  &
    COMPONENT=C
DEFINE MFRPS1 STREAM-VAR STREAM=RESOLID SUBSTREAM=CIPSD1  &
    VARIABLE=MASS-FLOW
DEFINE MFRPS2 STREAM-VAR STREAM=RESOLID SUBSTREAM=CIPSD2  &
    VARIABLE=MASS-FLOW
DEFINE MFRNC1 STREAM-VAR STREAM=RESOLID SUBSTREAM=NCPSD1  &
    VARIABLE=MASS-FLOW
DEFINE MFRNC2 STREAM-VAR STREAM=RESOLID SUBSTREAM=NCPSD2  &
    VARIABLE=MASS-FLOW
DEFINE MFRLIM STREAM-VAR STREAM=RESOLID SUBSTREAM=CISOLID  &
    VARIABLE=MASS-FLOW
DEFINE MOFPS1 STREAM-VAR STREAM=S3 SUBSTREAM=CIPSD1  &
    VARIABLE=MOLE-FLOW
DEFINE MOFPS2 STREAM-VAR STREAM=S3 SUBSTREAM=CIPSD2  &
    VARIABLE=MOLE-FLOW
DEFINE MDPSD1 STREAM-VAR STREAM=S3 SUBSTREAM=CIPSD1  &
    VARIABLE=MASS-DENSITY
DEFINE MDPSD2 STREAM-VAR STREAM=S3 SUBSTREAM=CIPSD2  &
    VARIABLE=MASS-DENSITY
DEFINE MDLIME STREAM-VAR STREAM=LIME SUBSTREAM=CISOLID  &
    VARIABLE=MASS-DENSITY
DEFINE MDRLIM STREAM-VAR STREAM=RESOLID SUBSTREAM=CISOLID  &
    VARIABLE=MASS-DENSITY
DEFINE MDAIR1 STREAM-VAR STREAM=AIR1 SUBSTREAM=MIXED  &
    VARIABLE=MASS-DENSITY
DEFINE MDNC1 STREAM-VAR STREAM=S3 SUBSTREAM=NCPSD1  &
    VARIABLE=MASS-DENSITY
DEFINE MDMC2 STREAM-VAR STREAM=S3 SUBSTREAM=NCPSD2  &
    VARIABLE=MASS-DENSITY
DEFINE MDRPS1 STREAM-VAR STREAM=RESOLID SUBSTREAM=CIPSD1  &
    VARIABLE=MASS-DENSITY
DEFINE MDRPS2 STREAM-VAR STREAM=RESOLID SUBSTREAM=CIPSD2  &
    VARIABLE=MASS-DENSITY
VECTOR-DEF PSD1 SUBS-ATTR STREAM=S3 SUBSTREAM=CIPSD1  &
    ATTRIBUTE=PSD1
VECTOR-DEF PSD2 SUBS-ATTR STREAM=S3 SUBSTREAM=CIPSD2  &
    ATTRIBUTE=PSD2
VECTOR-DEF RPSD1 SUBS-ATTR STREAM=RESOLID SUBSTREAM=CIPSD1  &
    ATTRIBUTE=PSD1
VECTOR-DEF RPSD2 SUBS-ATTR STREAM=RESOLID SUBSTREAM=CIPSD2  &
    ATTRIBUTE=PSD2
DEFINE MOFRAC MOLE-FRAC STREAM=S3 SUBSTREAM=MIXED  &
    COMPONENT=O2
DEFINE MODMIX STREAM-VAR STREAM=S3 SUBSTREAM=MIXED  &
    VARIABLE=MOLE-DENSITY
DEFINE MODPS1 STREAM-VAR STREAM=S3 SUBSTREAM=CIPSD1  &
    VARIABLE=MOLE-DENSITY
DEFINE MODPS2 STREAM-VAR STREAM=S3 SUBSTREAM=CIPSD2  &
    VARIABLE=MOLE-DENSITY
```

```
    DEFINE VISCO STREAM-PROP STREAM=S3 PROPERTY=PS-1
F    OPEN(7,FILE='F-1.txt')
F
F
C    TOTAL MASS FLOW RATE OF SUBSTREAM CIPSD
F    FTOTAL = MFPSD1+MFPSD2+MFNC1+MFNC2
F    +      +MFRPS1+MFRPS2+MFRNC1+MFRNC2
F    +      +MFLIME+MFRLIM
F
F    WRITE(7,*)'TOTAL FLOW RATE OF CIPSD(kg/s)',FTOTAL
F
C    MEAN MASS DENSITY OF TOTAL FLOW
F    DEN  = (MFPSD1*MDPSD1+MFPSD2*MDPSD2
F    +      +MFNC1*MDNC1+MFNC2*MDNC2
F    +      +MFRPS1*MDRPS1+MFRPS2*MDRPS2
F    +      +MFRNC1*MDRNC1+MFRNC2*MDRNC2
F    +      +MFLIME*MDLIME+MFRLIM*MDRLIM)
F
F    DENS =  1/FTOTAL*DEN
F    WRITE(7,*)'MEAN MASS DENSITY(kg/m^3)',DENS
F
C    VOLUMETRIC FLOW RATE OF TOTAL FLOW
F    VFTOT = FTOTAL/DENS
F    WRITE(7,*)'VOLUMETRIC FLOW RATE OF TOTAL FLOW(m^3/s)',VFSUM
F
C    CONCENTRATION OF OXYGEN
F    CONO2=MOFRAC*MODMIX
F    WRITE(7,*)'CONCENTRATION OF OXYGEN',CONO2
F
C    VISCOSITY OF MIXED STREAM
F    VIS = VISCO
F    WRITE(7,*)'VISCOSITY',VISCO,VIS
F
C    *=============================================================*
C          DEFINED VARIABLE TO EXTERNAL SUBROUTINE
C    *=============================================================*

C    DEFINED MOLAR DENSITY
F    DPSD(1) = MODPS1
F    DPSD(2) = MODPS2
F
F
C    DEFINED MOLAR FLOW RATE
F    FMOLE(1) = MOFPS1
F    FMOLE(2) = MOFPS2
F
F
C    DEFINED MOLE FRACTION FOR CALCULATED
F    FRAC(1) = MOFRAC
F    FRAC(2) = FRACO
```

```
F    FRAC(3) = FRAH2O

F

C    DEFINED MASS FLOW RATE OF CARBON INPUT STREAM

F    FCPSD(1) = MFC1

F    FCPSD(2) = MFC2

F

C    DEFINED MASS FLOW RATE OF CARBON RESOLID STREAM

F    FCRPS(1) = MFCR1

F    FCRPS(2) = MFCR2

F

C    *============================================================*

C         DEFINED VARIABLE TO EXTERNAL SUBROUTINE

C    *============================================================*

F

C    DEFINED MOLAR DENSITY

F    DPSD(1) = MODPS1

F    DPSD(2) = MODPS2

F

C    DEFINED MOLAR FLOW RATE

F    FMOLE(1) = MOFPS1

F    FMOLE(2) = MOFPS2

F

C    DEFINED MOLE FRACTION FOR CALCULATED

F    FRAC(1) = MOFRAC

F    FRAC(2) = FRACO

F    FRAC(3) = FRAH2O

F

C    DEFINED MASS FLOW RATE OF CARBON INPUT STREAM

F    FCPSD(1) = MFC1

F    FCPSD(2) = MFC2

F

C    DEFINED MASS FLOW RATE OF CARBON RESOLID STREAM

F    FCRPS(1) = MFCR1

F    FCRPS(2) = MFCR2

F

C    *============================================================*

C         PREPARE WEIGHT FRACTION OF PSD

C    *============================================================*

F

F    DO 5  I=1,5

F      WFPSD(I,1) = PSD1(I)

F      WFPSD(I,2) = PSD2(I)

F      RWFPSD(I,1)= RPSD1(I)

F 5    RWFPSD(I,2)= RPSD2(I)

F

F

F    WRITE(7,6)((WFPSD(I,J),J=1,2),I=1,5)

F 6  FORMAT(2X,'WFPSD',/2(1X,E10.3))

F    WRITE(7,7)((RWFPSD(I,J),J=1,2),I=1,5)

F 7  FORMAT(2X,'RWFPSD',/2(1X,E10.3))
```

```
F
F
C    *==========================================================*
C              LOWER REGION
C    *==========================================================*
F
C    SECTION AREA OF REACTOR
F    AREA = BEDW**2
F    WRITE(7,*)'AREA',AREA
F

C    VOLUMETRIC FLOW RATE OF AIR
F    VFAIR1 = MFAIR1/MDAIR1
F    WRITE(7,*)'AIR VOLUMETRIC FLOW RATE(m^3/s)',VFAIR1
F
C    AIR VILOCITY(m/s)
F    VAIR1=VFAIR1/AREA
F    WRITE(7,*)'AIR VELOCITY (m/s)',VAIR1
F
C    FUNCTION BETWEEN VELOCITY AND 1-VOIDAGE
F    VOI = -0.0884*DLOG(VAIR1)+0.279
F    VVOID(1)=1.-VOI
F    WRITE(7,*)'MEAN VOIDAGE OF DENSE BED',VVOID(1)
  EXECUTE BEFORE BLOCK B4

CALCULATOR C-2
F    COMMON/USER4/VFTOT,CONO2,VIS,VVOID,DPSD,FMOLE,VAIR1,BEDVV
F    COMMON/USER6/FCPSD1,WF2PSD
F    COMMON/USER7/DPSDU1,FMOLU1,VAIRU1,BEDT2
F
F    REAL*8 VVOID(4),DPSDU1(2),FMOLU1(2),WF2PSD(5,2),
F    +    FCPSD1(2),BEDVV(4),UGAS(4),BEDL(4),BDL(4)
F
F    DATA PHIS/0.806/,BEDLT/21.84/,VOIDS/0.999/,G/9.81/,DP/0.001/
  DEFINE MFPSD1 STREAM-VAR STREAM=S8 SUBSTREAM=CIPSD1 &
    VARIABLE=MASS-FLOW
  DEFINE MFPSD2 STREAM-VAR STREAM=S8 SUBSTREAM=CIPSD2 &
    VARIABLE=MASS-FLOW
  DEFINE MFNC1 STREAM-VAR STREAM=S8 SUBSTREAM=NCPSD1 &
    VARIABLE=MASS-FLOW
  DEFINE MFNC2 STREAM-VAR STREAM=S8 SUBSTREAM=NCPSD2 &
    VARIABLE=MASS-FLOW
  DEFINE MFLIME STREAM-VAR STREAM=S8 SUBSTREAM=CISOLID &
    VARIABLE=MASS-FLOW
  DEFINE MFMIX STREAM-VAR STREAM=S8 SUBSTREAM=MIXED &
    VARIABLE=MASS-FLOW
  DEFINE MOFPS1 STREAM-VAR STREAM=S8 SUBSTREAM=CIPSD1 &
    VARIABLE=MOLE-FLOW
  DEFINE MOFPS2 STREAM-VAR STREAM=S8 SUBSTREAM=CIPSD2 &
    VARIABLE=MOLE-FLOW
```

```
      DEFINE MFAIR1 STREAM-VAR STREAM=AIR1 SUBSTREAM=MIXED  &
        VARIABLE=MOLE-FLOW
      DEFINE MFAIR2 STREAM-VAR STREAM=AIR2 SUBSTREAM=MIXED  &
        VARIABLE=MOLE-FLOW
      DEFINE MFAIR3 STREAM-VAR STREAM=AIR3 SUBSTREAM=MIXED  &
        VARIABLE=MOLE-FLOW
      DEFINE MDPSD1 STREAM-VAR STREAM=S8 SUBSTREAM=CIPSD1  &
        VARIABLE=MASS-DENSITY
      DEFINE MDPSD2 STREAM-VAR STREAM=S8 SUBSTREAM=CIPSD2  &
        VARIABLE=MASS-DENSITY
      DEFINE MDNC1 STREAM-VAR STREAM=S8 SUBSTREAM=NCPSD1  &
        VARIABLE=MASS-DENSITY
      DEFINE MDNC2 STREAM-VAR STREAM=S8 SUBSTREAM=NCPSD2  &
        VARIABLE=MASS-DENSITY
      DEFINE MDLIME STREAM-VAR STREAM=S8 SUBSTREAM=CISOLID  &
        VARIABLE=MASS-DENSITY
      DEFINE MDMIX STREAM-VAR STREAM=S8 SUBSTREAM=MIXED  &
        VARIABLE=MASS-DENSITY
      DEFINE MODPS1 STREAM-VAR STREAM=S8 SUBSTREAM=CIPSD1  &
        VARIABLE=MOLE-DENSITY
      DEFINE MODPS2 STREAM-VAR STREAM=S8 SUBSTREAM=CIPSD2  &
        VARIABLE=MOLE-DENSITY
      DEFINE MOFRAC MOLE-FRAC STREAM=S8 SUBSTREAM=MIXED  &
        COMPONENT=O2
      DEFINE MODMIX STREAM-VAR STREAM=S8 SUBSTREAM=MIXED  &
        VARIABLE=MOLE-DENSITY
      VECTOR-DEF PSD1 SUBS-ATTR STREAM=S8 SUBSTREAM=CIPSD1  &
        ATTRIBUTE=PSD1
      VECTOR-DEF PSD2 SUBS-ATTR STREAM=S8 SUBSTREAM=CIPSD2  &
        ATTRIBUTE=PSD2
      DEFINE MFC1 MASS-FLOW STREAM=S8 SUBSTREAM=CIPSD1  &
        COMPONENT=C
      DEFINE MFC2 MASS-FLOW STREAM=S8 SUBSTREAM=CIPSD2  &
        COMPONENT=C
      DEFINE VISCO STREAM-PROP STREAM=S8 PROPERTY=PS-1
      DEFINE BEDVL BLOCK-VAR BLOCK=B4 VARIABLE=VOL SENTENCE=PARAM
      DEFINE BEDVU1 BLOCK-VAR BLOCK=B8 VARIABLE=VOL  &
        SENTENCE=PARAM
      DEFINE BEDVU2 BLOCK-VAR BLOCK=B11 VARIABLE=VOL  &
        SENTENCE=PARAM
      DEFINE BEDP BLOCK-VAR BLOCK=B8 VARIABLE=PRES SENTENCE=PARAM
F     OPEN(7,FILE='F-2.txt')
F
F
C     TOTAL MASS FLOW RATE OF SUBSTREAM CIPSD
F     FTOTAL = MFPSD1+MFPSD2+MFNC1+MFNC2+MFLIME
F
F     WRITE(7,*)'TOTAL FLOW RATE OF CIPSD(kg/s)',FTOTAL
F
C     MEAN MASS DENSITY OF TOTAL FLOW
```

```
F    DEN  = MFPSD1*MDPSD1+MFPSD2*MDPSD2
F    +    +MFN1*MDNC1+MFNC2*MDNC2+MFLIME*MDLIME
F

F    DENS = 1/FTOTAL*DEN
F    WRITE(7,*)'MEAN MASS DENSITY(kg/m^3)',DENS
F
C    VOLUMETRIC FLOW RATE OF TOTAL FLOW TO RCSTR
F    VFTOT = FTOTAL/DENS
F    WRITE(7,*)'VOLUMETRIC FLOW RATE OF TOTAL FLOW(m^3/s)',VFTOT
F
C    CONCENTRATION OF OXYGEN
F    CONO2=MOFRAC*MODMIX
F    WRITE(7,*)'CONCENTRATION OF OXYGEN',CONO2
F
C    VISCOSITY OF FLUID
F    VIS = VISCO
F    WRITE(7,*)'VISCOSITY',VIS
F
C    *===============================================================*
C           DEFINED VARIABLE TO EXTERNAL SUBROUTINE
C    *===============================================================*
F
C    DEFINE MOLAR DENSITY
F    DPSDU1(1) = MODPS1
F    DPSDU1(2) = MODPS2
F
C    DEFINED MOLAR FLOW RATE
F    FMOLU1(1) = MOFPS1
F    FMOLU1(2) = MOFPS2
F
C    MASS FLOW RATE OF CARBON FOR EACH COMPONENT IN INPUT
F    FCPSD1(1) = MFC1
F    FCPSD1(2) = MFC2
F
C    *===============================================================*
C            PREPARE WEIGHT FRACTION OF PSD
C    *===============================================================*
F
F    DO 5  I=1,5
F       WF2PSD(I,1) = PSD1(I)
F  5    WF2PSD(I,2) = PSD2(I)
F       WRITE(7,6)((WF2PSD(I,J),J=1,2),I=1,5)
F  6    FORMAT(2X,'WF2PSD',/5(1X,E10.3))
F

F
C    *===========================================================*
C               LOWER REGION
C    *===========================================================*
F
```

```
F    WRITE(7,*)'VOLUMETRIC FLOW RATE OF AIR (m^3/s)',VFAIR1

F    WRITE(7,*)'AREA',AREA

F    WRITE(7,*)'AIR VELOCITY (m/s)',VAIR1

F    WRITE(7,*)'MEAN VOIDAGE OF DENSE BED',VVOID(1)

F

F

C    *=============================================================*

C              UPPER REGION

C    *=============================================================*

F

C    VOLUMETRIC FLOW RATE FOR MIXED STREAM (m^3/s)

F    VFMIX = MFMIX/MDMIX

F


C    AIR VILOCITY(m/s)

F    VAIRU1 = VFMIX/AREA

F    WRITE(7,*)'AIR VELOCITY (m/s)',VAIRU1

F

C    NET SOLIDS CIRCULATION (Kg/(m^2 s)

F    GS = 30.0

F

F

C    DIMENSIONLESS (DP STAR) (m)

F    DPSAT = DP*(MDMIX*(DENS-MDMIX)*G/VISCO**2.)**(1./3.)

F    WRITE(7,*)'DIMENSIONLESS (DP STAR)',DPSAT

F

C    TERMINAL VELOCITY OF PARTICLE (m/s)

F    UTSAT = 1./(18./DPSAT**2.+(2.335-1.744*PHIS)/DPSAT**0.5)

F    WRITE(7,*)'UTSAT',UTSAT

F

F    UT= UTSAT/(MDMIX**2./(VISCO*(DENS-MDMIX)*G))**(1./3.)

F    WRITE(7,*)'TERMINAL VELOCITY OF PARTICLE (m/s)',UT

F

C    EQUIVALENT DIAMETER (m)

F    BEDD = 4.*AREA/(4.*BEDW)

F

C    BED LENGTH(m)

F    BEDL(1) = BEDV/AREA

F    BEDL(2) = BEDVU1/AREA

F    BEDL(3) = BEDVU2/AREA

F    BEDL(4) = BEDLT-(BEDL(1)+BEDL(2)+BEDL(3))

F    WRITE(7,*)'BEDL(I)',(BEDL(I),I=1,4)

F

C    TOTAL GAS CONCENTRATION (kmole/m^3)

C    GAS CONSTANT (atm cm^3)/(gmole k)

F    R = 82.056

F    BEDT2 = 1173

F    CONC =  BEDP*1000./(101325.*R*BEDT2)

F    WRITE(7,*)'CONC',CONC

F
```

```
C    SUPERFICIAL GAS VELOCITY(m/s)
F    UGAS(1) = MFAIR1/(AREA*CONC)
F    UGAS(2) = UGAS(1)+MFAIR2/(AREA*CONC)
F    UGAS(3) = UGAS(2)+MFAIR3/(AREA*CONC)
F    UGAS(4) = UGAS(3)
F    WRITE(7,*)'SUPERFICIAL GAS VELOCITY(m/s)',(UGAS(I),I=1,4)
F
C    FROUDE NUMBER
F    FR = UGAS(4)/(G*BEDD)**0.5
F    WRITE(7,*)'FR',FR
F
C    PARTICLE FROUDE NUMBER
F    FRT = UT/(G*BEDD)**0.5
F    WRITE(7,*)'FRT',FRT
F
C    MEAN AXIAL VOIDAGE IN THE FULLY DEVELOPED ZONE
F    PHI = 1.+5.6/FR + 0.47*FRT**0.41
F    VVOID(4) = 1./(1.+PHI*GS/(UGAS(4)*DENS))
F    WRITE(7,*)'PHI',PHI
F    WRITE(7,*)'VVOID(4)',VVOID(4)
F
C    DECAY CONSTANT
F    A = 5./UGAS(4)
F    WRITE(7,*)'DECAY RATIO',A
F
C    LENGTH OF THE ACCELERATION ZONE
F    BEDZ = (-1./A)*DLOG((VOIDS-VVOID(4))/(VOIDS-VVOID(1)))
F    WRITE(7,*)VOIDS,VVOID(4),VVOID(1)
F    WRITE(7,*)'BEDZ',BEDZ
F
C    HEIGHT IN CFBC AT ANY INTERVAL
F    BDL(1) = BEDV/AREA
F    BDL(2) = BEDZ/3.
F    BDL(3) = 2.*BEDZ/3.
F    BDL(4) = BEDLT-(BEDZ+BDL(1))
F    WRITE(7,*)'BDL(I)',(BDL(I),I=1,4)
F
F    BEDVV(1) = BEDV
F    BEDVV(2) = AREA*BDL(2)
F    BEDVV(3) = AREA*BDL(3)
F    BEDVV(4) = AREA*BDL(4)
F    WRITE(7,*)'BEDVV(I)',(BEDVV(I),I=1,4)
F
C    VOIDAGE AT ANOTHER INTERNAL
F    VVOID(2) = VOIDS + (VOIDS-VVOID(1))/(A*BDL(2))
F    +        *(DEXP(-A*BDL(2))-1)
F    VVOID(3) = VOIDS + (VOIDS-VVOID(1))/(A*BDL(3))
F    +        *(DEXP(-A*BEDZ)-DEXP(-A*BDL(2)))
F    WRITE(7,*)'VVOID(2)',VVOID(2)
F    WRITE(7,*)'VVOID(3)',VVOID(3)
```

EXECUTE BEFORE BLOCK B8

CALCULATOR C-3

```
F    COMMON/USER4/VFTOT,CONO2,VIS,VVOID,DPSD,FMOLE,VAIR1,BEDVV
F    COMMON/USER8/FCPSD2,WF3PSD
F    COMMON/USER9/DPSDU2,FMOLU2,VAIRU2,BEDT3,BEDVV2,VVOID2
F
F
F    REAL*8 VVOID(4),VVOID2(4),DPSDU2(2),FMOLU2(2),WF3PSD(5,2),
F    +    FCPSD2(2),BEDVV2(4),UGAS(4),BEDL(4),BDL(4)
F
F    DATA PHIS/0.806/,BEDLT/21.84/,VOIDS/0.999/,G/9.81/,DP/0.001/
     DEFINE MFPSD1 STREAM-VAR STREAM=S12 SUBSTREAM=CIPSD1 &
        VARIABLE=MASS-FLOW
     DEFINE MFPSD2 STREAM-VAR STREAM=S12 SUBSTREAM=CIPSD2 &
        VARIABLE=MASS-FLOW
     DEFINE MFNC1 STREAM-VAR STREAM=S12 SUBSTREAM=NCPSD1 &
        VARIABLE=MASS-FLOW
     DEFINE MFNC2 STREAM-VAR STREAM=S12 SUBSTREAM=NCPSD2 &
        VARIABLE=MASS-FLOW
     DEFINE MFLIME STREAM-VAR STREAM=S12 SUBSTREAM=CISOLID &
        VARIABLE=MASS-FLOW
     DEFINE MFMIX STREAM-VAR STREAM=S12 SUBSTREAM=MIXED &
        VARIABLE=MASS-FLOW
     DEFINE MFC1 MASS-FLOW STREAM=S12 SUBSTREAM=CIPSD1 &
        COMPONENT=C
     DEFINE MFC2 MASS-FLOW STREAM=S12 SUBSTREAM=CIPSD2 &
        COMPONENT=C
     DEFINE MOFPS1 STREAM-VAR STREAM=S12 SUBSTREAM=CIPSD1 &
        VARIABLE=MOLE-FLOW
     DEFINE MOFPS2 STREAM-VAR STREAM=S12 SUBSTREAM=CIPSD2 &
        VARIABLE=MOLE-FLOW
     DEFINE MFAIR1 STREAM-VAR STREAM=AIR1 SUBSTREAM=MIXED &
        VARIABLE=MOLE-FLOW
     DEFINE MFAIR2 STREAM-VAR STREAM=AIR2 SUBSTREAM=MIXED &
        VARIABLE=MOLE-FLOW
     DEFINE MFAIR3 STREAM-VAR STREAM=AIR3 SUBSTREAM=MIXED &
        VARIABLE=MOLE-FLOW
     DEFINE MDPSD1 STREAM-VAR STREAM=S12 SUBSTREAM=CIPSD1 &
        VARIABLE=MASS-DENSITY
     DEFINE MDPSD2 STREAM-VAR STREAM=S12 SUBSTREAM=CIPSD2 &
        VARIABLE=MASS-DENSITY
     DEFINE MDNPS1 STREAM-VAR STREAM=S12 SUBSTREAM=NCPSD1 &
        VARIABLE=MASS-DENSITY
     DEFINE MDNPS2 STREAM-VAR STREAM=S12 SUBSTREAM=NCPSD2 &
        VARIABLE=MASS-DENSITY
     DEFINE MDLIME STREAM-VAR STREAM=S12 SUBSTREAM=CISOLID &
        VARIABLE=MASS-DENSITY
     DEFINE MDMIX STREAM-VAR STREAM=S12 SUBSTREAM=MIXED &
        VARIABLE=MASS-DENSITY
```

```
      DEFINE MODPS1 STREAM-VAR STREAM=S12 SUBSTREAM=CIPSD1  &
         VARIABLE=MOLE-DENSITY
      DEFINE MODPS2 STREAM-VAR STREAM=S12 SUBSTREAM=CIPSD2  &
         VARIABLE=MOLE-DENSITY
      DEFINE MODMIX STREAM-VAR STREAM=S12 SUBSTREAM=MIXED  &
         VARIABLE=MOLE-DENSITY
      DEFINE MOFRAC MOLE-FRAC STREAM=S12 SUBSTREAM=MIXED  &
         COMPONENT=O2
      DEFINE VISCO STREAM-PROP STREAM=S12 PROPERTY=PS-1
      VECTOR-DEF PSD1 SUBS-ATTR STREAM=S12 SUBSTREAM=CIPSD1  &
         ATTRIBUTE=PSD1
      VECTOR-DEF PSD2 SUBS-ATTR STREAM=S12 SUBSTREAM=CIPSD2  &
         ATTRIBUTE=PSD2
      DEFINE BEDVL BLOCK-VAR BLOCK=B4 VARIABLE=VOL SENTENCE=PARAM
      DEFINE BEDVU1 BLOCK-VAR BLOCK=B8 VARIABLE=VOL  &
         SENTENCE=PARAM
      DEFINE BEDVU2 BLOCK-VAR BLOCK=B11 VARIABLE=VOL  &
         SENTENCE=PARAM
      DEFINE BEDP BLOCK-VAR BLOCK=B11 VARIABLE=PRES  &
         SENTENCE=PARAM
F     OPEN(7,FILE='F-3.txt')
F
F
C     TOTAL MASS FLOW RATE OF SUBSTREAM CIPSD
F     FTOTAL = MFPSD1+MFPSD2+MFNC1+MFNC2+MFLIME
F
F     WRITE(7,*)'TOTAL FLOW RATE OF CIPSD(kg/s)',FTOTAL
F
C     MEAN MASS DENSITY OF TOTAL FLOW TO RCSTR
F     DEN  = MFPSD1*MDPSD1+MFPSD2*MDPSD2
F     +     +MFNC1*MDNC1+MFN2*MDNC2+MFLIME*MDLIME
F     DENS = 1/FTOTAL*DEN
F
F     WRITE(7,*)'MEAN MASS DENSITY(kg/m^3)',DENS
F
F
C     VOLUMETRIC FLOW RATE OF TOTAL FLOW TO RCSTR
F     VFTOT = FTOTAL/DENS
F     WRITE(7,*)'VOLUMETRIC FLOW RATE OF TOTAL FLOW(m^3/s)',VFTOT
F
C     CONCENTRATION OF OXYGEN
F     CONO2=MOFRAC*MODMIX
F     WRITE(7,*)'CONCENTRATION OF OXYGEN',CONO2
F
C     VISCOSITY OF FLUID
F     VIS = VISCO
F     WRITE(7,*)'VISCOSITY',VIS
F
C     *=========================================================*
C          DEFINED VARIABLE TO EXTERNAL SUBROUTINE
```

```
C    *==========================================================*
F
C    DEFINE MOLAR DENSITY
F    DPSDU2(1) = MODPS1
F    DPSDU2(2) = MODPS2
F
C    DEFINED MOLAR FLOW RATE
F    FMOLU2(1) = MOFPS1
F    FMOLU2(2) = MOFPS2
F
C    MASS FLOW RATE OF CARBON FOR EACH COMPONENT IN INPUT
F    FCPSD2(1) = MFC1
F    FCPSD2(2) = MFC2
F
C    *================================================================*
C            PREPARE WEIGHT FRACTION OF PSD
C    *================================================================*
F
F    DO 5  I=1,5
F      WF3PSD(I,1) = PSD1(I)
F  5   WF3PSD(I,2) = PSD2(I)
F      WRITE(7,6)((WF3PSD(I,J),J=1,2),I=1,5)
F  6   FORMAT(2X,'WF3PSD',/5(1X,E10.3))
F
F
C    *=======================================================*
C             UPPER REGION
C    *=======================================================*
F
C    VOLUMETRIC FLOW RATE FOR MIXED STREAM (m^3/s)
F    VFMIX = MFMIX/MDMIX
F
C    AIR VILOCITY(m/s)
F    VAIRU2 = VFMIX/AREA
F    WRITE(7,*)'AIR VELOCITY TO UPPER (m/s)',VAIRU2
F
C    NET SOLIDS CIRCULATION (Kg/(m^2 s)
F    GS = 30.0
F
C    DIMENSIONLESS (DP STAR) (m)
F    DPSAT = DP2*(MDMIX*(DENS-MDMIX)*G/VISCO**2.)**(1./3.)
F    WRITE(7,*)'DIMENSIONLESS (DP STAR)',DPSAT
F
C    TERMINAL VELOCITY OF PARTICLE (m/s)
F    UTSAT = 1./(18./DPSAT**2.+(2.335-1.744*PHIS)/DPSAT**0.5)
F    WRITE(7,*)'UTSAT',UTSAT
F
F    UT= UTSAT/(MDMIX**2./(VISCO*(DENS-MDMIX)*G))**(1./3.)
F    WRITE(7,*)'TERMINAL VELOCITY OF PARTICLE (m/s)',UT
F
```

```
C    EQUIVALENT DIAMETER (m)
F    BEDD = 4.*AREA/(4.*BEDW)
F

C    BED LENGTH(m)
F    BEDL(1) = BEDV/AREA
F    BEDL(2) = BEDVU1/AREA
F    BEDL(3) = BEDVU2/AREA
F    BEDL(4) = BEDLT-(BEDL(1)+BEDL(2)+BEDL(3))
F    WRITE(7,*)'BEDL(I)',(BEDL(I),I=1,4)
F

C    TOTAL GAS CONCENTRATION (kmole/m^3)
C    GAS CONSTANT (atm cm^3)/(gmole k)
F    R = 82.056
F    BEDT3 = 1173
F    CONC = BEDP*1000./(101325.*R*BEDT3)
F    WRITE(7,*)'CONC',CONC
F

C    SUPERFICIAL GAS VELOCITY(m/s)
F    UGAS(1) = MFAIR1/(AREA*CONC)
F    UGAS(2) = UGAS(1)+MFAIR2/(AREA*CONC)
F    UGAS(3) = UGAS(2)+MFAIR3/(AREA*CONC)
F    UGAS(4) = UGAS(3)
F    WRITE(7,*)'SUPERFICIAL GAS VELOCITY(m/s)',(UGAS(I),I=1,4)
F

C    FROUDE NUMBER
F    FR = UGAS(4)/(G*BEDD)**0.5
F    WRITE(7,*)'FR',FR
F

C    PARTICLE FROUDE NUMBER
F    FRT = UT/(G*BEDD)**0.5
F    WRITE(7,*)'FRT',FRT
F

C    MEAN AXIAL VOIDAGE IN THE FULLY DEVELOPED ZONE
F    PHI = 1.+5.6/FR + 0.47*FRT**0.41
F    VVOID2(4) = 1./(1.+PHI*GS/(UGAS(4)*DENS))
F    WRITE(7,*)'PHI',PHI
F    WRITE(7,*)'VVOID2(4)',VVOID2(4)
F

C    DECAY CONSTANT
F    A = 5./UGAS(4)
F    WRITE(7,*)'DECAY RATIO',A
F

C    LENGTH OF THE ACCELERATION ZONE
F    BEDZ = (-1./A)*DLOG((VOIDS-VVOID2(4))/(VOIDS-VVOID(1)))
F    WRITE(7,*)VOIDS,VVOID2(4),VVOID(1)
F    WRITE(7,*)'BEDZ',BEDZ
F

C    HEIGHT IN CFBC AT ANY INTERVAL
F    BDL(1) = BEDV/AREA
```

```
F    BDL(2) = BEDZ/3.
F    BDL(3) = 2.*BEDZ/3.
F    BDL(4) = BEDLT-(BEDZ+BDL(1))
F    WRITE(7,*)'BDL(I)',(BDL(I),I=1,4)
F
F    BEDVV2(1) = BEDV
F    BEDVV2(2) = AREA*BDL(2)
F    BEDVV2(3) = AREA*BDL(3)
F    BEDVV2(4) = AREA*BDL(4)
F    WRITE(7,*)'BEDVV2(I)',(BEDVV2(I),I=1,4)
F
C    VOIDAGE AT ANOTHER INTERNAL
F    VVOID2(2) = VOIDS + (VOIDS-VVOID(1))/(A*BDL(2))
F    +        *(DEXP(-A*BDL(2))-1)
F    VVOID2(3) = VOIDS + (VOIDS-VVOID(1))/(A*BDL(3))
F    +        *(DEXP(-A*BEDZ)-DEXP(-A*BDL(2)))
F    WRITE(7,*)'VVOID2(2)',VVOID2(2)
F    WRITE(7,*)'VVOID2(3)',VVOID2(3)
   EXECUTE BEFORE BLOCK B11


CALCULATOR C-4
F    COMMON/USER10/FCPSD3,WF4PSD
F    COMMON/USER11/DPSDU3,FMOLU3,VAIRU3,BEDT4,BEDVV3,VVOID3
F    COMMON/USER12/UGAS
F
F    REAL*8 VVOID(4),VVOID3(4),DPSDU3(2),FMOLU3(2),WF4PSD(5,2),
F    +    FCPSD3(2),BEDVV3(4),UGAS(4),BEDL(4),BDL(4)
F
F    DATA PHIS/0.806/,BEDLT/21.84/,VOIDS/0.999/,G/9.81/,DP/0.001/
   DEFINE MFPSD1 STREAM-VAR STREAM=S16 SUBSTREAM=CIPSD1  &
      VARIABLE=MASS-FLOW
   DEFINE MFPSD2 STREAM-VAR STREAM=S16 SUBSTREAM=CIPSD2  &
      VARIABLE=MASS-FLOW
   DEFINE MFNC1 STREAM-VAR STREAM=S16 SUBSTREAM=NCPSD1  &
      VARIABLE=MASS-FLOW
   DEFINE MFNC2 STREAM-VAR STREAM=S16 SUBSTREAM=NCPSD2  &
      VARIABLE=MASS-FLOW
   DEFINE MFLIME STREAM-VAR STREAM=S16 SUBSTREAM=CISOLID  &
      VARIABLE=MASS-FLOW
   DEFINE MFMIX STREAM-VAR STREAM=S16 SUBSTREAM=MIXED  &
      VARIABLE=MASS-FLOW
   DEFINE MFC1 MASS-FLOW STREAM=S16 SUBSTREAM=CIPSD1  &
      COMPONENT=C
   DEFINE MFC2 MASS-FLOW STREAM=S16 SUBSTREAM=CIPSD2  &
      COMPONENT=C
   DEFINE MOFPS1 STREAM-VAR STREAM=S16 SUBSTREAM=CIPSD1  &
      VARIABLE=MOLE-FLOW
   DEFINE MOFPS2 STREAM-VAR STREAM=S16 SUBSTREAM=CIPSD2  &
      VARIABLE=MOLE-FLOW
   DEFINE MFAIR1 STREAM-VAR STREAM=AIR1 SUBSTREAM=MIXED  &
```

```
            VARIABLE=MOLE-FLOW
     DEFINE MFAIR2 STREAM-VAR STREAM=AIR2 SUBSTREAM=MIXED  &
            VARIABLE=MOLE-FLOW
     DEFINE MFAIR3 STREAM-VAR STREAM=AIR3 SUBSTREAM=MIXED  &
            VARIABLE=MOLE-FLOW
     DEFINE MDPSD1 STREAM-VAR STREAM=S16 SUBSTREAM=CIPSD1  &
            VARIABLE=MASS-DENSITY
     DEFINE MDPSD2 STREAM-VAR STREAM=S16 SUBSTREAM=CIPSD2  &
            VARIABLE=MASS-DENSITY
     DEFINE MDNC1 STREAM-VAR STREAM=S16 SUBSTREAM=NCPSD1  &
            VARIABLE=MASS-DENSITY
     DEFINE MDNC2 STREAM-VAR STREAM=S16 SUBSTREAM=NCPSD2  &
            VARIABLE=MASS-DENSITY
     DEFINE MDLIME STREAM-VAR STREAM=S16 SUBSTREAM=CISOLID  &
            VARIABLE=MASS-DENSITY
     DEFINE MDMIX STREAM-VAR STREAM=S16 SUBSTREAM=MIXED  &
            VARIABLE=MASS-DENSITY
     DEFINE MODPS1 STREAM-VAR STREAM=S16 SUBSTREAM=CIPSD1  &
            VARIABLE=MOLE-DENSITY
     DEFINE MODPS2 STREAM-VAR STREAM=S16 SUBSTREAM=CIPSD2  &
            VARIABLE=MOLE-DENSITY
     DEFINE MOFRAC MOLE-FRAC STREAM=S16 SUBSTREAM=MIXED  &
            COMPONENT=O2
     DEFINE MODMIX STREAM-VAR STREAM=S16 SUBSTREAM=MIXED  &
            VARIABLE=MOLE-DENSITY
     DEFINE VISCO STREAM-PROP STREAM=S16 PROPERTY=PS-1
     VECTOR-DEF PSD1 SUBS-ATTR STREAM=S16 SUBSTREAM=CIPSD1  &
            ATTRIBUTE=PSD1
     VECTOR-DEF PSD2 SUBS-ATTR STREAM=S16 SUBSTREAM=CIPSD2  &
            ATTRIBUTE=PSD2
     DEFINE BEDVL BLOCK-VAR BLOCK=B4 VARIABLE=VOL SENTENCE=PARAM
     DEFINE BEDVU1 BLOCK-VAR BLOCK=B8 VARIABLE=VOL  &
            SENTENCE=PARAM
     DEFINE BEDVU2 BLOCK-VAR BLOCK=B11 VARIABLE=VOL  &
            SENTENCE=PARAM
     DEFINE BEDP BLOCK-VAR BLOCK=B14 VARIABLE=PRES  &
            SENTENCE=PARAM
F    OPEN(7,FILE='F-4.txt')
F
C    TOTAL MASS FLOW RATE OF SUBSTREAM CIPSD
F    FTOTAL = MFPSD1+MFPSD2+MFNC1+MFNC2+MFLIME
F
F    WRITE(7,*)'TOTAL FLOW RATE OF CIPSD(kg/s)',FTOTAL
F
C    MEAN MASS DENSITY OF TOTAL FLOW TO RCSTR
F    DEN  = MFPSD1*MDPSD1+MFPSD2*MDPSD2
F    +      +MFNC1*MDNC1+MFNC2*MDNC2+MFLIME*MDLIME
F
F    DENS = 1/FTOTAL*DEN
F
```

```
F    WRITE(7,*)'MEAN MASS DENSITY(kg/m^3)',DENS
F
C    VOLUMETRIC FLOW RATE OF TOTAL FLOW TO RCSTR
F    VFTOT = FTOTAL/DENS
F    WRITE(7,*)'VOLUMETRIC FLOW RATE OF TOTAL FLOW(m^3/s)',VFTOT
F
C    CONCENTRATION OF OXYGEN
F    CONO2=MOFRAC*MODMIX
F    WRITE(7,*)'CONCENTRATION OF OXYGEN',CONO2
F
C    VISCOSITY OF FLUID
F    VIS = VISCO
F    WRITE(7,*)'VISCOSITY',VIS
F
F
C    *=============================================================*
C          DEFINED VARIABLE TO EXTERNAL SUBROUTINE
C    *=============================================================*
F
C    DEFINE MOLAR DENSITY
F    DPSDU3(1) = MODPS1
F    DPSDU3(2) = MODPS2
F
C    DEFINED MOLAR FLOW RATE
F    FMOLU3(1) = MOFPS1
F    FMOLU3(2) = MOFPS2
F
C    MASS FLOW RATE OF CARBON FOR EACH COMPONENT IN INPUT
F    FCPSD3(1) = MFC1
F    FCPSD3(2) = MFC2
F
C    *=============================================================*
C          PREPARE WEIGHT FRACTION OF PSD
C    *=============================================================*
F
F    DO 5  I=1,5
F       WF4PSD(I,1) = PSD1(I)
F  5    WF4PSD(I,2) = PSD2(I)
F       WRITE(7,6)((WF4PSD(I,J),J=1,2),I=1,5)
F  6    FORMAT(2X,'WF4PSD',/5(1X,E10.3))
F
F
C    *=============================================================*
C            UPPER REGION
C    *=============================================================*
F
C    VOLUMETRIC FLOW RATE FOR MIXED STREAM (m^3/s)
F    VFMIX = MFMIX/MDMIX
F
C    AIR VILOCITY(m/s)
```

```
F    VAIRU3 = VFMIX/AREA
F    WRITE(7,*)'AIR VELOCITY TO UPPER (m/s)',VAIRU3
F
C    NET SOLIDS CIRCULATION (Kg/(m^2 s)
F    GS = 30.0
F
C    DIMENSIONLESS (DP STAR) (m)
F    DPSAT = DP3*(MDMIX*(DENS-MDMIX)*G/VISCO**2.)**(1./3.)
F    WRITE(7,*)'DIMENSIONLESS (DP STAR)',DPSAT
F
C    TERMINAL VELOCITY OF PARTICLE (m/s)
F    UTSAT = 1./(18./DPSAT**2.+(2.335-1.744*PHIS)/DPSAT**0.5)
F    WRITE(7,*)'UTSAT',UTSAT
F
F    UT= UTSAT/(MDMIX**2./(VISCO*(DENS-MDMIX)*G))**(1./3.)
F    WRITE(7,*)'TERMINAL VELOCITY OF PARTICLE (m/s)',UT
F
C    EQUIVALENT DIAMETER (m)
F    BEDD = 4.*AREA/(4.*BEDW)
F
C    BED LENGTH(m)
F    BEDL(1) = BEDV/AREA
F    BEDL(2) = BEDVU1/AREA
F    BEDL(3) = BEDVU2/AREA
F    BEDL(4) = BEDLT-(BEDL(1)+BEDL(2)+BEDL(3))
F    WRITE(7,*)'BEDL(I)',(BEDL(I),I=1,4)
F
C    TOTAL GAS CONCENTRATION (kmole/m^3)
C    GAS CONSTANT (atm cm^3)/(gmole k)
F    R = 82.056
F    BEDT4 = 1173
F    CONC =  BEDP*1000./(101325.*R*BEDT4)
F    WRITE(7,*)'CONC',CONC
F
C    SUPERFICIAL GAS VELOCITY(m/s)
F    UGAS(1) = MFAIR1/(AREA*CONC)
F    UGAS(2) = UGAS(1)+MFAIR2/(AREA*CONC)
F    UGAS(3) = UGAS(2)+MFAIR3/(AREA*CONC)
F    UGAS(4) = UGAS(3)
F    WRITE(7,*)'SUPERFICIAL GAS VELOCITY(m/s)',(UGAS(I),I=1,4)
F
C    FROUDE NUMBER
F    FR = UGAS(4)/(G*BEDD)**0.5
F    WRITE(7,*)'FR',FR
F
C    PARTICLE FROUDE NUMBER
F    FRT = UT/(G*BEDD)**0.5
F    WRITE(7,*)'FRT',FRT
F
C    MEAN AXIAL VOIDAGE IN THE FULLY DEVELOPED ZONE
```

```
F    PHI = 1.+5.6/FR + 0.47*FRT**0.41
F    VVOID3(4) = 1./(1.+PHI*GS/(UGAS(4)*DENS))
F    WRITE(7,*)'PHI',PHI
F    WRITE(7,*)'VVOID3(4)',VVOID3(4)
F
C    DECAY CONSTANT
F    A = 5./UGAS(4)
F    WRITE(7,*)'DECAY RATIO',A
F
C    LENGTH OF THE ACCELERATION ZONE
F    BEDZ = (-1./A)*DLOG((VOIDS-VVOID3(4))/(VOIDS-VVOID(1)))
F    WRITE(7,*)VOIDS,VVOID(4),VVOID(1)
F    WRITE(7,*)'BEDZ',BEDZ
F
C    HEIGHT IN CFBC AT ANY INTERVAL
F    BDL(1) = BEDV/AREA
F    BDL(2) = BEDZ/3.
F    BDL(3) = 2.*BEDZ/3.
F    BDL(4) = BEDLT-(BEDZ+BDL(1))
F    WRITE(7,*)'BDL(I)',(BDL(I),I=1,4)
F
F    BEDVV3(1) = BEDV
F    BEDVV3(2) = AREA*BDL(2)
F    BEDVV3(3) = AREA*BDL(3)
F    BEDVV3(4) = AREA*BDL(4)
F    WRITE(7,*)'BEDVV2(I)',(BEDVV3(I),I=1,4)
F
C    VOIDAGE AT ANOTHER INTERNAL
F    VVOID3(2) = VOIDS + (VOIDS-VVOID(1))/(A*BDL(2))
F    +        *(DEXP(-A*BDL(2))-1)
F    VVOID3(3) = VOIDS + (VOIDS-VVOID(1))/(A*BDL(3))
F    +        *(DEXP(-A*BEDZ)-DEXP(-A*BDL(2)))
F    WRITE(7,*)'VVOID3(2)',VVOID3(2)
F    WRITE(7,*)'VVOID3(3)',VVOID3(3)
    EXECUTE BEFORE BLOCK B14


CALCULATOR C-5
F    COMMON/USER4/VFTOT,CONO2,VIS,VVOID,DPSD,FMOLE,VAIR1,BEDVV
F    COMMON/USER10/VAIRU2,VVOID2,BEDVV2
F    COMMON/USER13/VAIRU3,VVOID3,BEDVV3
F    COMMON/USER14/VOIDM,BEDVM,BEDL
F
F    REAL*8  VVOID(4),BEDVV(4),VVOID2(4),
F    +       BEDVV2(4),VVOID3(4),BEDVV3(4),
F    +       VOIDM(3),BEDVM(3),BEDL(4)
    DEFINE FLOW STREAM-VAR STREAM=AIR1 SUBSTREAM=MIXED  &
      VARIABLE=MASS-FLOW
    DEFINE BEDVL BLOCK-VAR BLOCK=B4 VARIABLE=VOL SENTENCE=PARAM


F    OPEN(7,FILE='F-5.txt')
```

```
F
F    WRITE(7,*)'VVOID',(VVOID(I),I=1,4)
F    WRITE(7,*)'BEDVV',(BEDVV(I),I=1,4)
F    WRITE(7,*)'VVOID2',(VVOID2(I),I=1,4)
F    WRITE(7,*)'BEDVV2',(BEDVV2(I),I=1,4)
F    WRITE(7,*)'VVOID3',(VVOID3(I),I=1,4)
F    WRITE(7,*)'BEDVV3',(BEDVV3(I),I=1,4)
F
C    *=========================================================*
C         UPPER REGION
C    *=========================================================*
F
C    FIRST INTERVAL
F    VOIDM(1) = (VVOID(2)+VVOID2(2)+VVOID3(2))/3.
F    BEDVM(1) = (BEDVV(2)+BEDVV2(2)+BEDVV3(2))/3.
F
C     SECOND INTERVAL
F    VOIDM(2) = (VVOID(3)+VVOID2(3)+VVOID3(3))/3.
F    BEDVM(2) = (BEDVV(3)+BEDVV2(3)+BEDVV3(3))/3.
F
C     THIRD INTERVAL
F    VOIDM(3) = (VVOID(4)+VVOID2(4)+VVOID3(4))/3.
F    BEDVM(3) = (BEDVV(4)+BEDVV2(4)+BEDVV3(4))/3.
F
F    WRITE(7,*)'MEAN VOID AT EACH INTERVAL',(VOIDM(I),I=1,3)
F    WRITE(7,*)'MEAN VOLUME AT EACH INTERVAL',(BEDVM(I),I=1,3)
F
C     THE HEIGHT OF EACH ZONE
F    BEDL(1) = BEDV/AREA
F    BEDL(2) = BEDVM(1)/AREA
F    BEDL(3) = BEDVM(2)/AREA
F    BEDL(4) = BEDVM(3)/AREA
     EXECUTE AFTER BLOCK B14

CONV-OPTIONS
    WEGSTEIN MAXIT=9999
    BROYDEN MAXIT=9999

STREAM-REPOR MOLEFLOW MASSFLOW MOLEFRAC PROPERTIES=PS-1

PROPERTY-REP PCES

REACTIONS R-1 USER
    PARAM SUBROUTINE=UKA31
    REAC-DATA 1 PHASE=V
    REAC-DATA 2 PHASE=V
    REAC-DATA 3 PHASE=V
    STOIC 1 CIPSD1 C -2. / MIXED O2 -1. / CO 2.
    STOIC 2 CIPSD2 C -2. / MIXED O2 -1. / CO 2.
    STOIC 3 MIXED CO -2. / O2 -1. / CO2 2.
```

REACTIONS R-2 USER
  PARAM SUBROUTINE=UKA32
  REAC-DATA 1 PHASE=V
  REAC-DATA 2 PHASE=V
  REAC-DATA 3 PHASE=V
  STOIC 1 CIPSD1 C -2. / MIXED O2 -1. / CO 2.
  STOIC 2 CIPSD2 C -2. / MIXED O2 -1. / CO 2.
  STOIC 3 MIXED CO -2. / O2 -1. / CO2 2.

REACTIONS R-3 USER
  PARAM SUBROUTINE=UKA33
  REAC-DATA 1 PHASE=V
  REAC-DATA 2 PHASE=V
  REAC-DATA 3 PHASE=V
  STOIC 1 CIPSD1 C -2. / MIXED O2 -1. / CO 2.
  STOIC 2 CIPSD2 C -2. / MIXED O2 -1. / CO 2.
  STOIC 3 MIXED CO -2. / O2 -1. / CO2 2.

REACTIONS R-4 USER
  PARAM SUBROUTINE=UKA34
  REAC-DATA 1 PHASE=V
  REAC-DATA 2 PHASE=V
  REAC-DATA 3 PHASE=V
  STOIC 1 CIPSD1 C -2. / MIXED O2 -1. / CO 2.
  STOIC 2 CIPSD2 C -2. / MIXED O2 -1. / CO 2.
  STOIC 3 MIXED CO -2. / O2 -1. / CO2 2.

BIOGRAPHY

Miss Chutima Montatip was born on August 26, 1982 in Chonburi, Thailand. She graduated her Bachelor's degree of Engineering in Department of Chemical Engineering, Faculty of Engineering, Suranaree University of Technology in 2004. She has continued her study in Master's degree of Engineering in Department of Chemical Engineering, Faculty of Engineering, Chulalongkorn University since 2004 and finished her study in 2007.